# DEVELOPMENT AND APPLICATIONS OF MINIATURIZED PROTEIN EXPRESSION SYSTEMS

By

QIAN MEI

A DISSERTATION PRESENTED TO THE GRADUATE SCHOOL
OF THE UNIVERSITY OF FLORIDA IN PARTIAL FULFILLMENT
OF THE REQUIREMENTS FOR THE DEGREE OF
DOCTOR OF PHILOSOPHY

UNIVERSITY OF FLORIDA

2007

To my grandfather, Chongjia Mei, who passed away in 2007. He will be always missed and I cherish the loving memories I had with him.

To my beloved parents, Yuzhu Zhou and Guifang Mei, who have unconditionally been supporting me through my entire life. They are my model for responsibility, strength, persistence and personal sacrifices. Without their encouragement and guidance, I would not have the goals I have achieved. I am so proud that I am their daughter.

To my husband and best friend, Hong Wang, whose constant love, encouragement, endless patience and passion enable me to complete this work.

To my dear sister, Xin Zhou, who has been always there for me, whenever good or bad time.

ACKNOWLEDGMENTS

It is my pleasure to express my gratitude to all those people without whom this dissertation would not be possible.

First and foremost I gratefully acknowledge my supervisor, Dr. Z. Hugh Fan, for his inspiration, guidance, mentoring, and support throughout my thesis. Dr. Fan has been cultivating an interdisciplinary environment by populating the laboratory with people from all different backgrounds, working on a number of different projects and introducing all sorts of new ideas from various fields. I also thank him for providing me an opportunity to grow as a student and engineer in the unique research environment he creates.

My next acknowledgement is to Dr. Steven Soper in Chemistry Department at Louisiana State University for providing me an opportunity to visit his lab and access the state-of-the-art fabrication facilities during the last year of my Ph.D program. Chapter 4 of this dissertation has been finished in his research lab. I appreciate Dr. Soper's generous support and supervision, and all scientific discussion and creative suggestions from his research group.

I thank Drs. Shouguang Jin, James Klausner, Malisa Sarntinoranont, and Roger Tran-Son-Tay for their time to serve on my supervisory committee and provide valuable comments and advice.

I thank Dr. Brian Cain for the access of a luminometer and Dr. Weihong Tan for the access of a fluorescence spectrometer.

I acknowledge Drs. Nancy Denslow, Quangfan Chen, Philip Laipis, Wei Lian, and Xinchun Shen for useful discussion.

My deep appreciation also goes to Carl Fredrickson and Andrew Simon for their contributions to the development and fabrication of devices used in this dissertation.

I thank Dr. Fan's entire Research Group, both former and current members, for their support and friendship. I sincerely cherish the moments we worked together as colleagues and friends.

Lastly, and most importantly, I wish to thank my parents, friends and entire extended family for providing a loving environment during my life.

TABLE OF CONTENTS

LIST OF TABLES

LIST OF FIGURES

Abstract of Dissertation Presented to the Graduate School
of the University of Florida in Partial Fulfillment of the
Requirements for the Degree of Doctor of Philosophy

DEVELOPMENT AND APPLICATIONS OF MINIATURIZED PROTEIN EXPRESSION SYSTEMS

By

Qian Mei

December 2007

Chair: Z. Hugh Fan
Major: Mechanical Engineering

Recent development in miniaturization provides an opportunity for performing chemical and biomedical research in a novel, fast and unique way. This dissertation presents miniaturized plastic devices for *in vitro* protein expressions (synthesis), as well as their downstream applications.

Biological synthesis of a protein includes the steps of gene transcription and protein translation, which are typically carried out in host cells. However, some proteins are difficult to be synthesized in cells due to their insolubility, degradation and cytotoxicity. To address some of these challenges, cell-free protein synthesis, a process called in vitro transcription and translation (IVT), has been developed. In this dissertation, IVT is first demonstrated in a microwell array for expression of proteins, including green fluorescent protein (GFP), chloramphenicol acetyl-transferase (CAT) and luciferase. The array device is then demonstrated for detecting toxin simulants, tetracycline (TC) and cycloheximide (CH), based on their inhibitory effects on protein synthesis. The differential response patterns from the array device for two toxin simulants suggest the feasibility of the detection concept.

One drawback of the microwell array is that it does not consist of any fluid manipulation. To address this, a nested-well array is then developed. The nested-well device possesses a

mechanism to supply nutrients continuously and remove byproducts, leading to higher protein expression yields. The productions of green fluorescent protein, chloramphenicol acetyl-transferase and luciferase are demonstrated in the device. In addition, the device is demonstrated for ricin detection. The calibration curve has been obtained between the luciferase expression yield and the ricin concentration.

Finally, a microfluidic device consisting of a straight channel with herringbone ridges at the bottom wall and a spiral channel is designed and fabricated to demonstrate enzymatic reactions. The device with the ridge feature has shown better mixing than one with a smooth wall when luminescent enzymatic reaction is implemented in the device. Morever, the device can be used to detect luciferse synthesized off chip.

# CHAPTER 1
# INTRODUCTION

In this chapter, miniaturization and the potential applications of miniaturized devices will be discussed first. It is followed by a brief introduction of basic principles and terminologies in molecular biology that are related to this interdisciplinary research.

## 1.1 Miniaturized Device and Its Applications

Richard Feynman presented two famous talks about the miniaturized tools and devices: one is titled "There is plenty of room at the bottom— an invitation to enter a new field of physics" at the annual meeting of the American Physical Society at the California Institute of Technology on December 29th, 1959;[1] the other is "Infinitesimal Machinery—Revisiting 'there is plenty of room at the bottom'" at the Jet Propulsion Laboratory in California on February 23th, 1983.[2] These talks invited scientists and engineers to explore the realm of ultra-small structures and systems. Though Feynman never coined any fashion word, like "nano" or "MEMS", he is now widely credited as the first visionary in the field of miniaturized devices, and more recently, nanotechnology.

Eleven months after his first talk, $1000 prize offered in Feynman's talk for "the first guy who makes an operating electric motor in 1/64 inch cube" was claimed by William McLellan.[1] Since then, the engineering community has made exponential progress in miniaturization in microelectronics, micro-electro-mechanical systems and nanotechnologies. The miniaturized computers were partially realized when he gave his second talk in 1983.

But he must be very disappointed by the slow progress in miniaturized biological systems, which he speculated in his talk: [1] (p. 62)

> ***The marvelous biological system.*** The biological example of writing information on a small scale has inspired me to think of something that should be possible. Biology is not simply writing information; it is *doing something* about it. A biological system can be exceedingly small. Many of the cells are very tiny, but they are very active; they

> manufacture various substances; they walk around; they wiggle; and they do all kinds of marvelous things---all on a very small scale. Also, they store information. Consider the possibility that we too can make a thing very small which does what we want---that we can manufacture an object that maneuvers at that level!

Chemists and biologists are beginning to understand the potential of miniaturization and starting to work closely with engineers to develop miniaturized devices.[3-5]

### 1.1.1 MEMS

Micro-Electro-Mechanical Systems (MEMS) are the miniaturized systems or devices that integrate electrical and mechanical components on a common silicon substrate through microfabrication technology.[6-10] The sizes of these components are from the submicrometer level to the millimeter level; and there can be any number, from a few to millions, in a particular system to complete a specific function.[11-16]

Traditionally, MEMS devices are achieved by repeating the deposition (thin film), patterning (photolithography) and etching steps on two major materials, silicon and glass.[8, 17, 18] Besides the fabrication technologies directly ported from the integrated circuit industry, new protocols have been developed in last three decades to manufacture mechanical elements, like gears, beams, springs, etc. in MEMS devices.[19]

During the last two decades, the MEMS devices shift rapidly from research lab to industry. Nexus market analysis predicted the market for microsystems will grow from $12 billion in 2004 to $25 billion in 2009 at the rate of 16% per year.[20] Examples of applications of MEMS devices are read/write head of hard drive, inkjet printer cartridge, automotive accelerometers and pressure sensors.

The topic of this dissertation is about BioMEMS, the most recent and dramatically expanding biological applications of MEMS.

### 1.1.2 BioMEMS, Lab-on-a-chip and MicroTAS

BioMEMS (biological or biomedical micro-electro-Mechanical system) gets its name from MEMS, but BioMEMS devices rarely use silicon or involve a moving part (like beams or gears), which are hallmarks of MEMS devices. It may be one of least precise terms to describe the application of MEMS and/or micro/nano technologies in biological system or bioanalytical chemistry. BioMEMS is now much more than a subset or division of MEMS, it is becoming a field into itself, uniquely identified by its materials, fabrication technologies, chemistry and physics.

While most researchers from engineering like to use BioMEMS to emphasize the microfabrication techniques used for manufacturing these miniaturized devices, chemists prefer to use Lab-on-a-chip (LOC) or micro total analysis system (MicroTAS or μTAS) to indicate that more than one processing steps are integrated on to a single platform to perform a well-defined analysis task or a specific function.[21] More and more researchers are now using these terms interchangeably. They sometimes also categorize devices without mechanical and/or electronic components, such as DNA or protein microarrays, under BioMEMS.

In the following part of this section, the material, fabrication, applications (Figure 1-1) and advantages of BioMEMS or LOC devices will be briefly reviewed.

BioMEMS devices are mainly fabricated with three categories of materials. They are (1) traditional MEMS materials, like silicon and glass; (2) plastic materials and polymers; (3) biomaterials, such as DNA, protein, cell and hydrogel.

At the inception of BioMEMS, silicon wafers and glass slides were used extensively because the MEMS fabrication technologies, such as lithography, bulk micromachining, surface machining, could be directly ported to fabrication such devices.[17, 22, 23] However, the cost of

such a device is very high. As reported by Manz et al. in 1998, the cost for each etched glass chip for continuous PCR amplification was $500 and for the apparatus was $4000.[24]

In last couple of years, more and more research groups started to use plastic materials and polymers. The main reasons of using plastic materials include: (1) low cost. The material itself and the compatible fabrication process are much less inexpensive than the silicon or glass and they can be used in disposable devices, reducing the possibility of cross-contamination of the re-used devices;[25-28] (2) multi-functionalities. There are different plastic materials and polymers with different chemical, physical and biological properties. A hard and glassy or a soft and rubbery chip with different chemically functionalized surface can be easily chosen from a doze of frequently used materials; (3) super biocompatibility. It's easier to interface polymer materials to the biological tissues. The lower toxicity, less immuno-inflammatory and bio-degradability permit *in vitro* applications of such devices. The fabrication methods for manufacturing plastic devices include soft-lithography, mold injection, hot embossing, laser ablation and micromilling.[29, 30] Most of these technologies still require a stamp, a mold, or a master fabricated with traditional MEMS technologies. Once the stamp is fabricated, the pattern on it can be mechanically transferred to hundreds to thousands of plastic chips. It is very cost-effective. The miniaturized devices used in this dissertation were made from PMMA (poly methyl methacrylate) and polycabonate by direct micromilling or hot embossing.

The third category is biomaterials, including biomolecules (DNA, protein, etc.) and hydrogel. Hydrogel is widely used in scaffold fabrication for artificial organ and other implantable medical devices. Lots of well-designed hydrogel may swell in responding to the environment, such as pH, temperature, etc., which makes it as a perfect component in closed-loop "smart devices".[31, 32] While the above mentioned two categories of materials are normally

fabricated with top-down methods (from large scale to small scale, like photolithography), the bottom-up approaches (from atoms or molecules to a specific pattern), such as self assembly, are widely used for biomaterials. "Nature is the best engineer".[33] Combining the top-down and bottom-up approaches, much more complex systems can be manufactured.

There are three categories of applications of BioMEMS devices: micro analysis, on chip synthesis and hybrid devices (Figure 1-1).

The micro analysis devices are typically classified as either microarrays or microfluidic separation devices. A DNA or protein microarray usually refers to a collection of miniaturized test sites, which are composed of DNA, protein, small molecules, probes, self-assembled or in situ synthesized on a solid substrate, permitting thousands or more tests to be performed at the same time. Developed in early 1990s, electrophoresis microchip is a typical microfluidic device for micro analysis.[27, 34-50] It is still one of the most active research topics in LOC and/or BioMEMS, and lots of efforts have been devoted to the integration and parallelization of microchip by different research groups. Burns et al. fabricated an integrated nanoliter DNA analysis device with microfluidic channels, heaters, temperature sensors and fluorescence detectors that could perform sample loading, mixing, PCR, electrophoresis and detection in a single chip.[51] Mathies group pioneered in the development of 16, 48 and 96 microchannel electrophoresis microchips for genotyping and DNA sequencing.[50, 52, 53] A recent success of parallelization is the 768 lane DNA sequencing system reported by Ehrlich et al. Within this system, two sets of 384 lanes could be alternatively cycled between electrophoresis and regeneration and the productivity was 4M bases.[54]

While majority research reports are about the micro analysis system, considerable efforts have been devoted to the on chip synthesis or microreactors since later 1990s. Take advantages

from the fast mixing,[55] improved mass and heat transfer from the microstructures in the microreactors,[56-58] and on chip (bio)chemical synthesis studies[59, 60] showed great success as predicted from the very beginning. One typical system is continuous-flow PCR microchip reported by Manz et al in 1998. Recent research focuses on the integration of multiple reaction steps, on line analysis feedback, the solution-based combinational synthesis which has the potential for oligonucleotide, and peptide library construction and gene assembly.[61-70]

There are full of challenges and opportunities to investigate the hybrid BioMEMS devices, such as implantable therapeutic devices and artificial organs. An ideal implantable therapeutic device composed of a sensor for monitoring level of biomolecules and controlling an actuator for drug or other therapeutic reagents delivery. A model system is glucose biosensor and insulin delivery system to relieve diabetes patients from repetitively injection of insulin.[71] Although there are many successful cases in either *in vivo* glucose detection or *in vivo* insulin delivery system, but no integrated system has been reported by now. This category of BioMEMS devices is not within the scope of this dissertation. Further information can be found in recent reviews.[72, 73]

After brief review of the materials, fabrication and applications of BioMEMS devices, we can answer this question: why we need miniaturized BioMEMS devices? Because there are several advantages of such devices, including: (1) small dimension of the components will reduce the weight, size and energy consumption of the device, leading to the high throughput, portable, and automatic complex system; (2) small amount of reagents may reduce the cost of the assay and small amount of analyte may save the precious sample consumption; (3) the performance (ultra-fast reaction rate, high resolution and sensitivity, etc.) of the device is greatly improved because of the fast mixing, heat exchange, and mass transfer; (4) the reliability of the

assay is improved because the batch fabrication processes make the low price, disposable device possible, and the confined miniaturized reactors almost eliminate the cross-contamination from different samples. These advantages and the potential commercial interest pull the miniaturized BioMEMS devices from emerging to burgeoning in last 15 years.

## 1.2 Protein Expression

In this section, the basic principles and terminologies of molecule biology related to this interdisciplinary work will be introduced.

### 1.2.1 DNA, RNA, Protein and Central Dogma

DNA or deoxyribonucleic acid, usually in the form of double strand helix, is the carrier of genetic information of all cellular forms of life and most viruses.[74] Each monomer of DNA is made from simple units, called nucleotides, which consist of a sugar (deoxyribose) with a phosphate group attached to it, and a base, which may be either adenine (A), guanine (G), cytosine (C), or thymine (T). The chemical bond between one phosphate to the next sugar form a backbone that links one nucleotide to the next. The bases protruding from the backbone can pair with bases from another strand of DNA to form double strand helix, as shown in Figure 1-2.

RNA or ribonucleic acid is slightly different from DNA. The sugar in the backbone is ribose and one of the four bases is different – uracil (U) replaces thymine (T). Unlike DNA, RNA is almost always a single-stranded molecule and has a much shorter chain of nucleotides. The hydroxyl group attached to the ribose is prone to hydrolysis, which makes RNA less stable than DNA. But RNA always contains secondary structure to prompt the stability.

Protein is a complex, high-molecular-mass and organic compound that is made from a long chain of amino acids, each linked to its neighbor through a peptide bond. Proteins constitute most of the dry mass of a cell and they are involved in nearly all biological processes of the

living cell, including regulation of cellular functions such as signal transduction and metabolism. Life, chemically speaking, is nothing but the functional activity of proteins.

Figure 1-3 shows the central dogma of molecular biology firstly enunciated by Francis Crick in 1958 and re-stated in a Nature paper published in 1970.[75] It summarized internal relations between DNA, RNA and protein and can be expressed in one sentence: DNA is transcribed to RNA, which is then translated to protein; but protein is never back-translated to RNA or DNA.

The central dogma can be represented by three major steps: (1) DNA replication: it transmits the genetic information from the parent cell to each daughter cell. It is carried out by a complex group of proteins that unwind the double stranded helix and using DNA polymerase and its associated proteins to faithfully replicate the original template; (2) transcription: the genetic information contained in DNA is transferred to mRNA. mRNA is synthesized and catalyzed by the RNA polymerase and four ribonucleoside triphosphates using DNA as a template with a polymerase specific promoter sequence; (3) translation: after transcription, mRNA will be transported out of nucleus and bound to ribosome. The sequence information of mRNA is translated to an amino acid chain (polypeptide) by tRNAs (transfer RNAs) and associated enzymes according to the three letter codons (Table 1-1). After translation, the peptide chain may require additional process or directly folds to a mature protein with a specific conformation.

Since Crick's paper published, there are a number of new facts have been discovered.[76-79] For example, the retroviruses can transcribe RNA to DNA and some viruses only have RNA genome.[76] But central dogma is still a very useful theory for guiding most experiments.

### 1.2.2 *In Vivo* and *In Vitro* (Cell Free) Protein Expression

*In vivo* protein expression process refers to protein synthesis in cells, which is already discussed in above section. A wealth of genetic and biochemical knowledge has been

accumulated both in prokaryotic cells (like E. *coli*) and in eukaryotic cells (like insect cells and mammalian cells). Several companies provide commercial cloning and protein expression kit with improved protein expression level and simplified protocols. However, there are still some drawbacks, including tedious labor in transfection, cell culturing and cell lysing, instability of mRNA and expressed protein, improper folding, and the aggregation or degradation of the protein products in the cell. In addition, it is impossible to synthesize proteins which are un-natural or toxic for the host cells.

*In vitro* or cell free protein synthesis is an attractive alternation of *in vivo* protein expression. As early as in 1950s, several groups independently demonstrated protein biosynthesis machinery can work in absence of cell integrity. The limitation of the first generation cell-free expression system based on crude cell extract is the short lift time, and as a consequence, low productivity. The first cell-free protein synthesis system was prepared from extracts of rat liver cells.[80] Later on, several E. *coli* extract systems were developed for translation.[81, 82] In 1970s, cell-free systems for translation of mRNA were made using wheat germ extract [83]and rabbit reticulocyte lysate.[84] The final yields of these original systems are relative poor, though the produced proteins have good biological activities. The limitation comes from two facts: one is the rapid depletion of high energy phosphate pool; the other is the accumulation of the byproducts during the protein synthesis that inhibit the reaction. In 1988, Spirin et al overcame the bottleneck of the *in vitro* protein synthesis system by demonstrating a continuous flow system to continuously supply the consumable substrates and remove the byproducts.[85] Following this work, several groups used different reagents exchange scheme to produce hundreds to thousands of microgram of proteins per milliliter of expression solution.[85-92] After testing the production of various function proteins (enzyme, antibody, hormone, etc) in

more than 40 laboratories, Roche introduced a Rapid Translation System (RTS) in 2001.[93] Theoretically, a cell-free protein synthesis could be prepared from any cell type. However, commercialized expression systems are based on E. *coli*, wheat germ and rabbit reticulocyte. These systems will be summarized in chapter 2.

Compared with *in vivo* protein expression system, the main advantages and potential application of cell free protein synthesis systems include:

1 Absence of the cell membrane eliminates steps associated with introducing DNA into cells, lysing cells and clearing lysate. More purified protein can be easily obtained.

2 Being compatible with the miniaturized and automated instrument, which can fulfill the high-throughput protein expression requirement in protein engineering and proteomic area.

3 The composition of the reaction mixture can be easily modified to favor post translational modification and protein folding.

4 The non-natural and chemically modified amino acids can be cooperated into the protein, which provides the possibility of protein engineering, protein function research and pharmaceutical studies.

5 The cytotoxic proteins and unstable or low expressed proteins can be obtained.

6 The procedure is extreme faster, making it highly suited for screening expression templates and conditions.

### 1.3 *In Vitro* Protein Expression on a Microchip

Cell-free mRNA translation in a microfabricated reactor made from a silicon wafer was first reported in 2000 by Hosokawa et al.[94] Polyphenylalanine, coded by polyuridylic acid, is synthesized by pumping two reactants into two inlets and mixing them through a T-shaped or H-shaped microchannel. The resulting product was collected from the outlet using a filter paper and then analyzed off the device by radioisotope assay. This work demonstrated the feasibility to implement cell-free transcription in a microfluidic device, though it showed only a polypeptide elongation step. Soon later, Nojima et al. showed the natural protein synthesis using the same device by cell-free translation of bacteriophage MS2 RNA.[95] The key drawback of this

device is the use of excessive accessories including external pumps and valves, and the lack of integration, making it difficult to be implemented in a high-throughput format.

Later on, an integrated PDMS-glass hybrid microreactor array was developed for *in vitro* protein synthesis by Yamamoto et al.[96] The microreactor array consisted of a reaction chip and a temperature control chip. The reaction chip composed of reaction chambers, flow channels and inlet/outlet reservoirs, is fabricated by casting PDMS replica on a silicon mold master, and then PDMS is bonded with a thin layer of PDMS to form closed chambers and channels. While the temperature control sensors are patterned on a glass chip through conventional photolithography. The microreactor array was aligned and bonded by placing the temperature control chip on bottom of the reaction chip. In our study, the performance of the microreactor array for *in vitro* protein synthesis was demonstrated by using DNA templates of Green Fluorescent Protein (GFP) and Blue Fluorescent Protein (BFP) in E. *coli* extract. The functional activity of GFP and BFP collected in the outlet reservoirs was successfully measured by the UV trans-illuminator. One limitation of this device is that the device was fabricated on a silicon wafer or a glass using traditional MEMS technology. Each device has to be fabricated individually, costing time and resources.

*In vitro* protein synthesis has also been demonstrated in the microplate format. Tabuchi et al. first reported a PMMA microchip was developed for cell-free protein synthesis in 2002.[97] The microchip was made by injection molding, with wells of 3 mm in diameter and 1 mm in depth. The synthesis of adipose-type fatty acid binding protein (A-FABP) was investigated on this microchip and the product was detected using Western blotting. Two years later, Angenendt et al. accomplished protein synthesis in microfabricated glass nanowell chip with submicroliter volumes, demonstrating enhanced throughput of protein production with reduced reagents.[68]

Two Proteins were synthesized on a chip with the coding genes of wt-GFP and β-galactosidase using E. *coli* extract. The biological activity of GFP and β-galactosidase was confirmed by a highly sensitive laser scanner with an excitation of 488 nm and an emission of 535 nm. Meanwhile, a microchamber array was fabricated using PDMS for *in vitro* protein synthesis by Kinpara et al.[98] The dimension of the chambers is about 100 (L) X 100(W) X 15 (D) μm, and the volume is about 150 pL. Polymer beads with immobilized GFP gene coding sequence were added to microchamber and mixed with E. *coli* extract. The expression of GFP was detected by fluorescence using an optical microscope.

In recent years, many research groups have attempted to perform *in vitro* protein synthesis on a microchip, but they only carry it out using either E. *coli* extract or rabbit reticulocyte lysate on one chip. In our study, we developed expression of three proteins in both E. *coli* extract and rabbit reticulocyte lysate on a plastic microwells chip by direct micromilling, and used the response pattern of an array for identification of two toxin simulants.[99] Miniaturized array format of *in vitro* protein synthesis suggests that it is possible to have high-throughput protein synthesis in microsacle from a DNA library. It has advantage of less reaction solution and low-cost. However, cell-free protein synthesis on a microchip usually stopped within 2 h, due to lack of substrate or inhibitory by accumulated by products. Therefore, the productivity of protein synthesis is poor on such a microchip.

### 1.4 Literature Review and Current Challenges

The challenge of BioMEMS is to integrate different components such as mciropumps and valves for mixing, purification and separation, and on-line detection on a single chip. In a miniaturized protein synthesis and analysis device, more challenges exist in performing fast, high-throughput and low cost synthesis, and sensitive assay. In addition, the poor productivity of *in vitro* protein synthesis limits the downstream applications because large amount of proteins

are required for traditional protein analysis. In 1988, large scale cell-free protein translation system using continuous flow mechanism was first reported by Spirin et al..[85] This system improved the production yield due to the extended duration of protein synthesis. It has been demonstrated that the duration time for protein synthesis can be 20-40 hours in E. *coli* and wheat germ extract, resulting in a significant increase in the final amount of product. However, the setup is bulky because it requires a peristaltic pump or HPLC pump, and the system is very complicated.

Later, simplified continuous exchange systems were reported by independent research groups using a dialysis bag or a flat dialysis membrane. For example, Kim and Choi developed the continuous exchange system that employed a dialysis membrane for large scale cell-free protein synthesis.[88] As shown in Figure 1-4, the reaction chamber was attached with a dialysis membrane at the bottom, and the chamber was immersed into a feeding solution containing all small molecular-weight substrate required for energy regeneration. Although the details of the membrane and the size of the chambers were not given, authors reported the synthesis of CAT protein can continue for up to 14 hours in this reactor. Continuous-exchange cell-free (CECF) systems proved to be so attractive that CECF instrument have developed Roche Diagnostic.[93]

However, there are very limited numbers of reports about protein synthesis in miniaturized devices using flow mechanism. As mentioned above, Hosokawa et al. first fabricated a simple T-shape and H-shape glass-silicon mixers to test cell-free translation of poly (U), which is not a functional protein.[94] Recently, a compartmentalized cell-free protein expression device was fabricated from PDMS to generate water-in-oil emulsion droplet as shown in Figure 1-5.[65] In this device, cell-free translation/transcription reaction solutions and red-shift GFP (rs-GFP) DNA template were pumped into two inlets in the Y-shape microchannel. At the cross-section of Y-

shaped inlets, a side channel was used to provide a carrier liquid. Discrete liquid droplets were compartmentalized to mimic an artificial cell by mineral oil as a carrier liquid and *in vitro* protein synthesis was carried out inside the liquid droplets. In the microfluidic channel, the formation of emulsion droplets may prevent the reagents from contacting with the microchannel wall and decrease dispersion during the transportation. However, the main problem for this experiment is that a heater is necessary to provide a temperature control for each droplet to obtain the detectable amount of synthesized red shift-GFP. Secondly, the microchannels must maintain hydrophobic surface to ensure the formation of emulsion droplets. Rough channel surface could also induce the fusion of individual emulsion droplet.

Recently, Hahn et al. published a short report and investigated a continuous-exchange cell-free protein synthesis system on a PDMS-based chip.[100] Expression of bacterial chloramphenicol acetyltransferase (CAT) was demostrated in this chip and the duration time for reaction is up to 16 h. But no detail information was further discussed, such as the size of reaction chamber, the effects of temperature and flow mechanism.

In our study, we considered easy and simplicity of device fabrication. Plastics are cheap and the devices can be disposable. Hence we chose PMMA and PC for this research work. Two different types of microfluidic devices were designed for *in vitro* protein synthesis. One is designed in a well-in-well array format employing a porous membrane to facilitate passive diffusion. The other is designed to contain three-dimension ridge structures in the bottom of microchannels to enhance mixing and reaction yield.

### 1.5 Objective and Organization of This Dissertation

Detection and identification of toxic agents are important for medical diagnostics, food/water safety testing, and biological warfare defense. One way to detect them is to use recombinant technology to engineer cytoplasmic or cell surface receptors for regulated or

specific changes in an organism after binding with an agent. An example is ricin, a plant toxin that is listed as one of potential warfare agents and known to be lethal by blocking protein synthesis in many cells of the human body.

The objective of this work is to fabricate a miniaturized high-yield protein expression system for detecting toxins. The detection method we proposed to explore is toxin's inhibition of protein expression (synthesis), which is one of action mechanisms toxin use to cause toxin effects. Biological synthesis of proteins typically take places in cells but it is challenging to use it directly as a sensor due to its slow process and maintenance requirement such as continuous supply of nutrients. To address them, we developed miniaturized devices that are composed of an array of units; each unit consists of a reaction chamber for protein expression and a feeding chamber for nutrient supply and byproduct removal. Different *in vitro* protein expression systems are evaluated in the device. This device has also demonstrated for screening anti-biotic inhibitors and ultra-fast ricin detection.

The significance of this work mainly lies in three aspects. First, the approach will provide a unique method to detect both known and new toxins. With the increasing ability to modify and engineer potential toxins, the ability to detect toxic agents that have not been identified or fingerprinted has become more important. To our knowledge, this new sensing principle using protein inhibition has not been studied. Second, the multiplexed IVT system offers a means for high-throughput protein expression that is needed by life sciences. As more and more new genes are being identified, there is a considerable need to determine the function and properties of the proteins these genes encode. Third, this study will also advance the field of microfluidics, bring forward sensor technology, and assist in understanding nanoliter-scale cellular reactions.

The rest of this dissertation is outlined as follows.

In chapter 2, different *in vitro* protein expression systems are evaluated in the miniaturized device consisting of an array of reaction chambers. As a proof of the concept for toxin detection, the expression yields of different proteins are measured in presence of antibiotic inhibitors.

In chapter 3, the performances of protein synthesis in the static and the continuous exchange reaction chamber are compared. Ultra fast and sensitive detection of a toxin, ricin, is employed as an example of the application of the continuous exchange protein synthesis device.

In chapter 4, microfluidic reactors are designed and fabricated to demonstrate enzymatic reactions. Bioluminescence produced by reaction of luciferase-luciferin was detected by a cooled CCD camera. Diffusion-based mixing and chaotic induced mixing in the microfluidic device was investigated and compared. The possibility of using such a microfluidic device for continuous flow protein expression will be discussed.

In chapter 5, the conclusion and future work will be described.

Table 1-1. RNA codon table

| First Position | Second Position | | | | Third Porsition |
|---|---|---|---|---|---|
| | U | C | A | G | |
| U | phenylalanine | serine | tyrosine | cysteine | U |
| | | | | | C |
| | leucine | | stop | stop | A |
| | | | stop | tryptophan | G |
| C | leucine | proline | histidine | | U |
| | | | | arginine | C |
| | | | glutamine | | A |
| | | | | | G |
| A | isoleucine | threonine | asparagine | serine | U |
| | | | | | C |
| | | | lysine | arginine | A |
| | * methionine | | | | G |
| G | valine | alanine | Aspartic acid | glycine | U |
| | | | | | C |
| | | | Glutanic acid | | A |
| | | | | | G |

* Start codon.

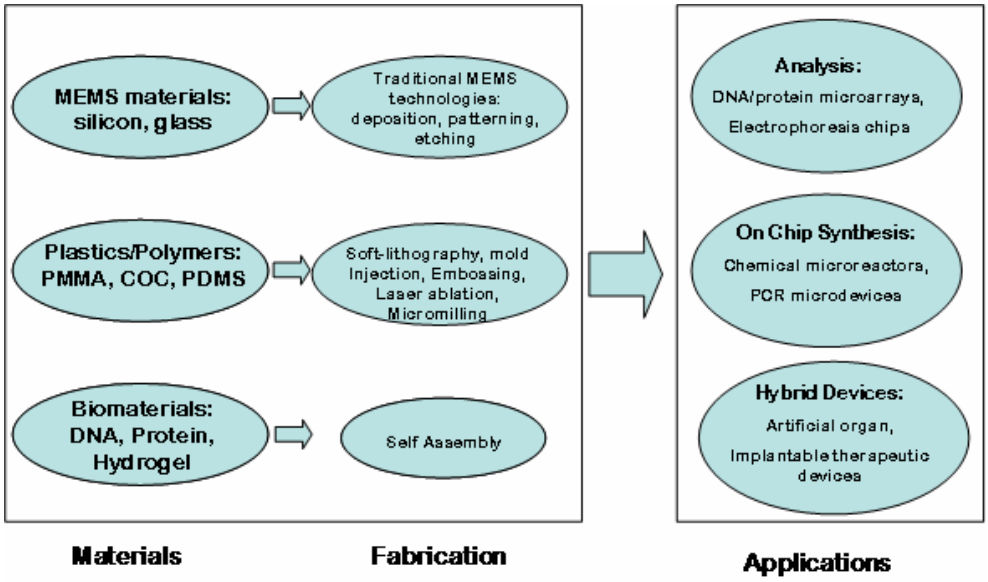


Figure 1-1. Materials, fabrication and applications of BioMEMS devices.

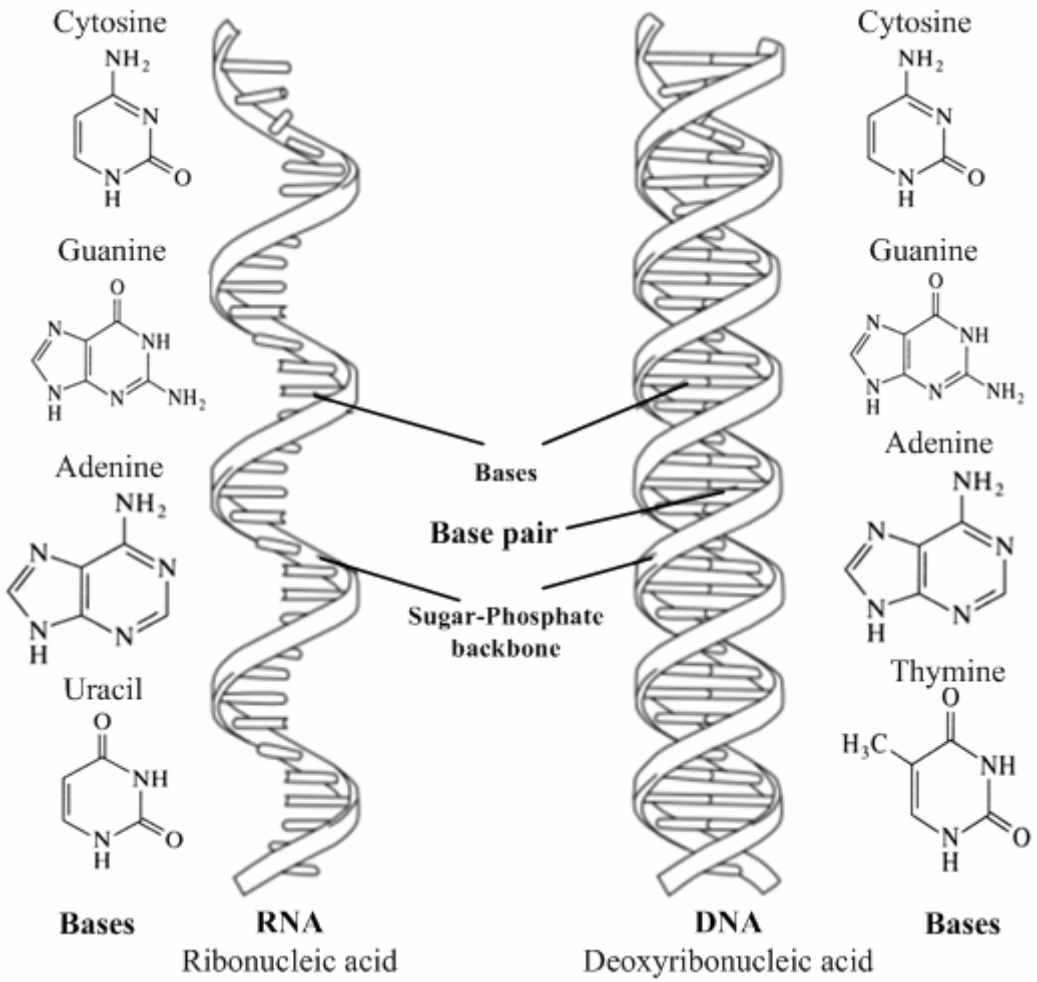


Figure 1-2. Structure of DNA and RNA.

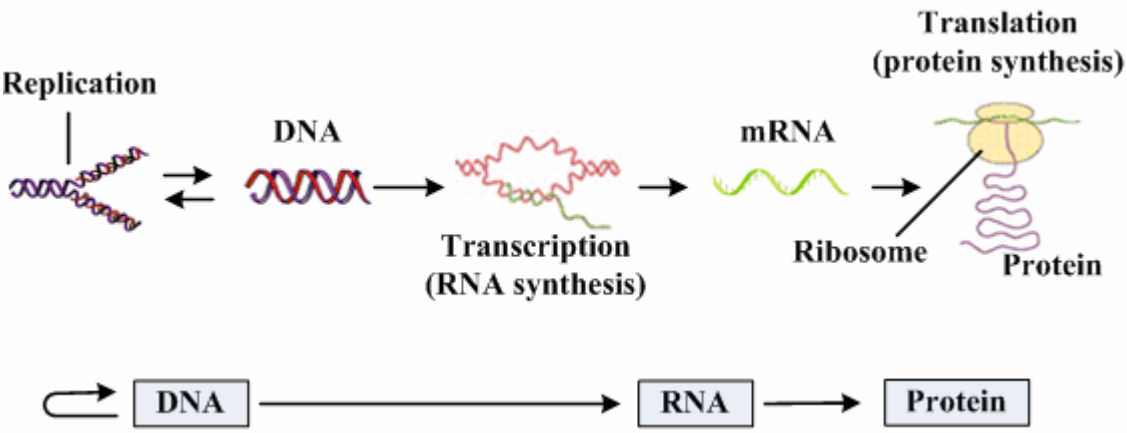


Figure 1-3. The central dogma of molecular biology.

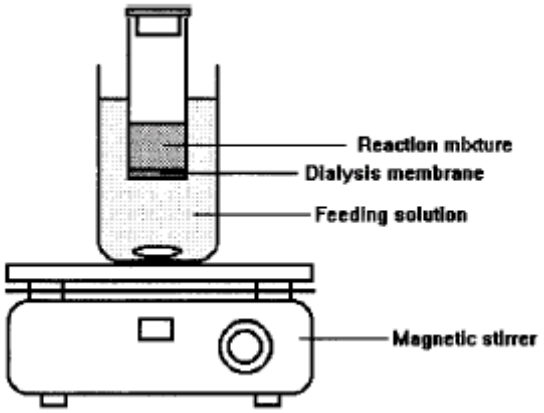


Figure 1-4. Schematic diagram of the continuous exchange of cell-free system, adapted from Kim and Choi.[88]

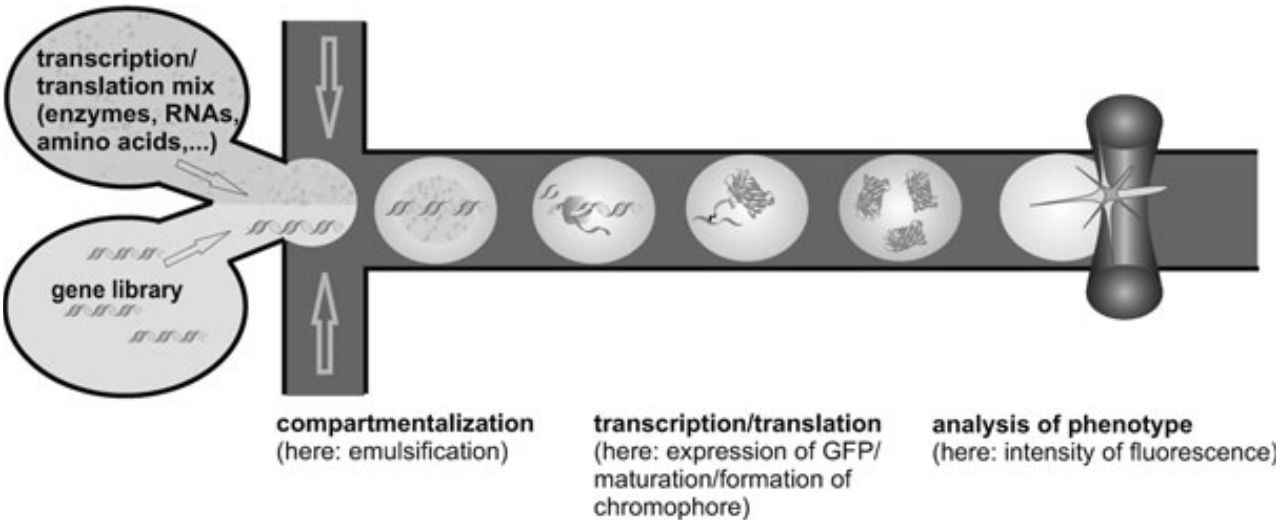


Figure 1-5. Schematic of *in vitro* red-shift GFP synthesis using emulsion droplets in microcrofluidic PDMS device by Dittrich et al.[65]

# CHAPTER 2
# *IN VITRO* PROTEIN EXPRESSION IN A MICROWELL DEVICE AND ITS USE FOR TOXIN DETECTION[1]

## 2.1 Introduction

Biological synthesis of a protein includes the steps of gene transcription and protein translation, which are typically carried out in host cells such as *Escherichia coli.* Although it is prevalent among academic and industrial labs, *E. coli*-based recombinant protein production has inherent limitations including formation of insoluble protein aggregates (inclusion bodies), degradation of proteins by intracellular proteases, low or no expression for the genes whose products are toxic to the host cell, and lack of post-translational modification.[101-103] To address some of these challenges, a few eukaryotic systems have been developed using *Saccharomyces cerevisiae*, insect or mammalian cells. In addition, cell-free protein synthesis, a process called *in vitro* transcription and translation (IVT), has been developed.[104-112] In IVT systems, a DNA template consisting of a coding sequence is transcribed into messenger RNA, either eukaryotic or prokaryotic lysate is then exploited to provide ribosome and additional components necessary for protein translation. The expression system may also be reconstituted from purified recombinant elements.[113, 114] IVT has been demonstrated for various applications, including in situ immobilization of expressed proteins onto solid surfaces,[66, 115] synthesis of drug transporters [116], polypeptide display,[117] gene expression,[118] and high-throughput screening.[119]

High-throughput protein production in an array format is desirable for genomics and proteomics. Completion of mapping the human genome has prompted strong interest in identifying the functions of newly discovered genes and the proteins encoded therein. To match high-throughput gene discovery, methods to produce a large number of proteins in parallel are

[1] A part of this chapter has been published in (99) Mei, Q.; Fredrickson, C. K.; Jin, S.; Fan, Z. H. *Anal Chem* **2005**, *77*, 5494-5500.

needed. *In vitro* protein expression has also been implemented in miniaturized devices[68, 95, 97, 98, 118, 120, 121] because miniaturization of analytical instruments has been one of major developments in the past decades.

In this chapter, we describe a device consisting of an array of miniaturized wells. The device was used for *in vitro* expression of three proteins, including green fluorescent protein (GFP), chloramphenicol acetyl-transferase (CAT), and luciferase. Two expression systems were used: a prokaryotic and a eukaryotic system. Differential inhibitory effects of two toxin simulants, tetracycline (TC) and cycloheximide (CH), on the protein expression yield were observed, providing a unique response pattern of the array device for each toxin. In addition, the quantitative relationship between the yield of expressed proteins and the amount of a toxin provide a calibration curves, leading to true analysis.

## 2.2 Background

*In vitro* protein synthesis systems are based on the cellular protein synthesis machinery to perform protein synthesis outside intact cells, and are divided into two types: prokaryotic and eukaryotic expression system. *In vitro* protein synthesis systems can be carried out either in a coupled manner, which requires an exogenous DNA as a template, or as an uncoupled system, in which messenger RNA (mRNA) is used as a template. Here we will focus on the coupled transcription-translation system (IVT).

### 2.2.1 Prokaryotic IVT System

The most commonly used prokaryotic system is derived from *Escherichia coli* lysate, including all the necessary enzymes and machinery for translation.[122] After two groups (Zubay; Gold and Scheiger) independently achieved some major improvements,[106-112] IVT has been widely used. The principal components of Zubay and Gold-Schweiger system are listed in Table 2-1. The major difference between them is Zubay's system contains 30,000 g centrifugation

supernatant (S30) *E. coli* lysate depleted of endogenous RNA and DNA, while Gold-Schweiger system is based on the ribosome-free and nucleic acid deprived of S100 fraction. In both systems, they contain an endogenous or phage T7 RNA polymerase, which transcribes mRNA from an exogenous DNA template. This RNA molecule is then used as template for translation. The DNA template may be either a gene cloned into a plasmid vector or a PCR amplified template. A ribosome binding site (RBS) is required for template translated in prokaryotic systems. During transcription, the 5' end of the mRNA becomes available for ribosome bind and translation initiation, allowing transcription and translation to occur simultaneously.

### 2.2.2 Eukaryotic IVT System

Eukaryotic IVT systems, such as rabbit reticulocyte lysate and wheat germ extract, are prepared from the cytoplasmic fraction. However, they lack endogenous RNA polymerase activity because the process of transcription only takes place in the nuclei of the cell, while protein synthesis is carried out in the cytoplasm of the cell, which is the major difference between the prokaryotic and eukaryotic cell. This limitation can be addressed by addition of an exogenous RNA polymerase. Purified *E. coli* RNA polymerase was first used to couple transcription and translation in eukaryotic IVT systems.[83, 123-126] Bacteriophage T7, T3 and SP6 RNA polymerases were then isolated to use in IVT systems and they were introduced into eukaryotic system to produce mRNA, using DNA template with corresponding promoters[92, 127, 128] (Table 2-2).

### 2.2.3 Choice of IVT Systems

Although any organism could potentially be used as a source to prepare an *in vitro* protein synthesis system, *E. coli* lysate, rabbit reticulocyte lysate and wheat germ extract are widely used and commercially available.[64, 84, 93, 129-131] The choice of a synthesis system is based on the origin and biochemical nature of synthesized proteins and their downstream applications. Generally,

prokaryotic IVT systems can provide higher yields and are suitable for structural analysis. However, eukaryotic IVT systems can allow a better platform for functional studies, especially for post-translational proteins. The comparison of prokaryotic and eukaryotic systems is summarized in Table 2-3.

## 2.3 Experimental

### 2.3.1 Reagents and Materials

The RTS 100 *E. coli* HY kit, two expression vectors containing the genes encoding green fluorescent protein (GFP) and chloramphenicol acetyl-transferase (CAT), and anti-6xHis were obtained form Roche Diagnostics GmbH (Mannheim, Germany). TNT Quick Coupled Transcription/Translation system, T7 luciferase DNA vector, luciferase assay reagent, phMGFP vector, PCR Master mix, PCR clean-up kit, DNA marker and nuclease-free water were from Promega Corporation (Madison, WI). RNA transcription kit was bought from Stratagene (La Jolla, CA) and RNA quantitation kit was from Molecular Probes (Eugene, OR). Primers were synthesized from Integrated DNA technologies (Coralville, IA). Acrylamide-bisacrylamide (electrophoretic grade, 5% C), tetramethylethylenediamine, sodium dodecyl sulphate (SDS), ammonium persulfate, tris(hydroxymethyl)aminomethane (Tris), glycine, sodium chloride, glycerol, bromophenol blue, β-mercaptoethanol, Tween-20, tetracycline, and cycloheximide were purchased from Fisher Scientific (Atlanta, GA). Polyvinylidene difluoride (PVDF) membranes (0.2 μm), and filter papers were from Bio-Rad Laboratories (Hercule, CA). Molecular weight standards, biotinylated secondary antibody and streptavidin-alkaline phosphatase were from Amersham Biosciences (Piscataway, NJ), while recombinant Green Fluorescent Protein (rGFP) and rabbit anti-GFP polyclonal antibody were from BD Biosciences (Palo Alto, CA). The phosphatase staining solution (Bromo-chloro-indoryl phosphate/Nitro Blue Tetrazolium, BCIP/NBT) was obtained from KPL (Gaithersburg, MD).

### 2.3.2 Device Fabrication

Polymethyl methacrylate (PMMA) is widely used in bioMEMS device fabrication. Its excellent optical properties, very low fluorescence background, and compatibility with chemical or biological reagents make it as the first choice of the materials for microfluidic device. Moreover, the fabrication steps are straightforward and cheap. A miniaturized device with an array of 2x3 wells was designed and fabricated for demonstrating the toxin detection concept. Two of such devices in Figure 2-1 form an array of 3x4 wells, which is the format for demonstrating toxin detection as discussed below. The device was made from PMMA (Lucite International, Cordova, TN) and the wells were created by a milling machine (Flashcut CNC, Menlo Park, CA). The distances between wells (center to center) are 9 mm according to the standards for microplates defined by the Society for Biomolecular Screening and accepted by the American National Standards Institute. This arrangement conforms the device to the alignment of 96-well plates and ensures compatibility with a variety of commercial fluid dispensing systems and plate readers. The diameter and depth of each well are 2.7 mm and 2.3 mm, respectively, providing the total well volume of ~13 μL. This is about 25 times smaller than the wells in conventional 96-well microplates. The decrease in the well size will significantly reduce reagent consumption for high-throughput assays. After fabrication, the device was sterilized by exposing to UV light for 30 minutes that ensured the consistency of the protein expression.

### 2.3.3 DNA Template for Cell-Free Protein Synthesis

GFP vector (Figure 2-2a), CAT vector (Figure 2-2b) and luciferase vector (Figure 2-2c) were used as the templates for the plasmid-based cell-free protein synthesis. For the experiments using linear DNA template produced by PCR for cell-free protein synthesis, the coding region of mutant GFP was amplified from the plasmid phMGFP (Figure 2-2d) using the forward and

backward primers given in Table 2-4. To generate linear DNA template, PCR Master Mix containing Taq DNA polymerase, was reconstituted per the manufacturer's recommendations. A PCR tube with 50 µl of the prepared solution was placed in a PTC-100 programmable thermal controller (MJ Research, Waltham, MA). PCR amplification consisted of 25 cycles, in which denaturation (94 °C) and annealing (57 °C) steps were 45 s, and the extension step (72 °C) was 1 min. The PCR products were purified using PCR-clean up kit (as manual instruction) prior to their use for protein expression. The amount of PCR products was determined by agarose gel electrophoresis and spectrophotometry. To prepare gel, agarose was dissolved in tris-boric acid-EDTA (TBE) buffer solution and cast into a gel slab. When solidified, it was immersed in TBE buffer containing ethidium bromide dye. The PCR products were added to the sample wells in the slab, which was placed in the separation cell and voltage was then applied. When separation was completed, the gel was removed from the cell, de-stained and rinsed to remove excess ethidium bromide, and imaged using a UV transilluminator.

### 2.3.4 Cell-Free Protein Synthesis

For the prokaryotic expression system, 50 µL of RTS 100 reaction solution was composed of 12 µL *E. coli* lysate, 10 µL reaction mix (proprietary composition, supplied in the kit by the manufacturer), 12 µL amino acids without methionine, 1 µL methionine, 5 µL reconstitution buffer (proprietary composition, supplied in the kit by the manufacturer), and 10 µL nuclease-free water containing 1 µg GFP or CAT vector. The reaction solution was then incubated in a microcentrifuge tube at 30 °C for 4 hours. For GFP, the reaction solution was stored at 4 °C for additional 24 hours for the maturation of GFP.

For the eukaryotic expression system, rabbit reticulocyte lysate or wheat germ extract was used. The reaction mix of 50 µL for luciferase synthesis was prepared by combining 40 µL TNT Quick master mix (proprietary composition, supplied in the kit by the manufacturer), 1 µL

methionine, and 9 μL nuclease-free water containing 1 μg luciferase vector. Wheat germ reaction mixture for monster GFP synthesis consisted of the following components: 25 μL wheat germ extract, 2 μL reaction buffer, 1 μL T7 RNA polymerase, 1 μL of 1 mM amino acid, 1 μL Ribonulease inhibitor and 19 μL nuclease-free water containing 2 μg of linear MonsterPTMP GFP template or 1 μg of phMGFP vector. Incubation was performed in a microcentrifuge tube at 30 °C for 1.5 hours. In certain experiments, the transcription and translation reactions were implemented sequentially. The plasmid template or PCR-product was incubated in a transcription mixture and then supplemented with wheat germ extract to initiate the translation reaction.

### 2.3.5 Toxin Inhibition Assay

For the toxin inhibition assay in a microcentrifuge tube, a stock solution of tetracycline and that of cycloheximide were prepared at 15 μg/μL and 10 μg/μL, respectively. A series of amounts of tetracycline or cycloheximide were added into protein expression mixture. The concentrations of toxins used are listed in the figures or text. To save reagents and match with miniaturized devices, 8 μL of prokaryotic or eukaryotic expression solution was used, making the total volume of each inhibition assay at 10 μL. For each set of experiments, a positive control (without inhibitor) and a negative control (without the expression vector) have also been included.

When the protein expression and toxin inhibition assays were implemented in the miniaturized device, the volume of the reaction mixture was reduced to 6.5 μL. Films with pressure-sensitive adhesive, so-called “PCR tape” (3M, Minneapolis, MN), were used to seal the wells to prevent evaporation.

### 2.3.6 Detection

We used Western blot, fluorescence or luminescence for measuring the yield of protein expression, depending on the property of the proteins expressed. Detection of expressed WT-GFP and CAT was achieved using Western blot. A reaction product solution of 1 μL was mixed with 15 μL of gel-loading sample buffer, which contains 50 mM Tris-HCl, pH 6.8, 2% W/V SDS, 0.01% W/V bromophenol blue, 10% V/V glycerol, and 5% V/V 2-mercaptoethanol. The mixture was then separated in a 15% SDS-polyacrylamide gel in the Mini-Protean III Cell system (BioRad). After electrophoresis, the gel was removed from the glass plates and then equilibrated in the transfer buffer, which is comprised of 48 mM Tris, 39 mM glycine, and 20% V/V methanol. PVDF membrane was pre-soaked with methanol, followed by soaking in the transfer buffer for 1 hour. The Mini Trans-Blot system (BioRad) was set up with pre-wetted fiber pad, filter paper, gel, and PVDF membrane according to the instruction from the manufacturer. The cassette and ice-cooling unit were placed in the tank that was filled with the transfer buffer.

After blotting, the PVDF membrane was removed from the trans-blot apparatus and blocked with 5% w/v non-fat dried milk in Tris-buffered saline (TBS) solution (with 0.05% Tween-20) for 1 hour at room temperature. After being washed three times (5 minutes each time) with TBS solution, the membrane was incubated for 1 hour at room temperature with 1 μg/mL anti-GFP polyclonal antibody for GFP product or 0.3 μg/mL anti-6xHis monoclonal antibody for CAT product, respectively. At the end of conjugation, the membrane was washed three times and then incubated with 1.5 μg/mL biotinylated secondary antibody at room temperature for 1 hour. Upon completion of the incubation, the membrane was rinsed again with TBS solution for three times, followed by incubation at ambient temperature for 30 minutes with a solution of streptavidin-alkaline phosphatase (1:2000 dilution from the stock solution). After

being washed, the membrane was immersed in chromogenic substrate (BCIP/NBT) for 3 minutes, followed by rinsing with water (to stop reaction). Images of protein bands were acquired with a color laser scanner (Canon); proteins bands were quantified using ImageJ from the National Institute of Health.[132]

Detection of synthesized WT-GFP and Monster™ GFP was also carried out by Spex Fluorolog spectrofluorometer (Jobin Yvon Inc, Edison, NJ). The excitation spectrum of WT-GFP was scanned from 350 nm to 500 nm with emission wavelength at 550 nm; and the emission spectrum was scanned from 450 nm to 580 nm with excitation wavelength at 470 nm. The emission spectrum of Monster™ GFP was collected from 450 nm to 580 nm with excitation wavelength at 480 nm.

Detection of luciferase expressed by IVT was achieved by SIRIUS luminometer from Berthold (Pforzheim, Germany). The luminometer was programmed to have a two-second delay, followed by a five-second measurement of luciferase activity. The expression product of 2 μL was added to a luminometer tube containing 40 μL of luciferase assay reagent and mixed evenly. The tube was then placed in the luminometer; and the data were acquired.

## 2.4 Results and Discussion

### 2.4.1 Toxin Detection Scheme

Multiplexed sensor array is a unique approach to obtain the fingerprint of a new agent. The concept of the sensor array for detecting toxins using IVT is illustrated in Figure 2-3. The device consists of an array of IVT wells; each well is designed to express one protein and thus functions as a sensor. The number of IVT sensors can be as high as 96 or its integral multiples, in the format of traditional microplates and can be easily adapted to commercial plate readers. Multiple wells (e.g., 3x4 wells circumscribed within the dashed lines and shadowed with diagonal lines) form one set, in which the top row is for the positive controls to express each of

three proteins, the second row for the negative controls, and the third and fourth rows are for the sample, allowing one repeat to enhance the precision. Use of the positive and negative controls and comparison of the signal from the sample wells with those in the control wells will reduce false positives and negatives. The set will express a group (three in this case) of pre-characterized proteins in different expression systems; the proteins and expression systems will be judiciously selected so that protein synthesis in each well is inhibited or affected differentially by different type of toxins. Therefore the unique response pattern (or signature) of a toxin due to different inhibitory effects will be registered and used as a tool for detection and identification. New agents will be identified by comparing the response pattern with signatures of known agents in a pre-acquired database. In the particular format illustrated, the rest of wells in the 96-well array can be designed to detect additional seven types of toxins if 12-well set is proved to be enough for the identification.

### 2.4.2 Plasmid-based Protein Expression

To demonstrate the concept of toxin detection by protein expression, we first synthesized three proteins in two types of expression systems. The first protein is wide type green fluorescent protein (WT-GFP), a widely-used fluorescent molecule with known DNA sequence and crystal structure.[133] Protein expression was carried out by using an expression vector as a DNA template, which consists of GFP coding sequence and the necessary regulatory elements including T7-RNA polymerase promoter, ribosome binding site, start codon, stop codon, and T7 terminator. The expression vector was mixed with *E. coli* lysate and a reaction mix consisting of T7-RNA polymerase, nucleotides, amino acids, and other reagents. WT-GFP product was confirmed by Western blotting and fluorescence spectrometry. The result of Western blotting is shown in Figure 2-4a. A clear band in lane 4 indicates the presence of WT-GFP in the expression product. According to pre-stained protein markers, the molecular weight of WT-GFP

expressed is estimated ~31 KD. Expressed WT-GFP contains a stretch of additional six histidines (6xHis) at its C-terminal, causing its molecular weight slightly larger than recombinant GFP (rGFP) purchased commercially. The negative control in the experiment contains all reagents except for the expression vector. The WT-GFP expression also can be quantified by fluorescence spectrometry. When it was excited with 488 nm light, the excitation and emission spectra of synthesized WT-GFP were shown in Figure 2-4b, indicating the synthesized WT-GFP folds properly and has biological activity.

The second protein is chloramphenicol acetyl-transferase (CAT), an enzyme responsible for bacterial resistance to an antibiotic drug, chloramphenicol. CAT was expressed in the same *E. coli* expression system; success of the protein expression was also confirmed using Western blot as shown in Figure 2-4c. According to pre-stained protein markers, the molecular weight of CAT expressed is estimated ~26 KD, which agrees with the value reported in the literature. The third protein is luciferase, an enzyme from firefly tails that catalyzes the production of light in the presence of luciferin , adenosine triphosphate (ATP), molecular oxygen and $Mg^{2+}$. Synthesis of luciferase was carried out using rabbit reticulocyte expression system as described in the experimental section. Detection of the expression product was achieved by monitoring the intensity of luminescence after mixing 2 μL of the product with luciferin , ATP, $O_2$ and $Mg^{2+}$. As shown in Figure 2-4d, the luminescence signal of the product is 5 orders of magnitude higher than that of the negative control.

### 2.4.3 Linear DNA Template-based Protein Expression

The WT-GFP gene originally cloned from *Montastrea cavernosa* can be expressed into the protein which tends to photobleach and is very dim. In addition, the correct folding of WT-GFP requires three distinct physical processes: the attainment of the correct three-dimensional structure, cyclization of the chromophore, and oxidation of the cyclized intermediate.[134] So the

folding of WT-GFP can not complete during transcription/translation in a cell-free system and it takes addition time to have biological activity. The mutants of GFP which have brighter fluorescence and fold more efficiently at 37 °C were developed, such as Monster$^{TM}$ GFP, enhanced GFP, blue fluorescent protein and yellow fluorescent protein. Monster$^{TM}$ GFP can produce fluoresces at least 20% brighter than other commercially available GFPs and the spectral properties of the Monster$^{TM}$ GFP are also slightly red-shifted. Peak excitation occurs at 505 nm, with a shoulder at 480 nm, and the peak emission occurs at 515 nm.

Monster$^{TM}$ GFP coding sequence was first amplified from phMGFP vector by PCR with corresponding primer. PCR products were purified by a PCR clean-up system and confirmed by the agarose gel electrophoresis (Figure 2-5). The results indicated that the length of PCR products is about 1190 bp, as same as we designed. The synthesized Monster$^{TM}$ GFP from PCR-amplified DNA or the vector using coupled transcription and translation synthesis was confirmed by fluorescent spectrometry (Figure 2-6). The excitation and emission spectra of the synthesized Monster$^{TM}$ GFP are consistent with those reported by Promega. The results also showed that the protein yield expressed from plasmid is higher than that from PCR amplified DNA, because the linear DNA are easily degraded by the endogenous nucleases, thus, the amount of mRNA molecules is limited. Unfortunately, the expression of Monster$^{TM}$ GFP can not be reproduced. Then PCR products were first transcripted to mRNA and then mRNA molecules were translated to protein but protein can not be detected by fluorescent spectrometry. The reasons may include: (1) the amount of expressed Monster$^{TM}$ GFP is too low to be detected using fluorescent spectrometry; (2) no Monster$^{TM}$ GFP was expressed due to rapid degradation of mRNA, thus terminates the translational reaction quickly.

### 2.4.4 Reaction Temperature

All of the protein expression experiments discussed above take place at the ambient temperature. For commercial RTS instruments from Roche, the recommended operation temperature is 30 $^{o}$C. As a result, we studied the effect of the reaction temperature on protein synthesis in microcentrifuge tubes. Temperature control is achieved by placing the tubes in a PCR machine. Figure 2-7a shows the Western blot image of GFP synthesized at room temperature and at 30 $^{o}$C. The GFP expression yield at room temperature is about 97% of that at 30 $^{o}$C, as shown in the quantitative illustration in Figure 2-7b. This result suggests that the GFP expression at room temperature is comparable to that at 30 $^{o}$C and it is not necessary to integrate a heater in the array device.

### 2.4.5 Inhibitory Effects of Toxins on Protein Synthesis

To illustrate the detection of toxins, we used tetracycline (TC) and cycloheximide (CH) as toxin simulants to study their inhibitory effects on protein expression. TC is an antibiotic substance produced by *Streptomyces* species.[135] It acts only on prokaryotic cells and it blocks binding of aminoaceyl-transfer RNA to A-site of ribosomes.[136] CH acts specifically on eukaryotic cells and it inhibits the activity of peptidyl transferase, an enzyme needed in the translocation reaction on ribosomes. Figure 2-8 shows the effects of a series of concentrations of TC or CH on the expression yields of GFP, CAT, and luciferase synthesized in two protein expression systems. As illustrated in Figure 2-8a, GFP synthesis was completely inhibited when 3000 ng/μL of TC was used. Partial inhibition was observed when a series of lower concentrations (300 ng/μL to 0.3 ng/μL) of TC was added. The experiment also included the positive control, in which no inhibitor (TC) was added. The negative control contained no expression vector, thus representing the background signal. These results suggest that a

qualitative and quantitative relationship exists between the expression yield and toxin amount, a critical figure of merit for a sensor.

The comparison between TC and CH for GFP production in the *E. coli* expression system is shown in Figure 2-8b and 2-8c. The expression yield for each protein was normalized against the expression yield of the positive control (without toxin), so that it is easier to compare the toxic effects. The results clearly indicate that TC has inhibitory effect on GFP production and the degree of inhibition is proportional to the amount of TC in the sample, whereas CH has a negligible effect on the yield of GFP production and the level of minor inhibition remained the same in the range of amount of TC we used. These results suggest that the differential inhibitory effects of a toxin on the expression of different proteins are possibly used for toxin detection.

Figure 2-8d and 2-8e exhibit similar disparity between TC and CH for CAT production in the *E. coli* expression system. Again, TC has inhibitory effect on CAT production and the degree of inhibition is proportional to the amount of TC in the sample, whereas CH has a negligible effect on the yield of CAT production and the level of minor inhibition remained essentially same in the range of amount of TC we used. Furthermore, comparison of Figure 2-8b and 2-8d indicates that although TC has inhibitory effect on both GFP and CAT production, the degree of inhibition per unit amount of TC differs between these two proteins, evident from the difference in the slopes of respective linear regression lines. These results further suggest that each toxin's differential inhibitory effects on expression of different protein can be used as a signature for toxin detection and identification.

The comparison between TC and CH for luciferase production in rabbit reticulocyte expression system is shown in Figure 2-8f and 2-8g. An opposite effect was observed; TC has a negligible effect on the luciferase production in the eukaryotic expression system, whereas CH

has a significant inhibitory effect and the degree of inhibition is proportional to the amount of CH present in the sample. The result indicates that different expression systems can be used to expand the variability, so that a unique response pattern can be obtained for toxin detection by using a set of proteins produced in different expression systems.

These results are significant because they indicate not only the feasibility of the concept of toxin detection presented in this work, but also the possibility of using IVT assay for high-throughput screening of drug candidates. We confirmed differential inhibitory effects of antibiotic inhibitors such as TC and CH on protein expression *in vitro*, in a way very similar to their effects on protein expression *in vivo*.[137] Therefore, an IVT array device may provide a great platform for searching for the best antibiotic drug candidates.

### 2.4.6 Miniaturized IVT Array

After the feasibility of toxin detection using protein expression is demonstrated in microcentrifuge tubes, we attempted IVT and toxin detection in a miniaturized well device. The design of the experiments was the same as in the shadowed area of the 96-well array in Figure 2-3, in which a set of 3x4 wells is assigned for detecting one toxin. Two of the 2x3 well devices in Figure 2-1 were combined to form a 3x4 well device. As illustrated in Figure 2-3, the first row of 3 wells was used as the positive control, expressing GFP and CAT vector in the *E. coli* expression system and luciferase vector in the rabbit reticulocyte expression system. These wells were free of toxins. The second row of 3 wells was used as the negative control without DNA vectors added. The third and forth rows of 3 wells were added with a certain amount of a toxin stimulant, either CH or TC, into the protein expression system. Figure 2-9a shows the response pattern of the IVT sensor array when 25 ng of TC was used whereas the response pattern of the same IVT array for 17 ng of CH is illustrated in Figure 2-9b. Although there is slight difference between two sample repeats for rows 3 and 4 for each toxin, the response pattern is reproducible

as expected. The significant difference in the response patterns between CH and TC clearly indicates that it is feasible to use IVT sensor array to detect and identify toxins.

Although we used Western blot and luminescence detection to monitor protein production in this concept demonstration, it should be feasible to use a common method for toxin detection. One of such methods is to use GFP as an indicator for the detection of protein expression due to its green fluorescence. GFP has been used for visualization, tracking, and quantification of a variety of proteins in cells after they are fused together.[133] An increase of fluorescence signal in an IVT well will indicate the production of GFP or GFP-fused proteins. Quantitative information may be obtained by comparing the fluorescence signals of sample wells and of reference wells, which include both positive and negative controls in the array device. Any variation or adverse effects will be cancelled out between control and sample wells. The magnitude of the signal can be correlated to the amount of proteins produced in the device. Indeed, we used a fluorescence spectrometer to confirm the production of GFP expressed as mentioned above. However, we did not use it for CAT and luciferase because we have not yet expressed them by fusion with GFP.

Rather than using GFP, we may also design the expression vector containing a coding sequence for expressing an additional stretch of six histidines (6xHis) at the C-terminal of the protein of interest. Many proteins produced by recombinant techniques are designed to contain a 6xHis tag, so that they can be purified through interactions between 6xHis tags and Ni-nitrilotriacetate chromatographic columns.[138, 139] Both GFP and CAT proteins produced in this work contain 6xHis tag, even though we did not need the purification step. A variety of biological assays are available for detecting the amount of 6xHis tag fused with a protein. There are many other tags that may be fused with proteins as reviewed in the literature.[138] In addition,

luminescence detection can also be used by fusing luciferase with proteins of interest, as demonstrated in the present report.

## 2.5 Conclusions

A novel concept for toxin detection is presented based on toxin's inhibition of biological protein synthesis—in the step of either DNA transcription or protein translation. We demonstrated the feasibility of the concept by (1) *in vitro* expression of four proteins either from plasmid or linear template, including wide type green fluorescent protein, chloramphenicol acetyl-transferase, luciferase, and Monster$^{TM}$ GFP; (2) confirming differential inhibitory effects of two toxin simulants, tetracycline and cycloheximide, on the expression yields of these proteins in either prokaryotic or eukaryotic expression system; (3) obtaining unique response pattern (or signature) of the 3x4 IVT array device for each toxin simulant.

Table 2-1. Principal composition of prokaryotic IVT systems.[122]

| Zubay's system | Gold-Schweiger |
|---|---|
| S30 of *E. coli* containing RNA polymerase, ribosomes, tRNAs, ARSes, and translation factors | S100 of *E. coli* containing RNA polymerase, ARSes and translation factor |
| Amino acids | ribosome |
| ATP, GTP, UTP and CTP | ATP, GTP, UTP and CTP |
| Energy regenerating system: PEP+PK, or CP+CK | Energy regenerating system: PEP+PK, or CP+CK |
| Sulfhydryl compounds: ME or DTT | Amino acids |
| cAMP | Total tRNA |
| Salts: $Mg^{2+}$, $Ca^{2+}$, $K^{+}$ and $NH_4^{+}$ | Sulfhydryl compounds: ME or DTT |
| DNA template | Salts: $Mg^{2+}$, $Ca^{2+}$, $K^{+}$ and $NH_4^{+}$ |
| | DNA template |

Abbreviation: ARSes, aminoacyl-tRNA synthetases; PEP, phophoenal pyruvate; PK, pyruvate kinase; CP, creatine phosphate; CK, creatine kinase; ME, mercaptoethanol; DTT, dithiotreitol

Table 2-2. Pricinpal composition of eukaryotic IVT systems.[122]

| Rabbit reticulocyte lysate | Wheat germ extract |
|---|---|
| Lysate containing ribosomes, tRNAs, ARSes, and translation factors | Extract containing ribosomes, tRNAs, ARSes, and translation factors |
| SP6,T3 or T7 RNA polymerase | SP6,T3 and T7 RNA polymerase |
| Amino acids | Amino acids |
| ATP, GTP, UTP and CTP | ATP, GTP, UTP and CTP |
| Energy regenerating system: CP+CK | Energy regenerating system: CP+CK |
| Sulfhydryl compounds: DTT | Sulfhydryl compounds: DTT |
| $Mg^{2+}$, $K^{+}$ and polyamine | $Mg^{2+}$, $Ca^{2+}$, $K^{+}$ and polyamine |
| Hemin, glutathione and cAMP | DNA template with SP6, T3, or T7 promoter |
| DNA template with SP6, T3, or T7 promoter | |

Table 2-3. Prokaryotic versus eukaryotic IVT systems.[102]

| | Prokaryotic | Eukaryotic |
|---|---|---|
| Ribosomes | 70S | 80S |
| Initiation factors | IF: 1, 2 and 3 | eIFs 1, 1A, 2, 2A, 2B, 3, 4A, 4B, 4E, 4F,4G, 5, 5A,6 |
| Elongation factors | EF-Tu, EF-Ts, EF-G | eEF1A, eEF1B, eEF2 |
| Termination factors | RF1, RF 2, RF3 | eRF1, eRF3 |
| Energy-regeneration system | PEP+PK, or CP+CK, or pyrucate+NAD+CoA | CP+CK |
| Sulfhydryl compounds | ME or DTT | DTT |
| Advantage | (1)Simplicity and university of DNA template design; (2)High translation rate. | (1)High stability; (2) Better compatibility with the synthesis of eukaryotic proteins |
| Disadvantage | (1)shorter reaction time; (2)High rate of degradation of DNA, mRNA and protein; (3)Aggregation of protein products | (1)Lower translation rate; (2)Complexity of design of DNA template |

Abbreviation: IF, initiation factor; EF, elongation factor; eEF, eukaryotic elongation factor; RF, release factor; eRF, eukaryotic release factor.

Table 2-4. Oligonucleotide primers used for mutant GFP.

| Orientation | Sequence (5'-3') |
|---|---|
| Forward | CAA CAG TCT CGA ACT TAA GC |
| Backward | AAA ACC TCC CAC ATC TCC |

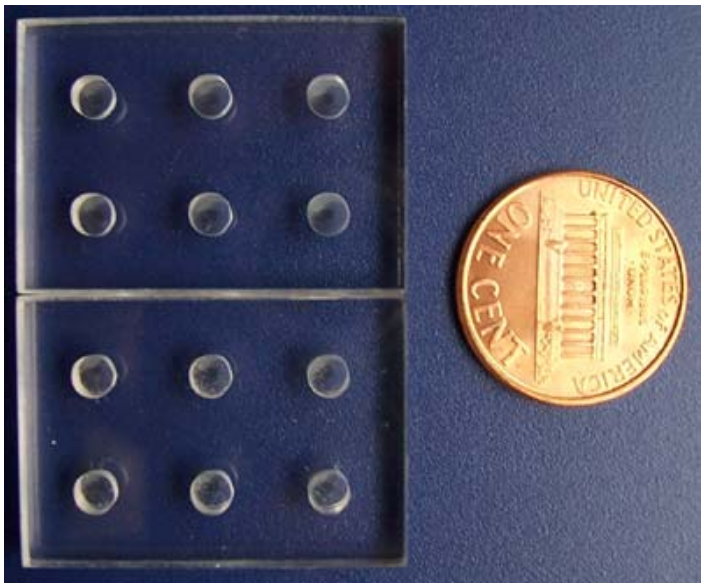


Figure 2-1. A picture of two devices forming an array (3x4) of 12 wells. A US penny is also pictured for comparison of the size. The wells in each device were laid out according to the standards of 96-well plates, but with ~25 time reduction in the well volume.

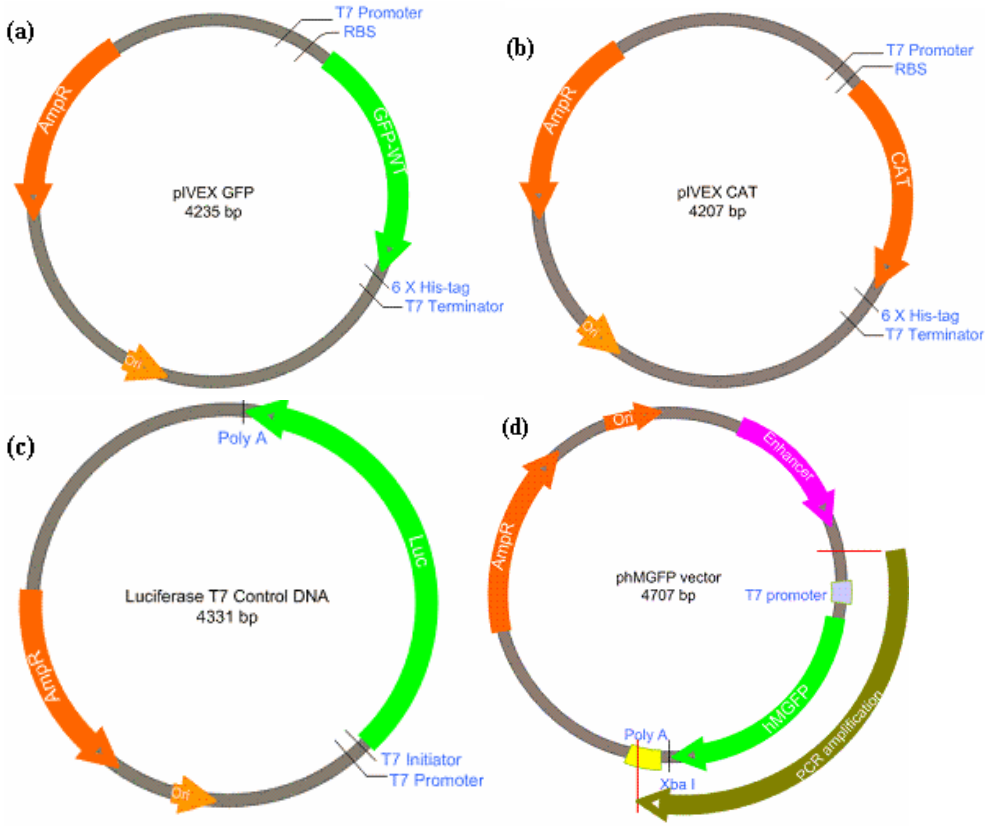


Figure 2-2. Vector maps. (a) pIVEX GFP vector map. (b) pIVEX CAT vector map. (c) Luciferase control DNA map. (d) phMGFP vector map. Additional description: ori, origin of plasmid replication; AmpR, b-lactamase gene (resistant to ampicillin).

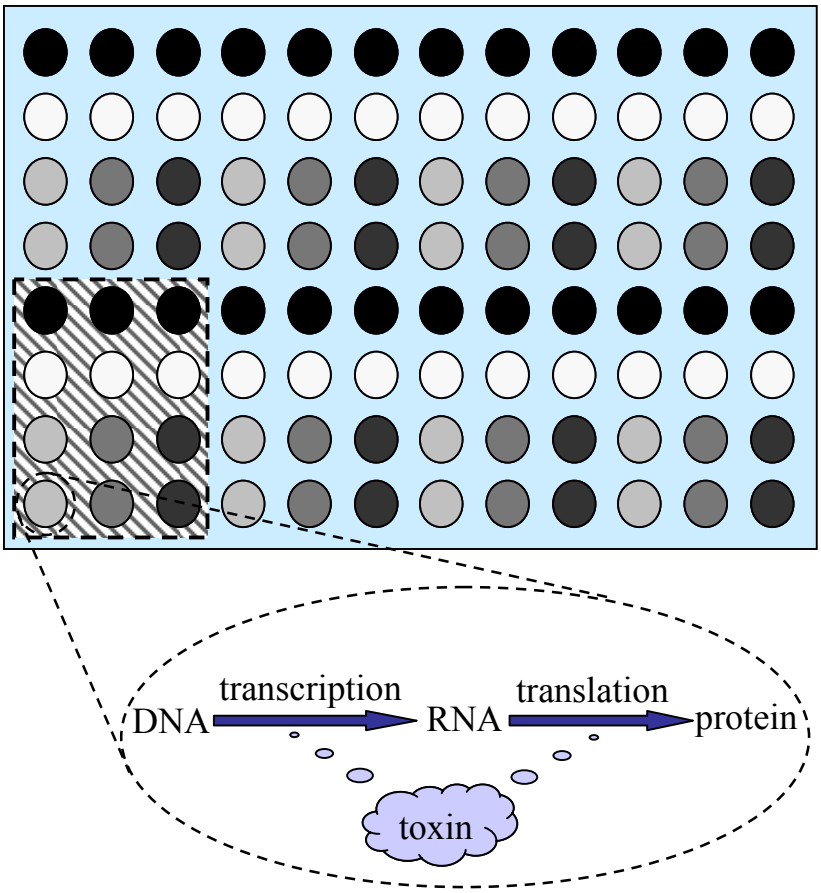


Figure 2-3. A device with an array (12x8) of wells for in vitro expression of a group of proteins. The area shadowed with diagonal lines indicates a subset (3x4) of 12 wells, among which the top row of 3 wells are for expression of three different proteins as the positive controls, the second row for the negative controls, and other two rows for the samples with one repeat for enhanced precision. Total of 8 series of such a 12-well set may be made for detecting different toxins. The insert in the expanded view shows transcription and translation steps in each well; and the processes may be inhibited by toxins.

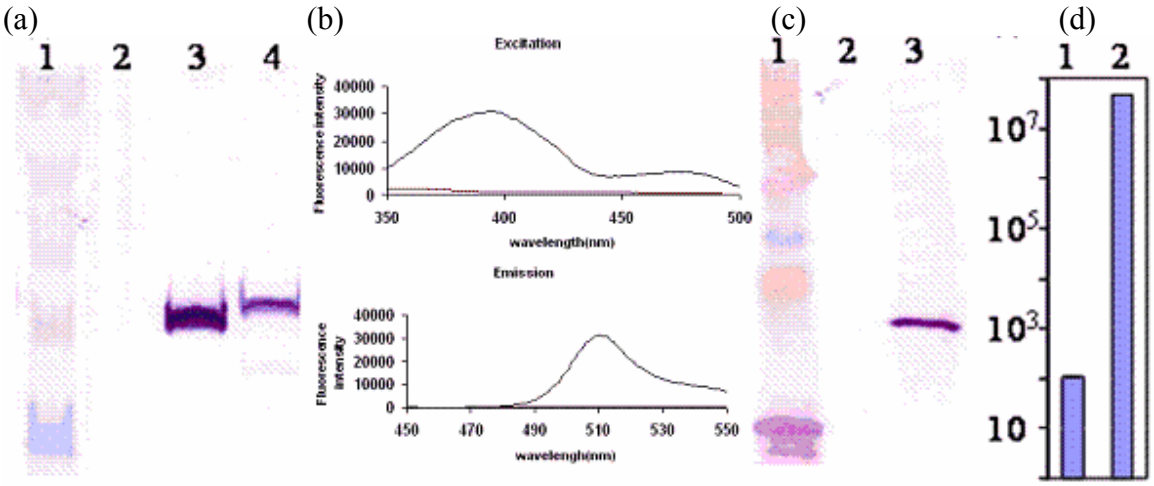


Figure 2-4. In vitro protein expression in microcentrifuge tubes. (a) WT-GFP expression confirmed by Western blot. Lane 1: pre-stained protein markers; 2: negative control; 3: recombinant GFP (rGFP) purchased; 4: GFP expressed. (b) WT-GFP confirmed by fluorescence spectrometry. Top: excitation spectrum; Bottom: emission spectrum. (c) CAT expression confirmed by Western blotting. Lane 1: protein markers; 2: negative control; 3: CAT expressed. (d) Luciferase expression confirmed by luminescence detection. Lane 1: negative control; 2: luciferase expressed. The intensity of luminescence in the y axis is in log scale.

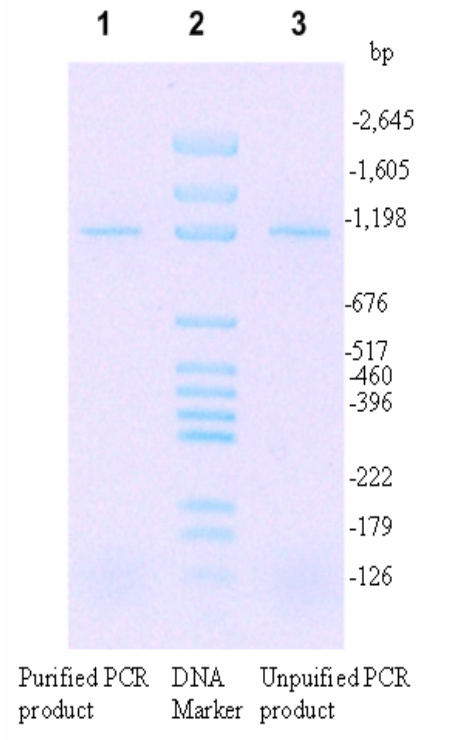


Figure 2-5. PCR analysis by agarose gel electrophoresis. Lane 1: PCR product after purification; Lane 2: DNA marker; Lane 3: raw PCR product.

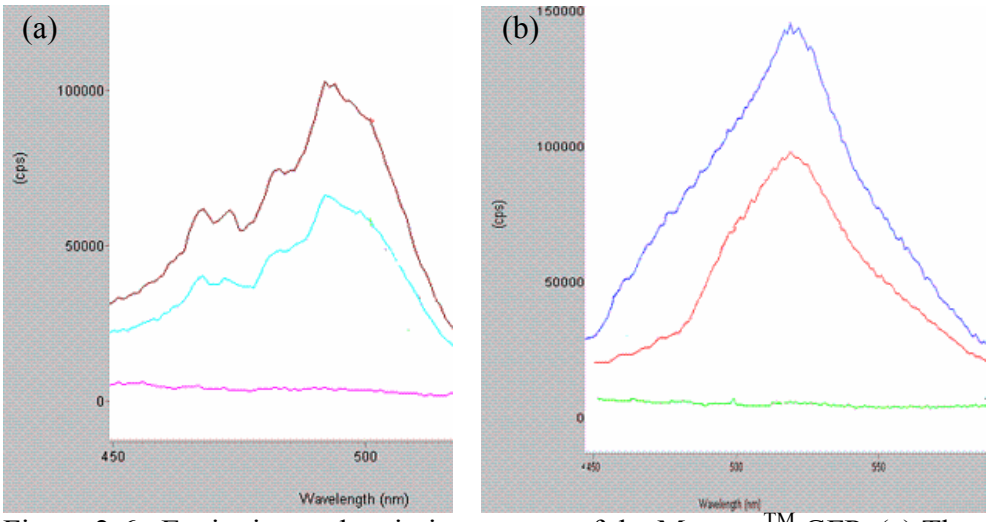


Figure 2-6. Excitation and emission spectra of the Monster™ GFP. (a) The excitation spectra of expressed Monster™ GFP. (b) The emission spectra of expressed Monster™ GFP, excited at 480 nm. Top curve: Monster™ GFP synthesized from phMGFP vector; Middle curve: Monster™ GFP synthesized from PCR-amplified DNA; Bottom curve: negative control.

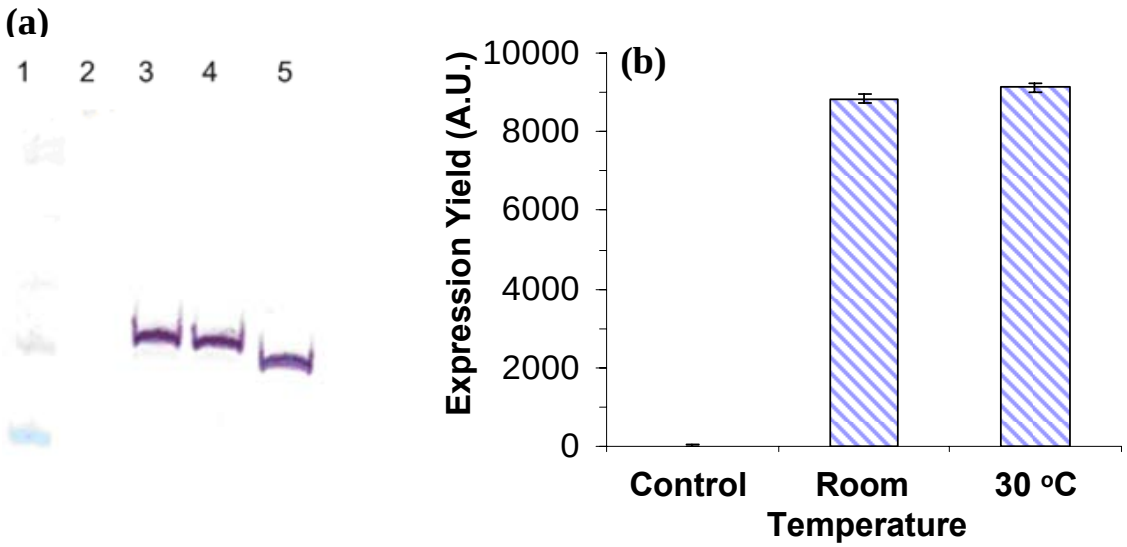


Figure 2-7. Comparison of in vitro GFP synthesis between at room temperature and at 30 °C. (a) Western blot analysis. Lane 1: pre-stained protein markers; 2: negative control; 3: GFP synthesized at room temperature. 4: GFP synthesized at 30 ◦C. 5: recombinant GFP (rGFP) purchased. (b) Quantitative comparison of the GFP expression yield between room temperature and 30 °C.

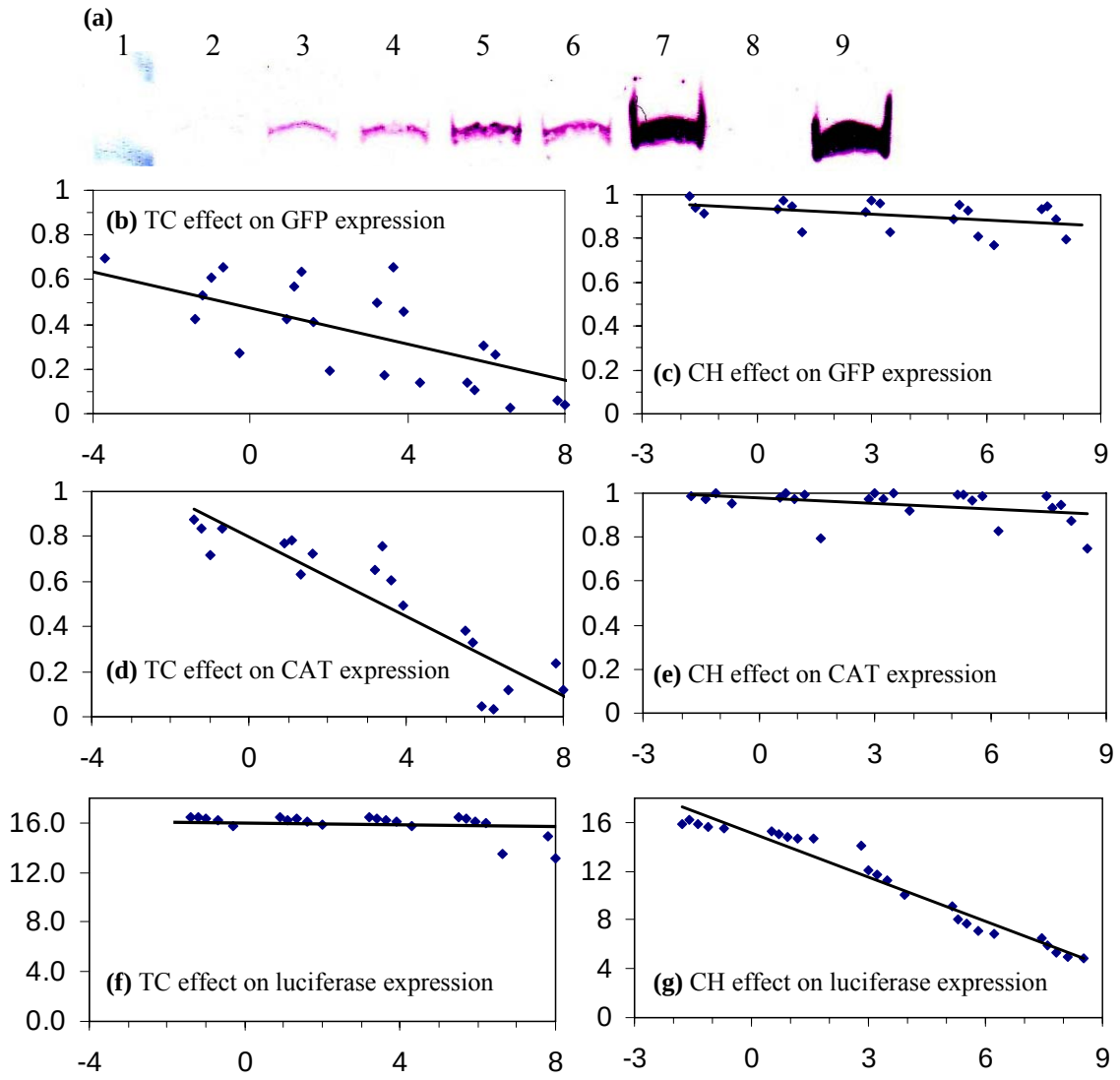


Figure 2-8. Inhibitory effects of TC and CH on cell-free protein expression in microcentrifuge tubes. (a) Western blot analysis confirms the inhibitory effects of TC on the expression yield of GFP in E. coli expression system. Lane 1: pre-stained protein markers; lanes 2-6: expression of GFP with 3000, 300, 30, 3, 0.3 ng/μL of TC, respectively; lane 7: positive control; lane 8: negative control; lane 9: rGFP purchased. (b-g) Inhibitory effects of TC (b, d, and f) or CH (c, e, and g) on the expression yield of GFP (b, c) in E. coli expression system, of CAT (d, e) in E. coli expression system, and of luciferase (f, g) in rabbit reticulocyte expression system. The expression yields of GFP and CAT were quantified by Western blotting while that of luciferase was measured by luminescence. All x axes are the concentration (ng/μL) of toxin, in log scale. Y axes are the amount of expressed protein either normalized to the positive control (b-e) or in log scale of luminescence signal (f, g).

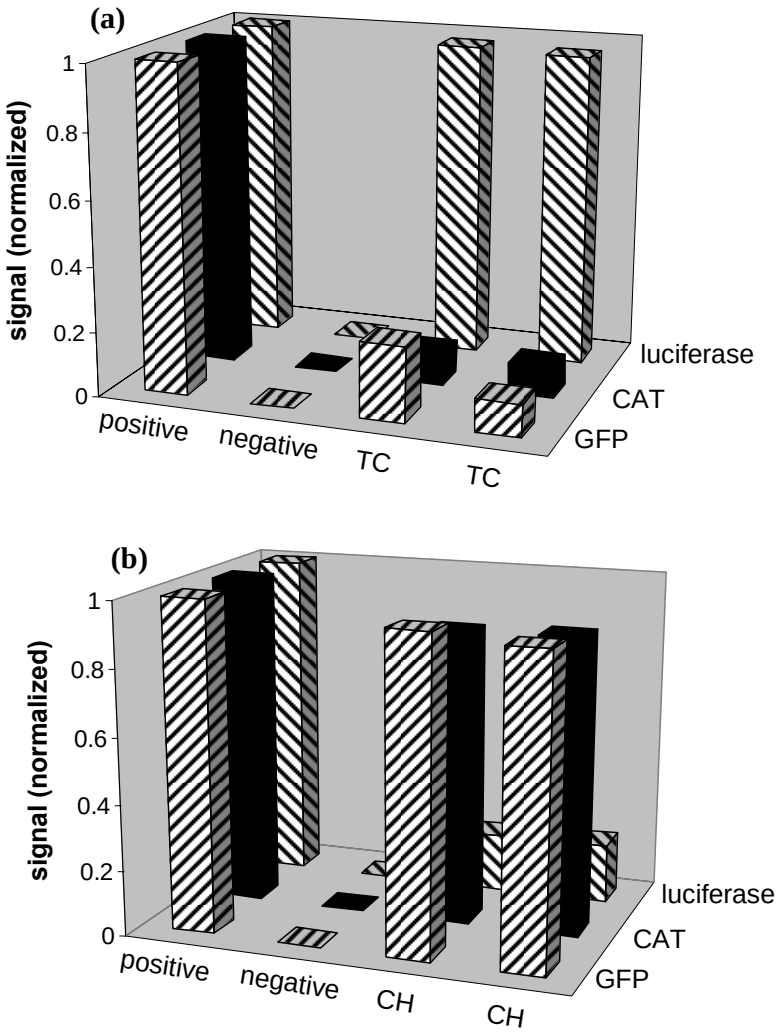


Figure 2-9. The response pattern of the 3x4 IVT sensor array for two toxin simulants, tetracycline (TC, a) and cycloheximide (CH, b). The experiments were carried out in two of the 2x3 well devices in Figure 1. The signals for the positive control were from the first row of 3 wells in the device, in which GFP, CAT, and luciferase were expressed in their respective expression systems. These wells were free of toxins. The signals for the negative control were from the second row of 3 wells in the device, in which the expression vector was not added. The signals for the samples were from the remaining two rows of 3 wells in the device, in which either 17 ng of CH or 25 ng of TC was added into the protein expression system.

# CHAPTER 3
# NESTED-WELL DEVICES FOR IN VITRO PROTEIN SYNTHESIS AND RICIN DETECTION[1]

## 3.1 Introduction

Detection and identification of toxic agents are important for medical diagnostics, food/water safety testing, and biological warfare defense. Methods to detect them include immunoassay,[142, 143] sensors,[144, 145] mass spectrometry,[146] and genetic analysis.[147-150] Nucleic acid-based genetic analysis, e.g., polymerase chain reaction (PCR), involves DNA amplification that offers high sensitivity and unambiguous identification. However, it is not applicable to toxins that contain no nucleic acids. One example of such toxins is ricin, which is listed as a Category B bioterrorism agent according to the Centers for Disease Control and Prevention[151] and was used as an agent in the letter sent to US congress in Feb. 2004. The structure, toxicity, mechanism of action, and current detection methods of ricin will be discussed in section 3.2. Immunoassay is advantageous over other methods due to its high sensitivity. However, it requires an antibody that is specific to the agent of interest and it often involves labor-intensive sample preparation. Therefore, it can not be used for detecting unknown or a new agent because an antibody is simply not available. With the increasing ability to modify and engineer potential warfare agents, a simple, fast, and highly sensitive method to detect agents is essential.

To address this challenge, we describe an approach that exploits the mechanism—by which toxins cause toxic effects—as the sensing scheme.[137, 152] For example, ricin acts on the 28S ribosomal subunit and prevents the binding of elongation factor-2, a critical component in the process of protein translation. That is, ricin kills people by blocking protein synthesis in cells

[1] A part of this chapter has been published in (140) Mei, Q.; Fredrickson, C. K.; Lian, W.; Jin, S.; Fan, Z. H. Ibid.**2006**, *78*, 7659-7664., and in (141) Mei, Q.; Fredrickson, C. K.; Simon, A.; Knouf, R.; Fan, Z. H. *Biotechnology Progress* **2007**, *23*.

of human body. Similarly, a number of biological toxins exhibit their toxin effects through inhibition of protein synthesis, including Shiga toxin, diphtheria, and exotoxin A.[137]

As discussed in chapter 2, *in vitro* protein synthesis has been inplemented in microwell IVT array. One of the major problems of IVT preformed in this microwell device is its short reaction time, thus significantly reduces protein expression yield. The problem has been addressed by the invention of continuous flow cell-free and continuous exchange cell-free systems, in which nutrients can be refurbished and inhibitory byproducts can be removed (summarized in section 3.2.2).

The nested-well device in this chapter consists of a mechanism for fluid manipulation. The performance of the device is demonstrated by synthesizing green fluorescent protein, chloramphenicol acetyltransferae, and luciferase. The production of IVT between the nested-well device and a microcentrifuge tube was compared. The effects of hydrostatic flow and connection depth on the protein product yield are also investigated. Higher protein expression yields can be obtained in the nested-well device, leading to larger detection signals (lower detection limit) when ricin is present. More importantly, this detection approach accomplishes signal amplification. For each copy of DNA, thousands of copies of proteins can be produced. The inhibitory effects of ricin on the production of each copy of protein are accumulated, leading to a significantly enhanced detection signal. In addition, ricin detection using the one-step operation of protein expression simplifies the detection procedure compared to ELISA that consists of many steps of applying reagents and washing.[153] The detection can be achieved in as short as 5 minutes.

## 3.2 Background

### 3.2.1 Ricin

Ricin, extracted from the seeds of the castor bean plant (*Ricinus communis*), is one of the most toxic and easily produced plant toxins. Ricin consists of two chains, A and B, connected by a disulfide bond. The B chain binds to galactose or N-acetylgalactosamine of glycoproteins and glycolipids on the surface of a eukaryotic cell, stimulating the endocytic uptake of the ricin. The A chain is an enzyme that binds and depurinates a specific adenine of the 28S ribosome RNA (rRNA). The adenine ring of the ribosome becomes sandwiched between two tyrosine rings in the catalytic cleft of the enzyme and is hydrolyzed by the enzyme N-glycosidase action. As a consequence, aminoacyl-tRNA can no longer bind to trancated 28S rRNA and protein synthesis is blocked in the cell, which lead to cell death and tissue image.[137, 154] The target adenine is a specific RNA sequence that contains the unusual tetranucleotide loop, GAGA. The B chain has two binding sites for galactose, and about 106 ricin molecules may bind per cell. However, just a single ricin molecule that enters the cytosol can inactivate over 1,500 ribosomes per minute and kill the cell.[155, 156]

Although ricin has been shown to inhibit tumor growth and it has been applied for cancer therapy,[157, 158] it is considered for biological weaponization and is listed as a Category B bioterrorism agent due to its extreme ease of production and high toxicity. The lethal dosage of ricin, which is lethal to 50% of the exposed population, is approximately 3-5 μg per kilogram of body weight.[159] Since ricin has no selectivity for specific cells, the clinical signs and symptoms of ricin intoxicity depend on the dose and the route of exposure. For example, inhalation causes cough, fever, nausea and pulmonary oedema; oral injection results in vomiting, diarrhea, hydration, low blood pressure, or necrosis of spleen, liver and kidneys.[160]

The methods to detect ricin at low concentration levels typically include enzyme-linked immunosorbent assay (ELISA)[161] and immunoassay using radioactive labeling.[162] Although offering high sensitivity, they involve many steps that are labor-intensive and time-consuming. For radio-immunoassay, the handling and disposal of radioisotopes are always environmental challenges. Recently, Ligler's group reported a fluorescence-based multianalyte immunosensor that has a detection limit of 25 pg/μL of ricin.[145, 163] Stine and Pishko exploited specific interaction between ricin and glycosphingolipids and developed a quartz crystal microbalance sensor with the detection limit of 5000 pg/μL of ricin.[164] Shankar et al. depicted an immunoassay-based magnetoelastic sensor that shows a detection limit of 5 pg/μL of ricin.[165] The detection limit and time required for detection of ricin are summarized in Table 3-1.

### 3.2.2 Continuous-Flow Cell-Free Protein Expression Systems

In an IVT system performed in the fixed volume of a microcentrifuge tube (Figure 3-1a), the main limitation is its short lifetime because reaction terminates as soon as any essential substrate is exhausted, or by-products accumulate to the level of inhibition, usually within 60 minutes. As a result, this leads to poor yield of protein. The major breakthrough was achieved by Spirin and coworkers with the invention of the continuous-flow cell-free (CFCF) system, in which the reaction products were continuously removed and the nutrients were continuous supplied.[85] This can also be achieved by a semi-permeable membrane, which maintains the high molecular weight components in the reaction chamber and separates it from feeding chamber containing the small molecular components. In this case, the nutrients are continuously supplied into and all the products including synthesized proteins are removed from the chamber by the forced flow of the feeding solution through an ultrafiltration membrane (Figure 3-1b).

The first CFCF system developed by Spirin was a modified Amicon 8MC mirco-ultrafiltration chamber.[85] Typically, the volume of the reaction mixture was 1 mL and the

feeding solution was pumped in with a constant flow rate of 1 mL/hour. The ultrafiltration membranes used in their report were Amicon PM-10, PM-30, XM-50, with respective molecular weight cut-offs of 10 KDa, 30KDa, and 50KDa. Both E. coli lysate and wheat germ extract were tested in this reactor for translation of various mRNA, resulting in extended reaction time (20-40 hr) of synthesis and a significantly high yield of products. The products are relatively small proteins including MS2 coat proteins (16 KDa), brome mosaic virus coat protein (19kDa) and calcitomin polypeptide (3.4KDa).[85]

Since then, several other groups reproduced and optimized the CFCE systems and realized coupled transcription-translation in the CFCF format. For examples, Endo et al. reported dihydrofolate reductase (DHFR) with enzymatic function was synthesized up to 20 hr using the same reactor as Spirin's.[86] Kigawa improved Spirin's design by using a HPLC pump instead of peristaltic pump to make better control of a constant flow rate.[87] In addition, Kigawa used a coupled *E. coli* IVT and produced active chloramphenicol acetyltransferase (CAT). Other similar reports are summarized in Table 3-2.

### 3.2.3 Continuous-Exchange Cell-Free System

Another simple way to allow continuous supply of nutrients and removal of products is to employ a dialysis bag or a flat dialysis membrane for the passive exchange of low molecular components, named as continuous-exchanged cell-free (CECF) systems[166] (Figure 3-1c). Kim reported 1.2 mg of CAT was synthesized in 1 mL dialysis bag and the reaction can extend up to 14 hr.[88] Kigawa developed a high-productive *E. coli* CECF system and the yield of CAT and RAS protein increased to 6 mg/mL over 21 hours of incubation.[101] More recently, Madin presented a highly productive wheat germ CECF system which can synthesize the amount of 0.5 to 1.5 mg/ml of several proteins, such as DHFR, GFP and luciferase in 24 hr.[167] As an alternative, a hollow fiber reactor with increased filtration area was proposed by Yamamoto.[168]

This modified configuration also enabled in situ concentration of extract, thus speeds the reaction rate.

The commercial CECF instrument with a programmable controlling temperature, supplemented with well-developed reagent kits, was launched on to the market by Roche Applied Science; this is called Rapid Translation Systems which use an optimized *E. coli* lysate or wheat germ extract. The production of various proteins can be synthesized up to 5 mg/mL in 24 hours.[93] Table 3-2 summarized nearly all published data so far reported on CFCF and CECF protein synthesis.

Although CFCF systems have several obvious advantages (purity and high yield of protein products), the operational complexities (pump and valve) limit the potential for practical use. Due to the simplicity and low cost, CECF systems became attractive to scientists during the past decade. In addition, CECF systems could be achieved in a miniaturized format and become a powerful tool for high-throughput expression of proteins, as discussed in following sections.

## 3.3 Experimental

### 3.3.1 Materials and Reagents

The RTS 100 wheat germ CECF kit, RTS 500 *E. coli* kit, and the expression vectors containing the gene of green fluorescent protein (GFP) and chloramphenicol acetyl-transferase (CAT) were obtained from Roche Diagnostics GmbH (Mannheim, Germany). T7 luciferase DNA vector, luciferase assay reagent, and nuclease-free water were acquired from Promega Corporation (Madison, WI). Ricin (MW 60 KDa) and ricin B chain (MW 32 KDa) were purchased from Vector Labs (Burlingame, CA) while ricin A chain (MW 29 KDa) and 2-mecaptoethanol were from Sigma (St. Louis, MO). The values of their molecular weight (MW) are provided by the respective manufacturers. Acrylic sheets with thickness of 0.25" (6.3 mm) and 0.22" (5.5 mm) was from Lucite International Inc.(Cordova, TN). The dialysis membrane

with the molecular weight cutoff of 8 KDa was obtained from Spectrum Labs (Rancho Dominguez, CA). 10 nm pore size of polycarbonate membrane was purchased from GE Osmonics Labstore (Minnetonka, MN) and polycarbonate membranes with 15 nm and 100 nm pore size were from Whatman Inc (Florham Park, NJ). A biocompatible epoxy (353ND-T) was bought from Epoxy Technologies (Billerica, MA).

### 3.3.2 Device Fabrication

The design of the nested-well device is shown in Figure 3-2a; it consists of two parts. The top part, tray, was fabricated by drilling through-holes and a common flange in a piece of 5.5 mm thick acrylic sheet using a CNC-mill (Flashcut CNC, Menlo Park, CA). The inside diameter of the hole is 3 mm, surrounded by a 1 mm thick wall, creating a structure with an outside diameter of 5 mm. The distance between the hole centers is 9 mm, following the microplate standards defined by the Society for Biomolecular Screening (SBS) and accepted by the American National Standards Institute. The bottom part, well, was created by milling an array of 4 mm deep wells into a piece of a 6.3 mm-thick acrylic sheet. The diameter of the wells is 7 mm; each well is concentric with the corresponding tray chamber when they are assembled. A picture of both parts in a 2 x 3 array is in Figure 3-2b.

A dialysis membrane is incorporated in the device to connect the two chambers as illustrated in Figure 3-2c, providing a means to supply nutrients continuously and remove the reaction byproducts. The membrane is glued to the bottom of each tray chamber using adhesives. Epoxy 353ND-T is cured at 80 $^{\circ}$C in an oven for 20 minutes. The assembled devices are rinsed with nuclear water and then sterilized by exposing to a UV light for 30 minutes to eliminate possible inhibition of enzymatic reactions.

### 3.3.3 *In vitro* Protein Expression

For the prokaryotic expression system, GFP and CAT were synthesized using a RTS 500 *E. coli* kit. Reaction and feeding solutions were prepared as recommended by the manufacturer. In brief, the reaction solution contained 0.525 mL *E.coli* lysate, 0.225 mL reaction mix, 0.27 mL amino acid without methionine and 30 μL methionine. The feeding solution consists of 8.1 mL feeding mix, 2.65 mL amino acid without methionine and 0.3 mL methionine. To run the protein synthesis in the miniaturized membrane device, the tray was filled with the 8 μL of the reaction solution containing GFP vector or CAT vector while 80 μL of the feeding solution was added to each well in the well plate. A biocompatible sealing tape was used to seal the tray to prevent evaporation. The device was placed on a shaker with a speed 100 rpm and incubated at room temperature for 2, 4, 6, 10, 14 and 20 hrs. As for comparison, 8 μL of reaction solution was dispensed into microcentrifuge tube and incubated the same time period as that of the membrane device. After GFP synthesis, the reaction tubes were stored at 4 °C overnight for the maturation of GFP. The synthesized GFP and CAT were analyzed using Western blotting.[99] Gel images are scanned by a flatbed scanning and quantified using ImageJ from the National Institute of Health.[132] GFP production is also confirmed by a microplate reader (Tecan Safire, Research Triangle Park, NC).

For the eukaryotic expression system, luciferase was synthesized using RTS 100 wheat germ expression kit. The reaction solution for trays was prepared by mixing 15 μL wheat germ extract, 15 μL reaction mix (provided in the kit), 4 μL amino acids, 1 μL methionine and 15 μL of nuclease-free water containing 1 μg of luciferase vector. For each tray chamber, 8 μL of the reaction solution was used. The feeding solution for wells was prepared by combining 900 μL feeding mix (provided in the kit), 80 μL amino acid and 20 μL methionine. In each well, 80 μL of the feeding solution was introduced. The tray and well plates were assembled and then placed

on a shaker (at room temperature) for a period of time (e.g., 0.5 hour). The amount of luciferase synthesized was determined by mixing the expression product with luciferase assay reagents, followed by luminescence detection in a luminometer (Berthold, Germany), as described in chapter 2[99]. When luciferase was synthesized in a microcentrifuge tube, the same reaction solution (8 μL) was used without the feeding solution.

### 3.3.4 Ricin Detection

Ricin is highly toxic to human. The material safety data sheet (MSDS) should be reviewed before handling this chemical. Ricin samples should be handled in dedicated laboratories and appropriate safety precautions are required when preparing ricin solutions. The personnel who perform the experiments must wear protective devices including a lab coat, gloves, and a face mask. Contaminated labware such as microcentrifuge tubes, pipet tips, and used devices are disposed into a biohazard container.

A series of concentrations of ricin A chain solutions, ranging from 0.035 to 0.69 nM, were prepared from a stock solution of 35 μM. To demonstrate ricin detection, 6 μL of the reaction solution (discussed above) is pipeted into the tray, followed by 2 μL of ricin samples. The volume of the feeding solution remained at 80 μL. For the positive controls in the same device, 2 μL of water was added. The negative controls contain no luciferase vector, providing with the background signal. To achieve lower detection limit, 4-hr protein expression was used, though ricin detection can be achieved in as short as 5 minutes.

The same protocol was used in studying the toxicity level of various forms of ricin, including whole ricin, ricin A chain, ricin B chain, heat-denatured ricin A chain, and whole ricin treated with 2-mercaptoethanol. Denature of Ricin A chain was achieved by heating the samples at 95 $^{o}$C for 5 minutes. Reduction of disulfide bond of two chains in ricin was carried out by

mixing ricin with 50 mM 2-mercaptoethanol, followed by the incubation of the mixture at 52 $^{o}$C for 10 minutes.

## 3.4 Results and Discussion

### 3.4.1 Device Design

As mentioned above, protein expression can be produced in a cell-free medium employing IVT. It is also well-recognized that high-yield protein expression of IVT can be attained in the flow of a feeding solution, but not under static conditions in a fixed volume.[85, 102] As a result, commercial bench-top instruments incorporate the principle of continuous flow with a magnetic stirrer.[93, 169] However, the bench-top instruments often employs milliliters of reagents[93] and it is difficult to achieve the high-throughput format as discussed by Angenendt et al.[68]

We fabricated a nested-well device consisting of a mechanism for fluid manipulation; it also has a potential to implement protein synthesis in a high-throughput format due to miniaturization. As illustrated in Figure 3-2, IVT was implemented in an array of units; each unit is for expression of one protein (e.g., GFP). Each unit in the device consists of a tray and a well (Figure 3-2c). The tray chamber is for the IVT reaction; the well is concentric with the corresponding tray chamber and functions as a nutrient reservoir. The well contains amino acids, adenosine triphosphate (ATP), and other reagents. The tray contains the cell-free expression mixture extracted from *E. coli* or wheat germs, as well as the same reagents in the well. The solution array is designed to conform with 96-well microplates, ensuring compatibility with a variety of commercial fluid dispensing systems and commercial plate readers for detection.

A dialysis membrane is glued to the bottom of the tray, connecting the tray and well and providing a means to supply nutrients and remove the reaction byproducts. The incorporation of membrane is critical [85, 129] because of two facts: (1) the flow of a nutrient-feeding solution will lead to higher expression yield compared to static conditions, because protein synthesis will not

terminate earlier due to fast depletion of the energy source (ATP); (2) removal of small molecular byproducts is also critical to high yield expression of proteins in a cell-free medium, because possible inhibition of protein synthesis by the byproducts (e.g., hydrolysis products of triphosphates) will not take place.

The connection between the tray and well chambers is a hollow circle, though it looks like a channel in the cross-sectional view in Figure 3-2c. The height of the connection ranges from 100 μm to 2 mm. One of the mechanisms for supplying nutrients from the well chambers to the tray chamber and for removing byproducts from the tray chamber to the well chambers is diffusion, the transport of species resulting from the difference in the concentration of solutes between two solutions separated by the membrane. The rate of diffusion is determined by the diffusion coefficient and the concentration gradient of solutes. In addition, the flow to supply fresh solution from the well to the tray is augmented by a hydrostatic pressure, which is caused by the difference in the solution level between the tray and well. When the well has slightly higher solution level than the tray, the pressure difference resulting from the height difference will drive nutrients from the well into the tray.

Incorporation of the membrane and fluidic connection enables continuous supply of nutrients and selective removal of small molecule byproducts. The nutrient-feeding solution will avoid fast depletion of the energy source, and the accumulation of small molecular byproducts will not take place. This device design allows protein synthesis to continue for up to 20 h with higher protein yield as discussed later.

Using the dimension discussed in 3.3.2, the volume of a tray chamber is 18 μL. We typically fill in the tray with 8 μL of an IVT solution; this volume is more than 2 orders of magnitude less than 1 mL of a reaction solution in RTS 500. Similarly, the volume of a well

chamber is 107 μL after a tray is placed inside. We typically fill in the well with 80 μL of a feeding solution; this volume is again more than 2 orders of magnitude less than 10 mL of a feeding solution in RTS 500. The decrease in the volume of both reaction mix and feeding resolution will significantly reduce reagent consumption when using IVT for high-throughput assays [170]

Although Figures 3-2 shows a 2 x 3 array device, an array of a higher number (e.g., 8 x 12) can be implemented as is readily appreciated by those in the field. As explained above, such an nested-well device has the following advantages: (1) less reagent consumption due to miniaturization; (2) higher protein expression yield due to incorporation of a mechanism for fluid manipulation; and (3) a potential to implement protein synthesis in a high-throughput format.

### 3.4.2 Protein Synthesis

To demonstrate the function of the nested-well device, GFP was synthesized using commercial E. *coli* system with a GFP coding sequence. GFP product was analyzed using Western blotting. Figure 3-3a show the Western blot image, and the signal intensity is plotted in Figure 3-3b. To show the effects of the flow manipulation, we did the same reactions in a microcentrifuge tube and found that protein expression ceased after 4 h. This result clearly illustrates the importance of incorporation of the dialysis membrane and fluidic connection in the device. Continuous supply of nutrients and selective removal of small molecule byproducts enable protein synthesis to continue for up to 20 h in the device, which is 5 times longer than the expression time in the tube. The longer expression time results in higher expression yield. The amount of GFP synthesized in the device is about 13 times larger than in the tube. The quantified data as shown in Figure 3-3b indicated the device design is proper.

Since GFP is naturally fluorescent, the expression product can also be quantified by fluorescence emission. Using a commercial microplate reader, the emission spectrum of

synthesized GFP is shown in Figure 3-4a, as is the spectrum of the recombinant GFP we purchased. The same fluorescence spectrum also confirms our success of GFP expression in the device. It should be noted that the GFP synthesized must be incubated at 4 $^{o}$C to let proteins fold correctly in order to have appropriate three-dimensional structures for fluorescence. Figure 3-4b shows the fluorescence intensity as the function of the incubation time. After 20 hours incubation, the fluorescence intensity reached the plateau. Fluorescence is a highly sensitive and widely used analytical method. But there are potential limitations when we try to use the fluorescence intensity to quantify the GFP expression in the microwell device. First, the long folding time of GFP lead slow response time. Even though lots of mutagenesis studies have improved the folding properties, the slow maturation time is still a big obstacle of practical application of GFP. Second, integrating the excitation light source into the microdevice will involve a lot of microfabrication time-consuming and costly steps. Moreover, it is very difficult to completely filter the excitation light in the chip, which may induce high background and greatly decrease the sensitivity of the system.

Similar expression has been achieved for chloramphenicol acetyl-transferase (CAT). CAT is expressed in the same *E. coli* expression system; success of the protein expression is confirmed by Western blotting in Figure 3-5a. The signal intensity as the function of the reaction time is shown in Figure 3-5b. These results also suggest longer expression time can be achieved in the device than in the tube. As a result, the production yield increased more than 22 fold in the device. This confirms that we have achieved the desired fluid manipulation, both continuous feeding of the nutrient solution and removal of the byproducts, in the device.

Because of the limitation of fluorescence detection on the chip, we further investigated a low background bioluminence system. Synthesis of luciferase is carried out using wheat germ

expression system. Detection of the expression product is achieved by monitoring the intensity of luminescence after mixing the product with luciferin and ATP as reported previously [140]. Figure 3-6 indicates the production yield of luciferase increased more than 2.6 fold in the device than that in a microcentrifuge tube. In addition, luciferase folding can be processed during the process of translation.[171] These results suggest that we achieved the desired fluid manipulation in the device.

### 3.4.3 Hydrostatic Flow

As mentioned above, one mechanism for supplying nutrients from the well to the tray is the hydrostatic flow due to the difference in the solution level between the tray and well. We studied the effects of the fluid level difference on the protein expression yield. Figure 3-7 shows the protein expression yield temporal profiles when the fluid level difference changes from -0.5 mm to 2 mm. The fluidic connection depth is fixed at 500 μm. When the height is -0.5 mm, i.e., a reverse flow from the tray to the well exist, protein expression is significantly hindered due to depletion of the expression components in the tray. When the fluid level difference is near 0, the expression yield increases 183% and normal temporal profile is observed. In this condition, the fluid flow should be primarily due to diffusion and agitation. When the fluid level difference increases from 0 to 2 mm, the expression yield increases 38%, presumably due to additional hydrostatic flow. This result indicates that hydrostatic flow plays a role in the replenishing nutrients in the device.

The flow of material across the membrane is believed to be driven by a three possible mechanisms: hydrostatic pressure, osmotic pressure, and diffusion.

Hydrostatic pressure is due to the difference in solution levels on both sides of the membrane; any difference will result in a pressure gradient across the membrane. The magnitude of the pressure difference is given by

$P = \rho gh$

where P is the hydrostatic pressure, ρ is the density of fluid, g is gravitational acceleration, and h is the height difference between liquid interfaces of the reaction and feeding chambers

Osmosis is the spontaneous net movement of water across a dialysis membrane from a region of high solvent potential to an area of low solvent potential when a solute concentration gradient is present. Osmosis likely take place because solutions possess different strengths, and water crossing the membrane from the dilute side to the concentrated side in an attempt to balance the concentrations. The magnitude of osmosis is given by Van't Hoff's equation:

$\pi = cRT$

where π is the osmotic pressure, c is concentration, R is the universal gas constant, and T is temperature in Kelvin. This equation predicts that the osmotic pressure will be higher when concentration is greater (Note that it doesn't depend on what the solute is, just its overall concentration; if the solution has many solutes, c is the overall concentration regardless of species).

Transport of materials across the semi-permeable membrane should be governed by Fick's law of diffusion, which in one-dimensional form is expressed as:

$$N_A = -D_A \frac{dC_A}{dy}$$

In this equation, $N_A$ represents the molar flux of A with respect to a fixed reference frame (mol/t $L^2$), $D_A$ is the mass diffusion coefficient, and $C_A$ is the concentration. By integrating this equation and applying the boundary conditions (concentrations on each side of the membrane and membrane thickness), we find that

$$N_A = D_A \frac{C_{A,high} - C_{A,low}}{\delta}$$

This equation suggests that if the solutions on either side of the membrane have different concentrations, solute will travel from the region of high concentration to region of low concentration.

Since solutions in the feeding and reaction chambers are from Roche, the exact compositions are unknown. Our calculation below indicates that the concentration of amino acid is same between the reaction and feeding chamber. In addition, Kim et al. mentioned that the concentration and the components in reaction solution and feeding solution are identical except for RNA polymerase, DNA template, and tRNA mixture.[88] The following calculation is based on the concentration of components provided by Kim et al:[88]

At the beginning of reactions:

$C_{amino\ acid,\ tray}$= 500 μM $C_{amino\ acid,\ well}$= 500 μM

$C_{ATP,\ tray}$= 1.2 mM $C_{ATP,\ well}$= 1.2 mM

$C_{byporduct,\ tray}$= 0 $C_{byproduct,\ well}$=0

Δh=2 mm

Hydrostatic pressure=ρg Δh=(998) (9.8) (0.002)=19.5608 Pa

$\pi_{tray}=\pi_{well}$

$N_{tray}=N_{well}$

In the middle of reactions, the concentrations are unknown, making calculation difficult. However, we believe that the molecules of amino acids and ATP diffuse from the well to tray due to higher concentration in the well whereas by-products diffuse from the tray to the well. Moreover, the total concentration of solutes is likely slightly higher in the tray, thus the osmosis will drive water from the tray to well. However, this effect should be overcome by the hydrostatic difference.

### 3.4.4 Effects of Membrane Pore Size

Different pore sizes of membranes have an effect on transportation of molecules through the membrane. 10 nm, 15 nm and 100 nm pore size of polycarbonate membrane and polycarbonate membranes are studied for CECF protein synthesis. The field emission scanning electron microscopy (SEM) images of 100 nm and 10 nm pore size of PC membrane at room temperature and 170 ◦C are shown in Figure 3-8 and Figure 3-9. The images indicated increasing temperature has negligible effects on the pore size of PC membrane.

The chip with the connection depth of 0.5 mm was created and the effects of membranes on the yield of protein synthesis were investigated. Luciferase was synthesized using a RTS 100 wheat germ expression kit. For each inner chamber, 6 μL of the reaction solution was used; while in outer chamber, 120 μL of the feeding solution. The amount of luciferase synthesized was determined by mixing the expression product with luciferase assay reagents, followed by luminescence detection in a luminometer, as described previously.[99] The yield of luciferase production among the device with different membranes and a microcentrifuge tube are compared and plotted in Figure 3-10. The results indicated the polycarbonate membranes with 10 nm and 15 nm pore size can improve the yield of protein expression, while no significant change using 100 nm pore size of polycarbonate membrane on protein expression compared with a microcentrifuge tube. The yield of luciferase synthesized in the device using polycarbonate membranes with 10 nm and 15 nm pore size are about 2.3 fold and 1.8 fold higher than in a microcentrifuge tube. However, the yield of luciferase production in the device using polycarbonate membranes is less than that using a dialysis membrane. The result indicated the pore size of membranes is critical for CECF protein synthesis. The dialysis membrane with the molecular weight cutoff 6 KDa-8 KDa contains tortuous pores of 2 nm in average. The pore is large enough to allow small molecular weight substrates (amino acids, ATP and PPi) pass

through, but that are small enough that larger molecular weight compounds (e.g., proteins and ribosome) cannot get through. However, polycarbonate membranes contain uniform, cylindrical pores. With the increasing of pore size, the large molecules such as the synthesized protein, polymerase and ribosome can not be retained in the inner chamber. Therefore the leaking of synthesized protein will reduce the productivity of protein synthesis. In the following experiment, the dialysis was selected for the best results.

### 3.4.5 Biological Signal Amplification

As discussed above, ricin causes toxic effects by inactivating ribosomes and inhibiting protein synthesis in biological cells and then leading to cell death and tissue damage.[137, 154] We exploit its toxicity mechanism as the sensing scheme to detect ricin. This detection method possesses inherent biological signal amplification, as illustrated in Figure 3-11. For each copy of DNA, thousands of copies of proteins can be produced. This is estimated by the amount of DNA vector used and the amount of the corresponding proteins produced in IVT. The inhibitory effects of ricin exist on the production of every copy of protein, as shown in Figure 3-11. As a result, the detection signal (i.e., the difference between the sample and the positive control) is accumulated, leading to an amplified signal.

This signal amplification is similar, to some degree, to the enzyme-enabled signal amplification in ELISA. Intrinsic to ELISA is the addition of reagents conjugated to enzymes; assays are then quantified by the build-up of colored products after the addition of the corresponding product. The signal amplification results from the enzyme that catalyzes a certain amount of substrates to detectable products. Two widely-used enzymes are horseradish peroxidase and alkaline phosphatase, which transfer o-phenylene diamine and p-nitrophenylphosphate, respectively, and generate colored products. Therefore, we expect the detection method based on protein inhibition has comparable sensitivity with ELISA.

### 3.4.6 Detection of Ricin by *In Vitro* Protein Synthesis

To demonstrate the detection of ricin, we studied its inhibitory effects on luciferase expression by adding a series of concentrations of ricin A chain into the IVT reactions in the array device. As shown in Figure 3-2a, the units on the left of the array are for the positive controls (free of ricin), the units in the middle for the negative controls (no DNA vectors), and the units on the right are for samples. Two rows of each unit are for repeat experiments to enhance the precision. The positive and negative controls are used for quantification as well as for reducing false positives and negatives for toxin detection. As shown in Figure 3-12a, the expression yield of luciferase indicated by the luminescence decreased with the concentration of ricin A chain. However, the expression yield remained the same when the ricin A chain was heat denatured and its toxicity was deactivated (open circles). The error bar of each data point indicates the standard deviation that was obtained from three repeat experiments. The calibration curve is obtained by plotting the detection signal (i.e., the difference between the samples and the controls) as a function of the ricin concentration (Figure 3-12b). A linear relationship exists from 0.035 to 0.69 nM. For a larger concentration range, a non-linear behavior of inhibition reactions is observed as expected. The detection limit is calculated to be 0.01 nM (0.3 ng/mL) by using the criterion that the signal-to-noise ratio is three times the standard deviation of the blank. Since the detection signal is dependent on the accumulation of inhibitory effects of ricin on protein production, longer protein expression (within the ascending range of the curve in Figure 3-12) will lead to lower detection limit. The result in Figure 3-12 was obtained after 4 hours of protein expression, at which protein expression yield just reaches a plateau as indicated in Figure 3-7.

However, luciferase can be synthesized in as short as 5 minutes, as shown in Figure 3-13a. Similar to the result in Figure 3-6, when a longer expression time was used, we also observed the

difference in the luciferase expression yield between the miniaturized device and a microcentrifuge tube when a short expression time (<30 minutes) was used. The result suggests that enough difference takes place in as short as 5-minute. A short IVT time is critical for those applications that need a quick response. We confirmed that we were able to detect ricin within 5 minutes, as shown Figure 3-13b, though the detection limit is higher than when a longer expression time is used.

### 3.4.7 Toxicity Level of Ricin

It is well known that ricin is a dimer, in which B chain binds to cell surface, allowing A chain to penetrate the cell to inhibit protein synthesis.[154, 172-176] In other words, the toxicity of ricin comes from the A chain. Since IVT does not provoke dissociation of the A-B dimer, all experimental results discussed above are from ricin A chain. If whole ricin (with A and B chains) is used, it will be interesting to see what the toxic effect is in the IVT device. The literature indicates that the A chain alone has a greater inhibitory effect on translation than does the complete ricin molecule.[177] As shown in Figure 3-14, we observed the similar result in IVT device. The A chain has highest toxicity, B chain has no detectable toxicity, and whole ricin shows a toxicity level slightly less than the A chain. However, 2-mercaptoethanol-treated ricin is as effective as A chain due to reduction of disulfide bond between two chains.

We also studied the effects of heat-denature on the ricin. We observed that there was a negligible inhibitory effect on luciferase expression when ricin A chain was heat-denatured and its biological activity was disabled (Figures 3-12a and 3-13b). In other words, there was no significant difference between the positive controls (free of ricin) and the one with the denatured ricin A chain. We can infer from these results that the IVT method can detect the toxicity level of ricin after physical and/or chemical treatments.

## 3.5 Conclusions

An array of nested wells with microfluidic connection has been developed for cell-free protein expression. The array device is fabricated by milling a tray chamber from acrylic and polycarbonate, attaching a porous membrane, and then nesting it in a well chamber. The device has been demonstrated for *in vitro* synthesis of GFP, CAT, and luciferase. The duration of protein expression is significantly extended due to continuous feeding of nutrients and removal of byproducts. The reactions in the wells with the feature of continuous-exchange last 5-10 times longer than the same reactions in a microcentrifuge tube. The production yield in the device is 13-22 time higher than that in the conventional reaction vessels (either microcentrifuge tubes or 96 well plates).

We also demonstrated the capacity of our device for ricin detection using the mechanism of protein expression pathway. Protein expression in our device can sustain a translation reaction as long as 20 h, thereby the expression efficiency is high. Moreover, the miniaturized device has the further advantage of reducing the volume of reagents, thus the costs. The nested-well device appears to perform better for ricin detection, offering better sensitivity, larger dynamic range and shorted detection time. The array device has potential to be used for high-throughput protein synthesis and parallel functional analysis.

Table 3-1. Summary of methods for detection of ricin.

| Research group | Methods | Labeling | Limit of Detection | Detection time | Reference |
|---|---|---|---|---|---|
| Ramakrishnan | Immunoassay | $^{125}I$ | 50 pg/tube | 30 h | [178] |
| Leith | ELISA | Avidin/biotin immunoperoxidase | 0.2 pg/μL | 30 h | [179] |
| Narang | Immunoassay | Cy5 | 0.1 pg/μL | 1 h | [180] |
| Dill | Immunoassay | Horseradish Peroxidase | 0.3 pg/ μL | 4 h | [181] |
| Rubina | Immunoassay | Cy3 | 0.1 pg/ μL | 30 h | [182] |
| Yu | Immunoassay | No label | N/A | N/A | [183] |
| Shyu | Immunoassay | Gold particles | 50 pg/ μL | 10 min | [184] |
| Shankar | Immunoassay | Alkaline phosphatase | 5 pg/ μL | 30 h | [165] |
| Wadkins | Immunoassay | Cy5 | 25 pg/ μL | 1.5 h | [163] |
| Stine | Quartz crystal microbalance sensor | No label | 5000 pg/ μL | 6 h | [164] |

Table 3-2. Summary of IVT system.

| Expression System | Reaction System | Protein synthesized | Duration hours | Yield (mg/mL) | Reference |
|---|---|---|---|---|---|
| E. coli | CFCF | MS2 coat protein | 20 | 0.1 | [85] |
| Wheat germ | CFCF | BMV coat protein | 20 | 0.18 | [85] |
| E. coli | CFCF | Calcitonin | 40 | 0.06 | [85] |
| E. coli | CFCF | CAT | 25 | 0.1 | [185] |
| Rabbit reticulocyte | CECF | CAT | 34 | 0.1 | [92] |
| Wheat germ | CFCF | DHFR | 24 | 0.2 | [92] |
| Wheat germ | CFCF | DHFR | 20 | 0.917 | [86] |
| E. coli | CECF | CAT | 14 | 1.2 | [88] |
| E. coli | CECF | CAT | 15 | 1.5 | [87] |
| E. coli | CECF | CAT | 8 | 3.5 | [186] |
| Wheat germ | CECF | DHFR | 60 | 4 | [167] |
| Wheat germ | CECF | Luciferase | 60 | 1.1 | [167] |
| Wheat germ | CECF | TMV RNA replicase | 72 | 0.6 | [167] |
| E. coli | CECF | GFP | 21 | 4.4 | [187] |
| Wheat germ | CECF | DHFR | 30 | 0.8 | [188] |
| E. coli | RTS 500 | CAT | 24 | 0.9 | [169] |
| E. coli | RTS 500 | DHFR | 24 | 0.2 | [93] |
| E. coli | RTS 500 | GFP | 24 | 5.9 | [189] |
| E. coli | RTS 500 | Erythropoietin | 24 | 0.3-2.2 | [190] |
| Wheat germ | RTS 100 | GUS | 24 | 0.05 | [191] |
| Wheat germ | RTS 100 | SHR | 24 | 0.794 | [191] |
| Wheat germ | RTS 100 | SRC | 24 | 0.95 | [191] |
| Wheat germ | RTS 500 | SHR | 24 | 1.07 | [191] |
| Wheat germ | RTS 500 | SRC | 24 | 1.34 | [191] |

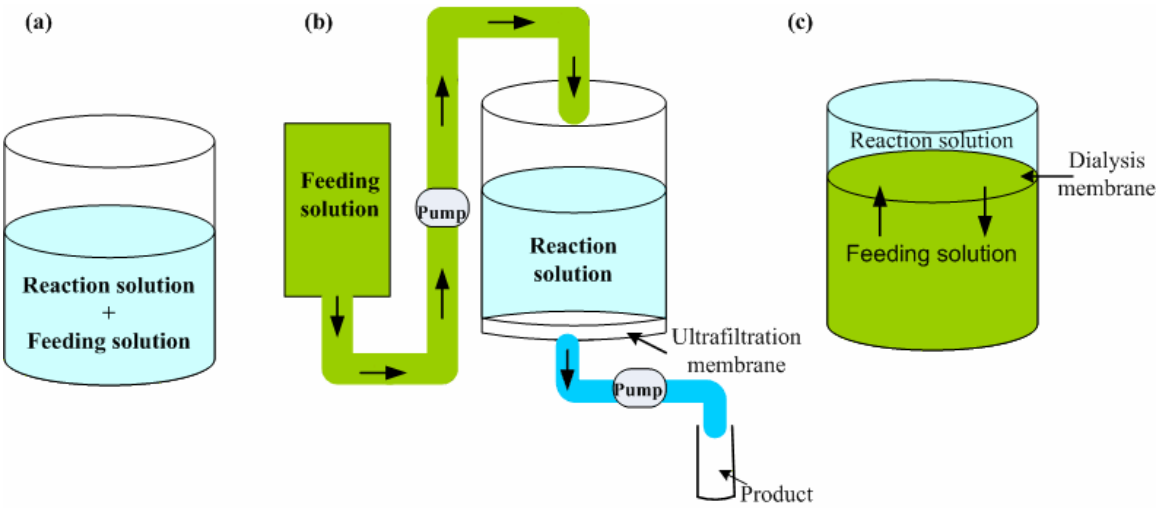


Figure 3-1. Schematic representations of current formats for IVT system. (a) batch (a microcentrifuge tube); (b) continuous-flow cell-free (CFCF) system; (c) continuous exchange cell-free (CECF) system.

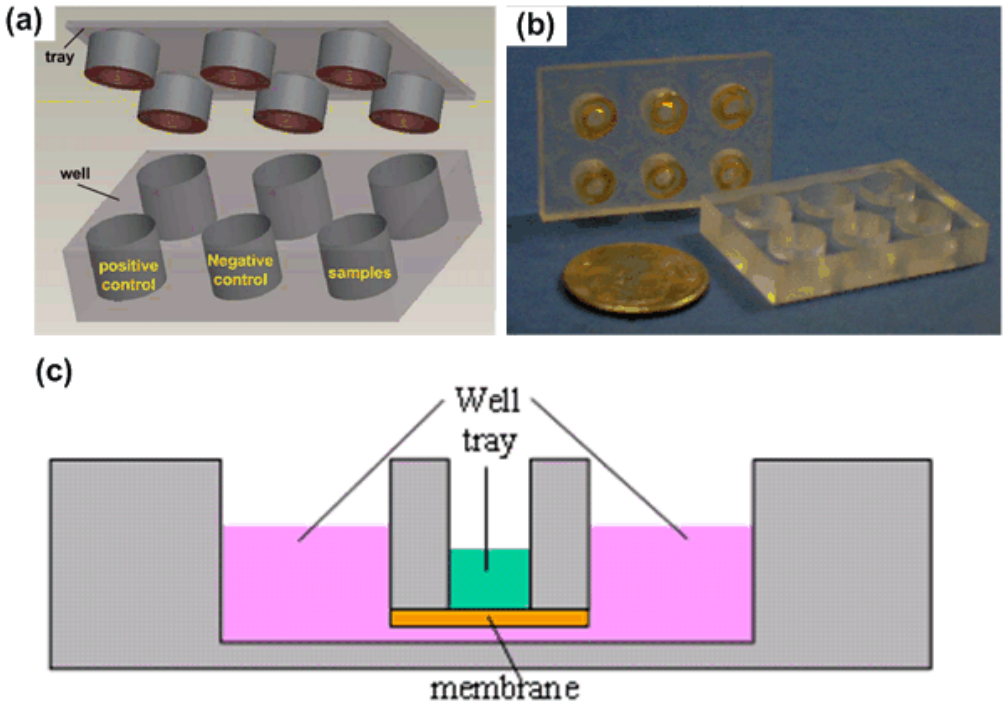


Figure 3-2. Illustrations of an array device I for protein synthesis. The units are laid out according to the standards of 96-well plates (i.e., 9 mm pitch). The tray chamber is for IVT reactions; the well chamber is concentric with the corresponding tray chamber and functions as a nutrients reservoir. (a) Three dimensional view; (b) Picture of both parts; (c) Cross-sectional view of a tray nested in a well, showing the dialysis membrane and fluidic connection.

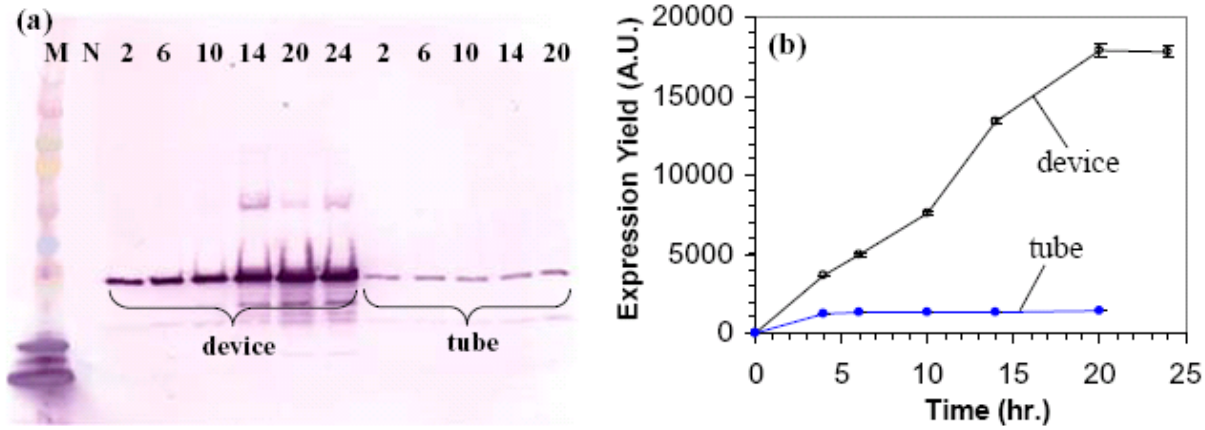


Figure 3-3. Comparison of in vitro GFP synthesis between a device and a microcentrifuge tube. (a) Western blot analysis of GFP expressed. The first lane is protein markers (M) and the second lane is the negative control (N); the lanes on the left are for GFP expressed in the device and the numbers on the top indicate the reaction time (hours); and the lanes on the right are for GFP expressed in the tube and the reaction time is also indicated on the top. (b) The production yield of GFP as the function of the expression time. The data for the device are represented by the open circles while those for the tube are by the closed circles.

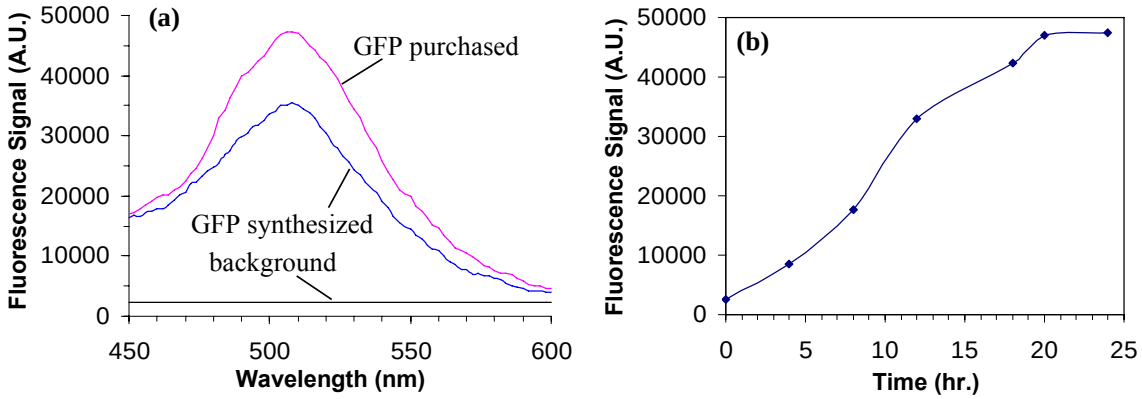


Figure 3-4. (a) Comparison of fluorescence emission spectrum between GFP synthesized and GFP purchased. The excitation wavelength is 488 nm. 5 µL of GFP synthesized is mixed with 35 µL of pH 7.4 PBS buffer to fill in the 50 µL of cuevette. The concentration of GFP purchased is 2 µg/mL in this spectrum. (b) The fluorescent signal as the function of the folding time.

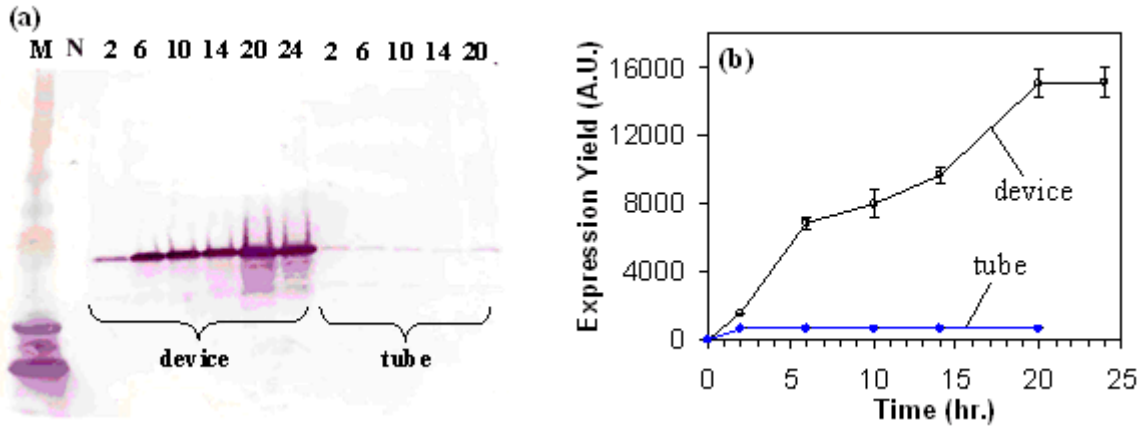


Figure 3-5. Comparison of *in vitro* CAT synthesis between a device and a microcentrifuge tube. (a) Western blot analysis of CAT expressed. The first lane is protein markers (M) and the second lane is the negative control (N); the lanes on the left are for CAT expressed in the device and the numbers on the top indicate the reaction time (hours); and the lanes on the right are for CAT expressed in the tube and the reaction time (hours) is also indicated on the top. (b) The production yield of CAT as a function of the expression time. The data for the device are represented by the open circles while those for the tube are by the closed circles.

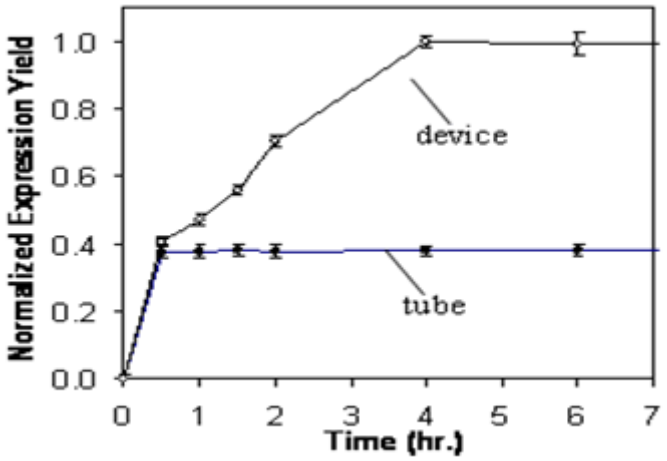


Figure 3-6. Production yield of luciferase as a function of the expression time in the device or in a microcentrifuge tube.

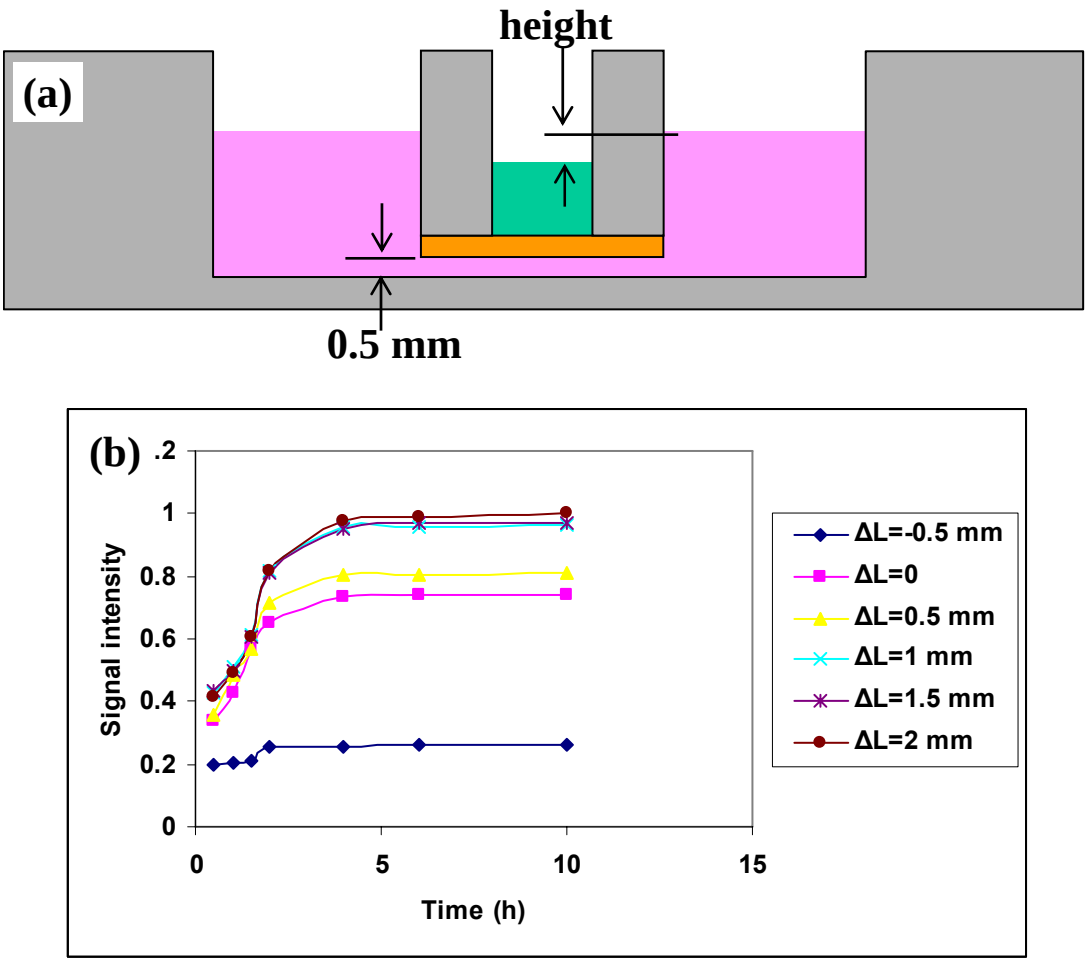


Figure 3-7. The effects of the fluid level difference on the protein expression yield. (a) Device cartoon illustrating the fluid level difference between the tray and well chambers when the connection depth is fixed at 500 μm. (b) Luciferase expression yield as the function of the IVT time. The expression yield is normalized against the experiment showing the highest luminescence signal.

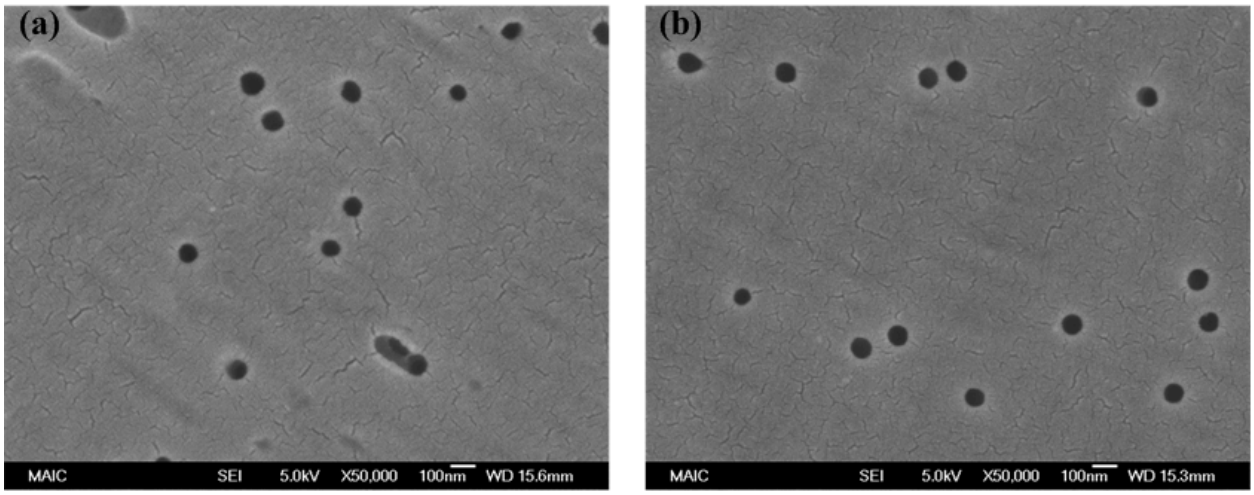


Figure 3-8. SEM images of polycarbonate membrane with 100 nm pore size. (a) room temperature. (b) 170 ◦C.

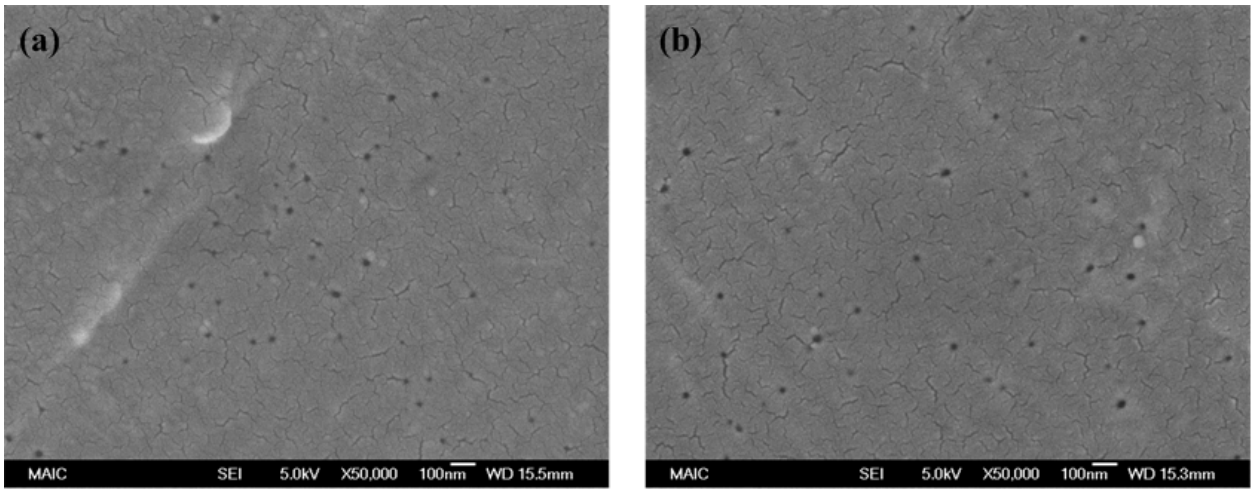


Figure 3-9. SEM images of polycarbonate membrane with 10 nm pore size. (a) room temperature. (b) 170 ◦C.

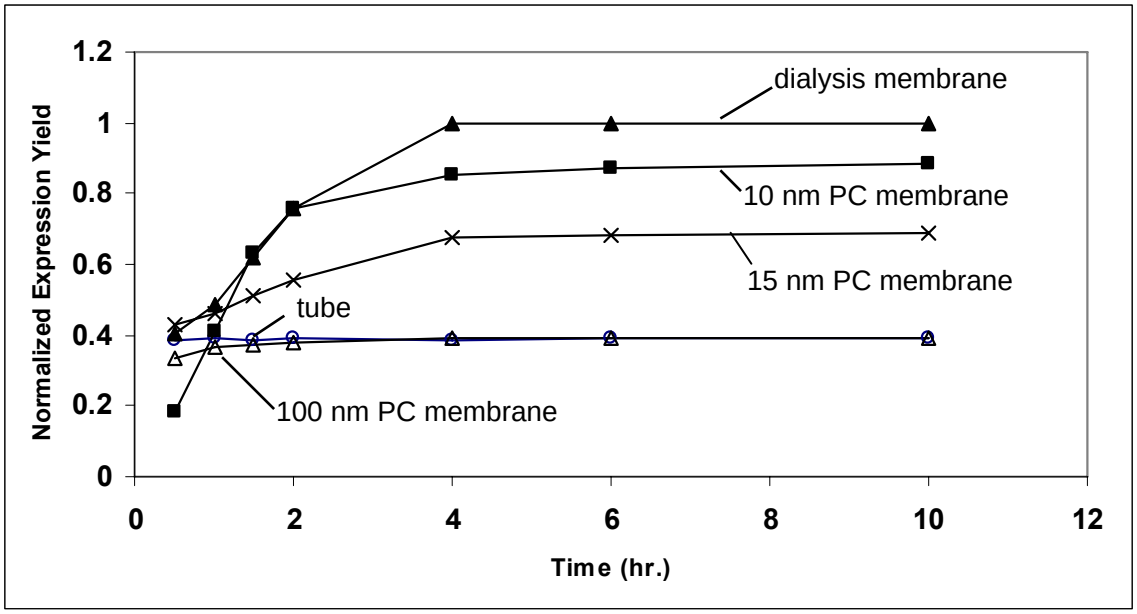


Figure 3-10. Production yield of luciferase as a function of time in the nanopore membrane devices, in the dialysis membrane or in a microcentrifuge tube.

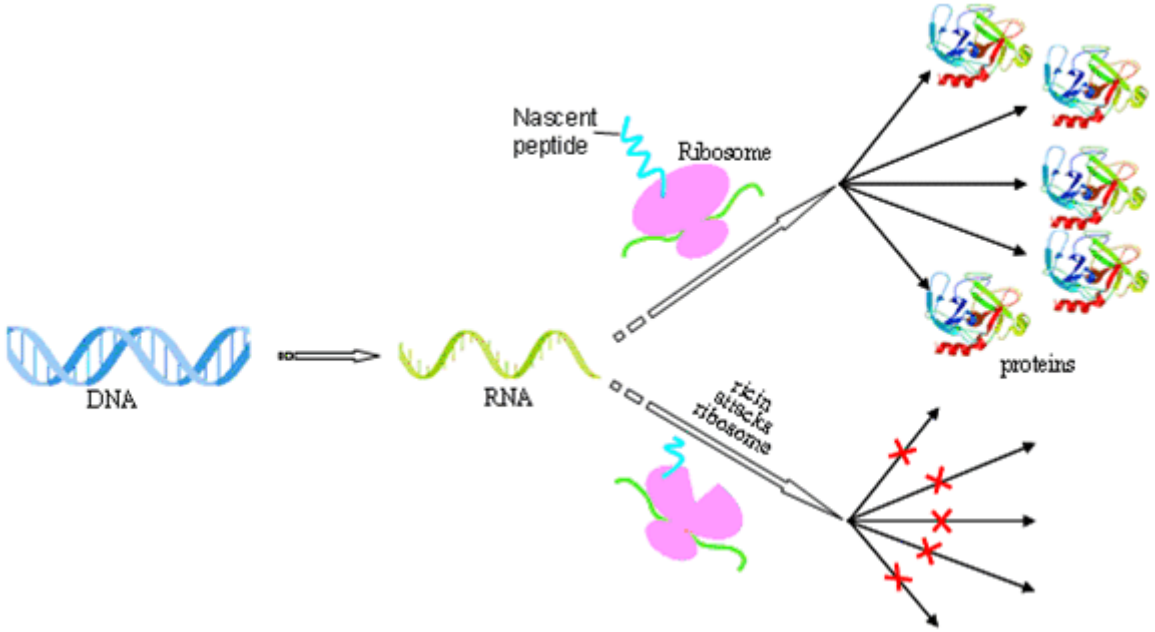


Figure 3-11. Signal amplification as a result of the inhibitory effects of ricin on the production of every copy of protein. Thousands of copies of a protein can be expressed from each copy of DNA when ricin is absent. While ricin is present, the damaged ribosome (indicated with a dent) is unable to produce the corresponding proteins.

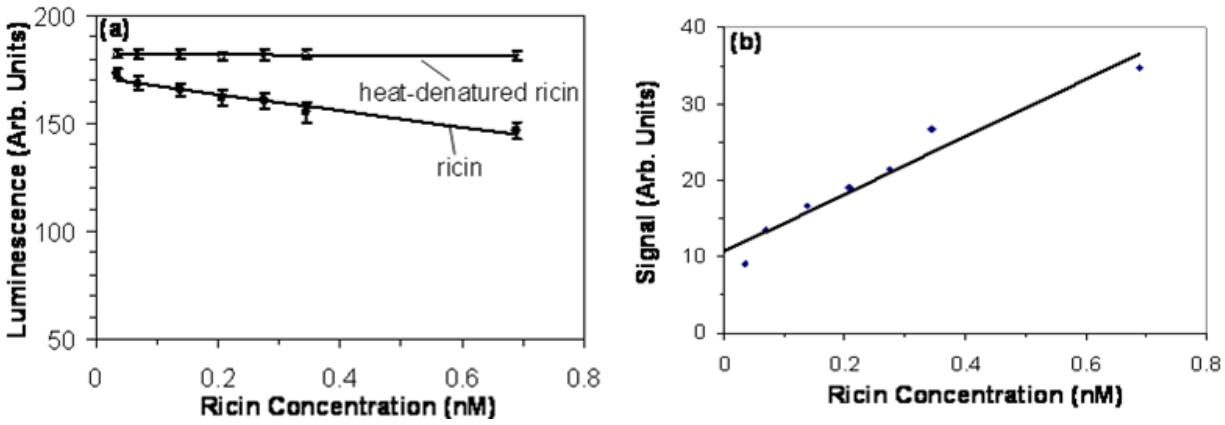


Figure 3-12. The inhibitory effects of ricin on the production yield of luciferase. (a) The expression yield of luciferase (indicated by the luminescence) is plotted as a function of the concentration of ricin A chain (solid circles) and heat-denatured ricin A chain (open circles). Experiments were carried out in the device and the expression time was 4 hours. The error bars are the standard deviation obtained from three repeat experiments. Lines are the best fit of linear regression of the experimental results. (b) Calibration curve for ricin detection. The signal is the difference between the samples and the controls.

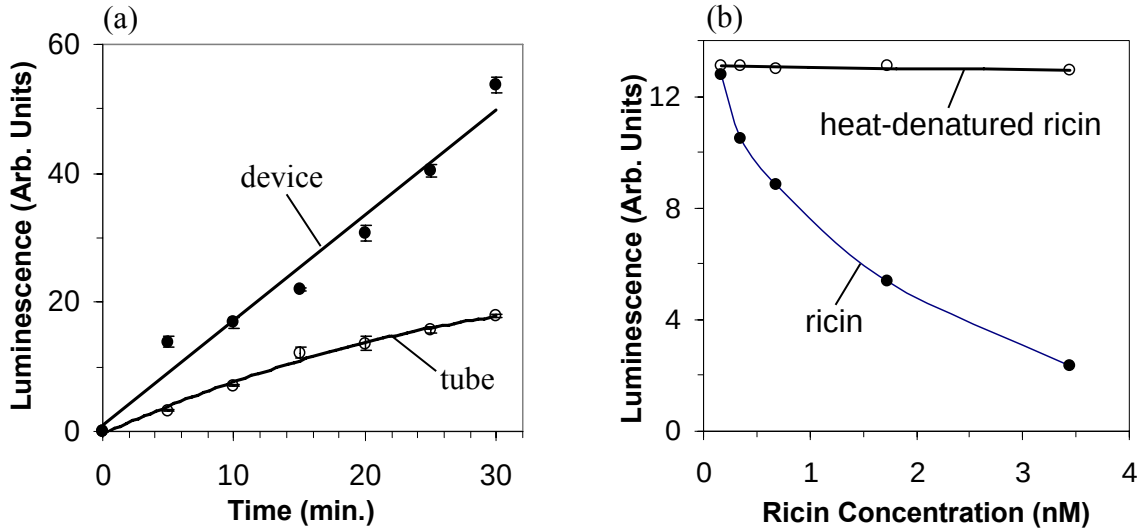


Figure 3-13. Synthesis of luciferase and detection of ricin in a few minutes. (a) Luciferase production as a function of the expression time in a miniaturized device or in a microcentrifuge tube. The expression yield is indicated by the luminescence. A circular DNA vector was used. (b) Protein expression yield, indicated by luminescence, decreased with the concentration of ricin A chain when the expression time was fixed at 5 minutes (solid circles). However, the expression yield remained the same when the ricin's toxicity was deactivated by heat denature (open circles).

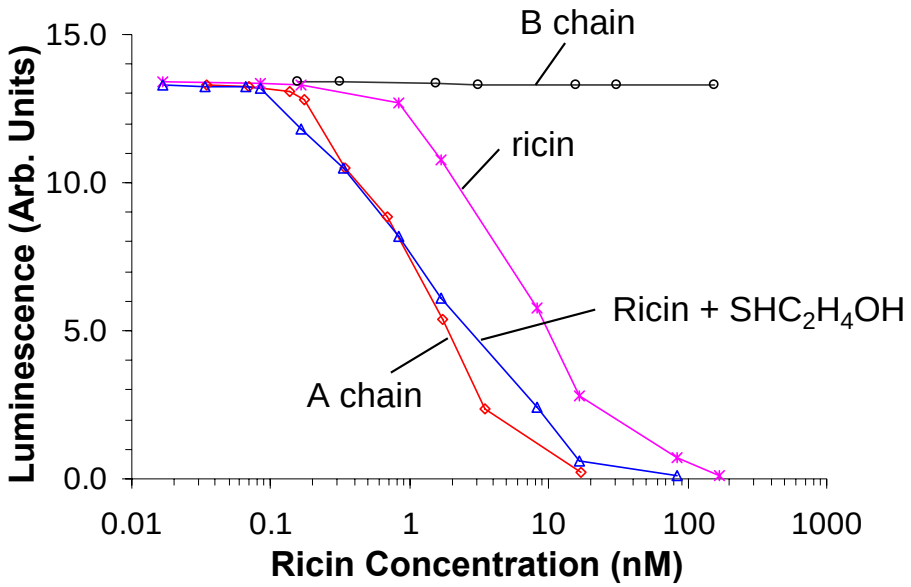


Figure 3-14. Comparison among ricin A chain, B chain, whole ricin, and ricin treated with 2-mercaptoethanol. Luciferase expression yield, indicated by luminescence, is plotted with the concentration of each reagent.

# CHAPTER 4
# FABRICATION OF A MICROFLUIDIC DEVICE AND ITS APPLICATION TO BIOLUMINESCENCE DETECTION

## 4.1 Introduction

As briefly discussed in the first chapter, the purpose of this project is to fabricate an integrated microfluidic system for protein expression that can be used for toxin detection. The system also has a potential to be used in applications like large scale protein engineering, drug screen, etc. So we are more interested in fabricating a protein synthesis and analysis device instead of a protein preparation device. For the latter one, improving the total yield of synthesized protein is one of the most important research focuses and there are several commercialized systems available, like RTS ProteoMaster commercialized by Roche.

To fabricate a miniaturized protein synthesis and analysis device, challenges lie in performing ultra-fast, high sensitive, high throughput and low cost synthesis and assay. There are very limited numbers of reports about protein synthesis in microfluidic devices. Endo et al. fabricated a simple T-shaped mixer to test cell-free translation of poly (U).[95, 192] Fujii et al developed a PDMS-glass hybrid device with temperature controller and successfully synthesize GFP and BFP.[121] More recently, a compartmentalized cell-free protein expression device was fabricated to generate water-in-oil emulsion for protein synthesis.[65]

However, no protein with biofunctionality has been expressed in microfluidic devices in all these papers, including our previous results. The reason is that effective mixing plays an important role for the success of most chemical and biochemical reactions. in the microscale.[193-201] It is well known that the flows inside the microchannels are predominantly laminar due to low Renolds number (Re) and mixing is typically dominated by diffusion.[202, 203] When the mixing relies on molecular diffusion, the total mixing time can be calculated by the following Equation 4-1:

$$t = \frac{d^2}{2D} \tag{4-1}$$

where t, d, and D are the time needed to obtain mixing, the thickness of diffusion path and diffusion coefficient, D, respectively. In order to enhance the mixing performance, a variety of mechanisms to effectively mix in microfluidic devices have been studied and reported. These devices can be categorized as using either active[204-210] or passive mixing[194, 211-234] methods. Most active micromixers facilitate rapid mixing by stirring flow, which require external sources, such as ultrasonic,[205] magnetic force,[208, 210] electro-kinetic field[207, 209] and an acoustic wave.[204, 206] Although these active micromixers are more effective in mixing performance, they are difficult to fabricate, operate and integrate with microfluidic devices. On the other hand, passive micromixers exert no energy input except for the mechanism provided to drive flows at a constant rate. They usually use channel geometry to stir or divide fluids, increasing the interfacial area between fluids and shortening the diffusion length.

Two methods of passive mixing include multi-lamination and chaotic advection. Multi-layer or multi-stage micromixers are designed to twist and split fluids and then to speed fluid mixing in the channel.[215, 220, 223, 226, 230, 235] A representative example is a micromixer with a three-dimensional serpentine channel developed by Liu et al.[211] A serpentine flow channel keeps twisting and stretching the interface between the two fluids, which is effectively at high flow rate (Re =70). This kind of micromixers is not suitable for expensive biological samples or reagents because a large volume of liquid is required. In addition, the microstructures in these mixers are complex, requiring complicated fabrication process such as multi-step lithography or multi-layer stacking. The micromixers based on chaotic advection using simple microstructures in a microchannel have been reported by several research groups in recently years.[212, 213, 218, 219, 228, 229, 236-240] One of most promising examples is the mixer with the bas-relief structure initially

proposed by Stroock et al.[212] In the mixer, helical flows can be produced in a microchannel with patterned grooves over a wide flow rate range ($0.01 \leq Re \leq 10$) and efficient mixing can be obtained in a short distance.

In this chapter, I discussed microfluidic devices consisting of a straight microchannel patterned with herringbone ridges and a spiral channel. The devices we fabricated relatively simple fabrication processes are designed for bioluminescence detection of enzymatic reactions. The PMMA microfluidic devices are replicated by hot embossing with a brass mold, in which the microstructures are milled by a high-precision micromilling machine. The bioluminescent luciferase-luciferin reaction is undertaken in the microflow devices to study the effect of the channel structure on intensity of light emission. The detection of limit of bioluminescent assay in the device is determined. In addition, the factors affecting the enzymatic reaction on the intensity of luminescence are investigated as the function of the flow rate.

## 4.2 Experimental

### 4.2.1 Materials and Reagents

PMMA polymer sheet (5 mm thickness) and cover film (250 μm thickness) were obtained from Plexiglas MC (GE Polymershapes, New Orleans, LA). QuantiLum® recombinant luciferase, T7 luciferase DNA vector, TNT wheat germ extract system and luciferase assay system were acquired from Promega (Madison, WI), while acetylated bovine serum albumin (BSA) was from Sigma-Aldrich (St. Louis, MO). Phenolphthalein, sodium hydroxide and Alconox were from Fisher Scientific (Atlanta, GA).

### 4.2.2 Device Design and Fabrication

The design of microfluidic device is shown in Figure 4-1a. Two devices, called device I and device II, are used in bioluminescent reaction experiments. Each microfluidic deivce is composed of T-shaped inlets, a straight channel connected to a spiral channel, and one outlet.

Device II possesses herringbone ridges in the straight channel for better mixing whereas device I does not. The detail of herringbone ridges is illustrated in an exploded view in the figure insert. All straight and spiral channels are 200 μm wide and 100 μm deep, except where specified otherwise. The herringbone ridge is 50 μm wide and 25 μm high. The patterns of the devices are designed using AutoCAD and then milled in a 6.3 mm thick brass (353 engravers brass, McMaster-Carr) with a high-precision micromilling machine (Kern MMP 2522). Micromilling i carried out at 40,000 rpm using 500-, 200- and 50 μm-diameter milling bits with the corresponding feeding rate of 200 mm/min, 120 mm/min and 15 mm/min using procedures described previously.[241] The negative relief of the pattern is hot embossed into the PMMA sheets using a commercial hydraulic press (Precision Press TS-21-H-C, City of Industry, CA). The brass mold and PMMA substrate are put into a vacuum chamber to remove air at the pressure of 8 kPa. During hot embossing, the mold is heated at 150 °C and then pressed to PMMA substrate with a force of 1000 lb for 4 min. Following embossing, the chamber is removed from the press and the embossed PMMA substrate was cooled. After the holes are then drilled at the ends of each channel serving as solution reservoirs for samples into and out of the device, the devices are thoroughly cleaned with 0.5% Alconox solution and DI water in an ultrasonicated bath and dried with compress air. For the final assembly, the open face of microchannel on PMMA substrate is thermal bonded to a thin PMMA film. That is, the PMMA device and thin film are clamped between two glass plates and put in a convection oven at 107 °C for 20 min. Figure 4-2 shows a picture of the assembled plastic device and the convection oven used in our study.

### 4.2.3 Mixing of Phenolphthalein and NaOH

Phenolphthalein is a pH indicator and changes its color from colorless to pink when the value of pH is larger than 8. It is easy to observe the color change by the naked eye so the

reaction between phenolphthalein and NaOH is used to simply demonstrate the performance of the device. 1% phenolphthalein and 0.05 mol/L NaOH are injected into microchannels by a syringe pump (PHD 2000, Harvard Apparatus, Holliston, MA) at the flow rate of 1 μL/min. When phenolphthalein and NaOH meets and reacts inside the channel, the color change are observed and captured by Nikon upright microscope equipped with a DXM 1200 color CCD camera.

### 4.2.4 Simulation

Computational simulation of 3D flow field and two-fluid mixing through a microchannel based on Finite Volume Method was carried out in the computational fluid dynamics (CFD) package, CFD-ACE (ESI Group, Huntsville, AL). The depth and width of the channel are set at100 μm and 200 μm, while the width and height of the ridge are set at 50 μm and 25 μm. 1.2-mm and 6-mm-long channels corresponding to one cycle of herringbone ridges and five cycles of herringbone ridges are examined. The 3D geometric models of microchannel and 8-node hexahedral elements are built by CFD-GEOM to achieve a stable solution. The density of mesh elements for the 1.2-mm-long channel is studied and optimized to speed up convergence and produce accurate simulation results. The flow module in CFD-ACE is used to solve the incompressible Navier-Strokes equations. The simulations are run with an assumption of a steady and laminar flow of a Newtonian fluid. Both inlets are assigned with a pressure of 10 Pa. Pure fluid 1 and fluid 2 are in the two inlets; their diffusion coefficient (D) is set at $1.0 \times 10^{-6}$ $cm^2/s$. No-slip condition is assumed at all channel walls and the outlet is set at atmospheric pressure. Conjugated Gradient Squared (CGS) and Preconditioning (Pre) solver are used for velocity and species, and Algebraic MultiGrid (AMG) solver is used for pressure correction. The central differencing scheme (with blending set to 0.1) and second-order upwind scheme are

adopted for the velocity and concentration calculations, respectively. The maximum iteration is 1000, while the convergence critical is $10^{-4}$ and minimum residual is $10^{-18}$.

### 4.2.5 Bioluminescence Reaction

Luciferase, an enzyme found in the firefly, catalyzes luciferin oxidation in the presence of adenosine triphosphate (ATP), magnesium ion as well as oxygen and generates the light with a peak emission at ~560 nm. A luciferase assay kit contains optimal concentration of luciferin, magnesium, ATP and coenzyme; appropriate reconstitution of these components forms luciferase assay reagents (LAR). A series of dilution of recombinant luciferase from 14.6 ng/mL to 14.6 μg/mL is obtained in 1 x cell culture lysis reagent (provided by the luciferase assay kit) with 1 mg/mL acetylated BSA; they are used to investigate the detection of limit in microfluidic devices. Addition of BSA prevents luciferase from nonspecific adsorption to the walls of the device, eliminating possible background signal.

*In vitro* synthesis of luciferase is carried out in wheat germ extract as previously reported. Briefly, The reaction mix of 50 μL for luciferase synthesis was prepared by combining 25 μL wheat germ extract, 2 μL reaction buffer, 1 μL T7 RNA polymerase, 1 μL of 1 mM amino acid, 1 μL Ribonulease inhibitor and 19 μL nuclease-free water containing 1 μg of luciferase DNA vector. Incubation was performed in a microcentrifuge tube at 30 °C for 1.5 hours.

Recombinant luciferase or synthesized luciferase and LAR are injected into a device by a syringe pump with two 50-μL glass syringes (SGE International Pty. Ltd., Austin, Texas) at a constant flow rate. The syringes are connected to the fused-silica capillaries through low dead volume luer-to-microtight assembly (P-662, Upchurch Scientific, Oak Harbor, WA), and the capillaries are glued into reservoirs on microchip to deliver the reagents into microchannel. Various volumetric flow rates are tested to investigate the effect of the flow rate on the enzymatic catalysis of bioluminescence. A thermoelectrically cooled (-70°C) CCD camera

(Roper Scientific Instrumentation, Trenton, NJ) coupled with an optical lens subsystem (4X Zoom) is used to capture the image of luminescence along the channel direction. The device is installed on a X-Y stage, so that different region in the device can be imaged as shown in Figure 4-3. The setup is in a black box to reduce the background signal. For each measurement, an image of 1024 x 1024 pixels was collected with an exposure time of 60 s. The quantitative data of each image are analyzed quantitatively using the software Winview 32.

## 4.3 Results and Discussion

### 4.3.1 Device Fabrication

As mentioned above, we exploit a high-precision micromilling machine to fabricate a mold, which was then used as the master for replicating microfluidic device. The approach is simple, with low cost and quick turn-around time. In addition, the mold can be used for a wide range of thermoplastics by hot embossing, compress molding or injection molding.

The devices are made from polymethylmethacrylate (PMMA). The straight channel in device II contains staggered herringbone mixer (SHM) as reported. Alternating cycles of asymmetric herringbone ridges are incorporated to improve the mixing efficiency because interfacial area and the bulk advection will increase due to the three dimension ridge structures.[212] The spiral channel is designed to obtain enough length for possible long time reaction in the device. The layout of the device is shown in Figure 4-1. The device consists of two inlet channels joined by a T-junction, a straight channel of 6.6 mm length, a 56-mm-long spiral channel, and an outlet. Several sets of T-junctions inlets are designed to enclose numbers of herringbone ridges in the channel. Each set is comprised of 5 cycles of asymmetric herringbone structures, which are composed of twenty single ridges. Only the first set of inlets numbered 1 and 2, and the fifth set of inlets numbered 9 and 10 are used in this work. The

straight channel in device I is smooth without any feature, functioning as the baseline control to evaluate the performance of the herringbone structure channel.

### 4.3.2 Embossing Fidelity

As discussed before, hot embossing is an easy and mass-productive method for replication of the micropatterns. The embossing is achieved by pressing a brass mold into the PMMA substrate at desired temperature in a vacuum chamber and then the desired microstructures are transferred into the plastic substrate within a few minutes. The topology of the plastic device is the negative image of the brass mold so the device has the exactly same pattern as the microfabricated brass mold. The brass mold and the embossed PMMA device coated with a thin layer of Au are observed under scanning electron microscopy (SEM) to examine the detail features. The pictures in Figure 4-4a and b show the SEM photography of the brass mold and plastic device with the portion of staggered herringbone structure. The plastic substrate shown in Figure 4-4b is a negative image of Figure 4-4a, i.e., a ridge becomes a channel. The results indicate the microstructures are successfully transferred from the mold to the plastic device at a high degree of fidelity.

The depth of groove (or the height of ridge) and width are determined and quantified by a non-contact profiler (Nanovea ST 400, Allentown, PA). Typical 3D profiler results are shown in Figure 4-5. The depth and width of the channel are 100 μm and 200 μm, while the height of the ridge is about 25 μm. The replication of the overall layout in Figure 4-5a and b shows additional evidence of a high degree of fidelity during the transfer from the brass mold to plastic substrate.

### 4.3.3 Holes Drilling

Before final assembly of PMMA substrate and thin film, access holes are drilled at the end of each channel to serve as reservoirs for samples and wastes. Originally, 1 mm-diameter holes are drilled by a milling machine. The end of the capillaries (OD 360 μm) is glued into a hole on

the assembly device as shown in Figure 4-6. It is noted that when two solutions are injected into the microchannels, the air bubbles are continuously produced inside the channel at the first 30 µl solution pumping in both device I and II (Figure 4-7), which has an effect on mixing of the solutions. It also can be seen from Figure 4-7b that a small bubble is always trapped by the ridge structure and it is difficult to remove the bubble from the channel. In some cases, the solution flows from one inlet to the other. This phenomenon can be explained by the large dead volume formed in the reservoir during the fabrication process. Figure 4-8a provides a clear view of the dead volume in the reservoir when the OD 360 µm of capillary sits into a 1 mm-diameter hole. To shrink the dead volume, the small size of holes is created using laser ablation technique. 400 µm-diameter of holes were drilled by a UV laser with 264 nm wavelength. After inserting 360 µm OD of capillary into the laser drilled hole, no dead volume is observed under the microscope as shown in Figure 4-8b.

### 4.3.4 Reaction of Phenolphthalein and NaOH

To evaluate the performance of device I and II, a simple experiment of mixing phenolphthalein and NaOH was first carried out. Two solutions of 1% phenolphthalein and 0.05 mol/L NaOH were pumped into the microchannels at the flow rate of 1 µL/min. As discussed before, when phenolphthalein meets and reacts with NaOH, its color changes from colorless to pink. Therefore, the interface between two solutions can be easily observed by the pink color. Figure 4-9 shows the experimental results for the device I and II. In the case of device I, two solutions flow in parallel and the reaction only takes place only at the center of the channel so that the interface is clearly observed. The fully mixing is not achieved at the spiral channel only by pure diffusion as indicated in Figure 4-9a. However, figure 4-9b shows the mixing has been completely achieved after the solutions pass through a set of the herringbone structure. We can

obviously tell the advantage of device I over device II by naked eyes. It should be mentioned that the air bubbles are produced in both devices due to large dead volume of the reservoir.

### 4.3.5 Effect of Herringbone Ridges

As discussed in Section 4.2.4, luciferase and LAR are pumped through inlets 1 and 2 into the microchannel simultaneously. When luciferase meets with LAR at the T-intersection, catalytical reactions start and generate the luminescence. Therefore, the mixing efficiency can be inferred from the luminescence detected. Figure 4-10 shows the top view luminescence images of both devices I and II, when the flow rate is at 1 μL/min and the concentration of luciferase is 14.6 μg/mL. These images are obtained from a cooled CCD camera. Only a part of channel is recorded due to the field view of the camera. In microdevice I without herringbone structures, two solutions flow in parallel in a laminar flow as expected. Two solutions interact with each other only in the centerline of the entire channel, as suggested by the stable interface in Figure 4-10a. The thickness of the luminescent trace slowly increases along the channel. The mixing is not completed even at the end of the spiral channel. In contrast, the interfacial line between two fluids disappeared almost immediately after they enter into the region containing herringbone structures, as shown in Figure 4-10b. Two fluids were completely mixed before the end of the region with herringbone ridges.

The mixing efficiency is analyzed by calculating the intensity of the luminescence on a line perpendicular to the microchannel by the following formula:[94]

$$\bar{I} = \frac{\Delta y \sum_i I_i}{w I_{\max}} \tag{4-2}$$

where $\bar{I}$, $\Delta y$, $I_i$, w and $I_{max}$ represent the normalized average intensity, interval between sampling points, intensity at sampling point i, width of the channel and maximum intensity

among the sampling points. The numerator in Equation 4-2, $\Delta y \sum_i I_i$, defines the area of intensity profile.

The normalized average intensity, based on equation (2), at different positions downstream for device I and II is plotted in Figure 4-11. The luminescence intensity in device I increases along the microchannel from 0.11 at the inlet to 0.3 at the distance of 30 mm. However, the signal of device II increases from 0.76 to 0.99 and reach the maximum at 24 mm, which consists of three sets of herringbone pattern. The average intensity of the device II grows much faster that of the device I, indicating that alternate repetition of the set of herringbone structure improves fluid mixing efficiently. It is shown that the normalized average intensity I can be represented by the equation:[218-220]

$$I=1-\exp(-x/\lambda) \qquad (4\text{-}3)$$

where x is channel axis and λ is a required mixing length. It can be seen that I is 0 at the cross of inlets and reaches 1 at certain length of the channel. λ is considered as a required mixing length when the intensity I increase from 0 to 0.632.[218-220] The required mixing length of device I and II are 88.18 mm and 5.41 mm, respectively. It is shown that the required mixing length of device II is 16 fold shorter than device I. These results indicate that device II has better mixing performance and one set of herringbone ridge is enough to improve the mixing efficiency.

Several research groups have reported the computational work concerning the staggered herringbone mixer, including the geometric effects on the mixing performance and the velocity profiles in the mixer.[213, 228, 236, 238] Here we utilize the CFD simulation results of the concentration distribution in the microchannel to visualize the process of mixing. Figure 4-12 displays the concentration distributions along the channel of both devices, indicating the mixing processes of those two devices are totally different. From Figure 4-12b, it can be seen that the

distortion of the interface in the channel with herringbone structure, where there is no distortion occurred in the straight channel. The simulation results are highly consistent with the experiment results, as shown in Figure 4-11.

### 4.3.6 Simulation Results

Several research groups have reported the computational work concerning the staggered herringbone mixer, including the geometric effects on the mixing performance and the velocity profiles in the mixer.[213, 228, 236, 238] Here we utilize the CFD simulation results of the concentration distribution in the microchannel to visualize the process of mixing. The density of mesh elements for 1.2 mm of channel length is first studied. The typical dimension of mesh elements are set at 0.833, 1.5625, 3.125, 6.25 and 12.5 μm, corresponding to the number of mesh elements at 344926, 256418, 205842, 180554 and 167920. The concentration distributions in the cross-section of the ridge channel with different numbers of the mesh element are shown in Figure 4-12. Figure 4-13 indicates that the computational residue plot is converged for velocity, pressure, and sample concentration when the dimension of mesh element is set at 3.125 μm. Simulations indicate higher number of the mesh elements could achieve more accurate concentration distribution in the channel, although all the residue plots (data are not shown) show the solution is converged. It is known that large number of mesh elements requires longer time to achieve the results, though it may give more accurate solution. For 6 mm long channel, we choose the medium dimension size of 2.5 μm, therefore the number of mesh element is about 1299780. Figure 4-14 displays the concentration distributions along the channel of both devices, indicating the mixing processes of those two devices are totally different. From Figure 4-14b, it can be seen that the distortion of the interface in the channel with herringbone structure, where there is no distortion occurred in the straight channel. The simulation results are highly consistent with the experiment results, as shown in Figure 4-11.

### 4.3.7 Detection of Limit

The luciferase protein is frequently used as a reporter gene for measuring promoter activity or transfection efficiency in biological studies. As a result, we studied the detection limit of luciferase and dynamic range of detection using the current setup. To obtain these results, a series of concentrations of luciferase is pumped into Devices I or II. Both luciferase and LAR are pumped at the constant flow rate of 1 μL/min, while LAR concentration maintains at the constant. Since the intensity of generated light is proportional to the amount of luciferase in the reaction when luciferin and ATP are in excess,[242] we can get a calibration curves between the light intensity and luciferase concentration. Figure 4-15 shows the luminescent intensity in the region of spiral channel as a function of luciferase concentration. The plots display a linear relationship in both devices as expected. The error bar of each data point indicates the standard deviation that was obtained from three repeat experiments. The data shoe a dynamic detection range from 0.7 μg/mL up to 14.6 μg/mL and a correlation coefficient ($R^2$) of 0.997 using microfluidic device 1. However, the detection limit for microfluidic device II is 0.0146 μg/mL and the dynamic range is up to 14.6 μg/mL with $R^2$ of 0.994. The detection limit for luciferase was defined as the concentration of luciferase producing an analytical signal equal to three-times the standard deviation of the blank bioluminescence intensity. The sensitivity for luciferase in the mircodevice II was increased by 48 fold compared to that in device I. Therefore, the sensitivity for luciferase obtained in the microfluidic device with the herringbone structure can be used to detection of *in vitro* synthesized protein in microfluidic device.

### 4.3.8 Effect of Flow Rate

The dependence of the luminescence intensity on the flow rate was investigated in device I and II. Reagents are introduced in inlets 9 and 10 and only one set of herringbone feature is contained in the channel. The concentration of luciferase is 14.6 μg/mL. Figure 4-16 shows the

CCD image of the spiral channel at the various flow rates. Calculated normalized intensity was plotted as the function of location for both devices, as shown in Figure 4-17. For the range of flow rates from 1 to 8 μL/min, the signal intensity of device II is much higher than that of device I, which confirms again the herringbone structure in the channel providing much more efficiency of mixing. Based on Equation 4-3, the required mixing lengths of device II are 5.75, 6.97, 9.67 and 12.79 mm, and those of device I are 77.94, 97.18, 116.78 and 176.40 mm, corresponding to the flow rates of 1, 2, 4 and 8 μL/min. These results indicate that the required mixing length increases as flow rate increases.

No surprising, mixing intensity in the device I decreases with increasing flow rate due to the reduction in the molecular diffusion of the reactants. However, luminescence intensity in the microreator II reduces with the increase of the flow rate, which could be explained the light generated from the luciferase assay reaction is the rate-determining. In such type of enzymatic reaction in the micro scale, mixing and reaction occur simultaneously rather than consecutively so that reactions may be limited by insufficient mixing.[243] DeLuca and MaElroy presented evidence indicating there are two distinct rate-limiting steps that occur after rapid mixing of ATP, luciferin and luciferase before maximum light emission reaches.[242] After mixing, there is a lag of 25 msec at room temperature before any light is emitted and then the rate of light emission rises slowly to the maximum in about 0.3 sec. Therefore, the decrease of the luminescence intensity can probably be attributable to a reduction in the residence time of the reactants, since the increase in the flow rate could be responsible for the decrease in the residence time of the reactants.

### 4.3.9 Detection of Synthesized Luciferase

*In vitro* synthesis of luciferase is carried out using wheat germ extract in the microcentrifuge tube as reported previously. Synthesized luciferase and LAR are pumped into

the inlets 9 and 10 using both devices I and II at the flow rate of 1 μL/min. Detection of the expression product is achieved by monitoring the intensity of luminescence after mixing the product with LAR. Figure 4-18 shows the experimental results of online detection of synthesized luciferase in device II. The amount of synthesized luciferase in a microcentrifuge tube is about 0.0146 ng/μL according to the detected signal and the calibration curve in Figure 4-16. However, the sample can not be detected using device I. It is suggested *in vitro* luciferase synthesis could be carried out in the device II.

## 4.4 Conclusion

We have developed a microfluidic device consisting of the straight channel with the herringbone ridge at the bottom wall and the spiral channel for luminescence detection. The PMMA microfluidic device was hot embossed from the brass mold, which was fabricated with a high-precision micromilling machine. Therefore, the fabrication of PMMA devices can be easily implemented with low cost. The efficiency for the luminescence detection of luciferase in the microfluidic device was relied on the microstructure of the channel within the devices, indicating the device with herringbone feature has a better mixing performance. It may be noted that luminescence intensity decreased as the flow rate increased for both devices. In addition, the device II can be used to detect *in vitro* synthesized luciferase. A device with a similar feature may be used for cell-free protein synthesis and online detection.

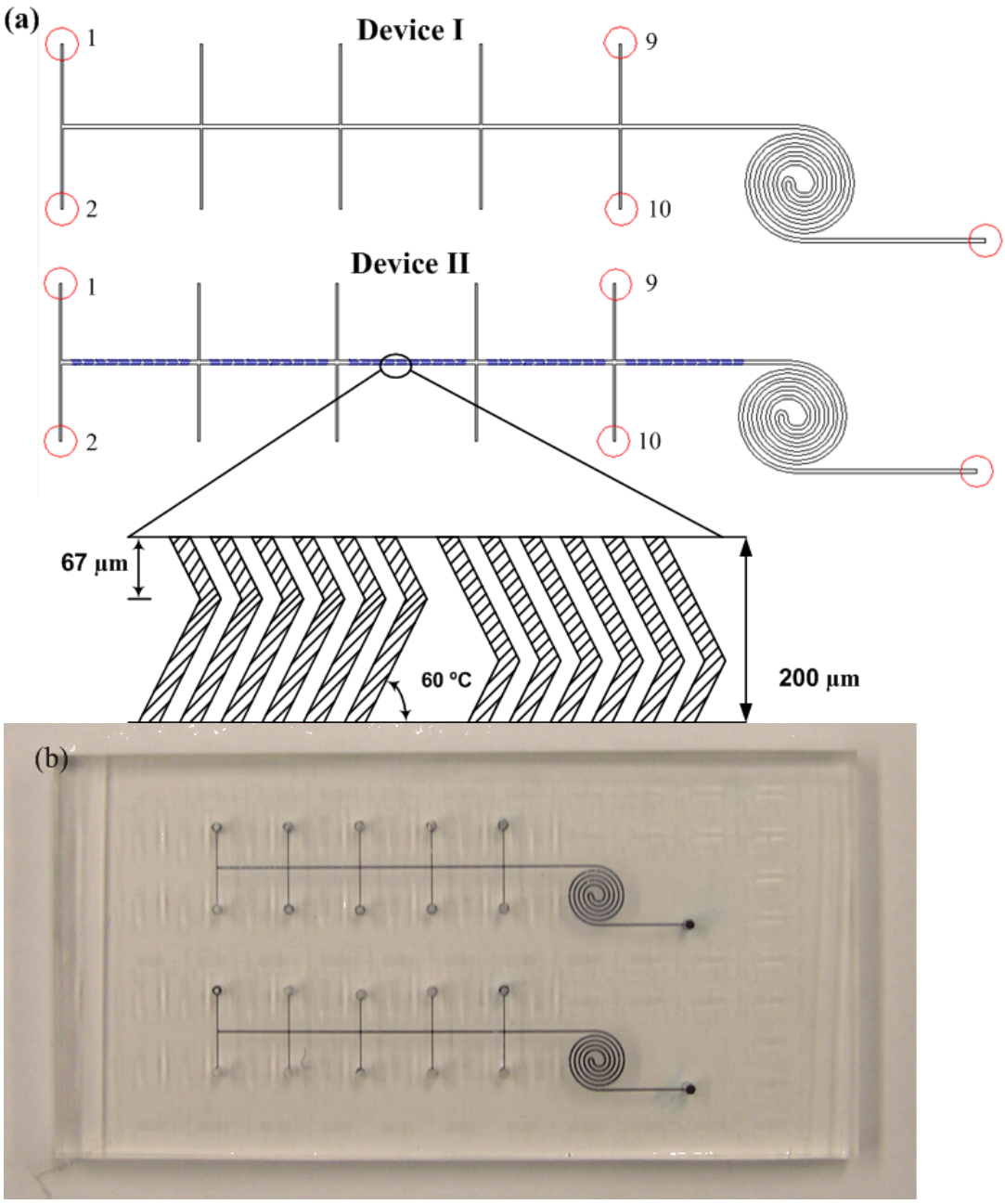


Figure 4-1. (a) Schematic diagrams of two types of microfluidic devices; Top: Microfluidic device I; Bottom: Microfluidic device II. Both devices consist of multiple T-shaped inlets, a straight channel, a spiral channel for reactions and one outlet. Device II possesses herringbone ridges in the straight channel whereas device I does not. The depth and width of all channels are 100 µm and 200 µm, except where specified otherwise. The pattern and geometry of the staggered herringbone groove. The groove is 50 µm wide and 30 µm deep. (b) Picture of a plastic microfluidic device for luciferase detection. Channels and wells are in the plastic substrate, which is thermal bonded with a thin film.

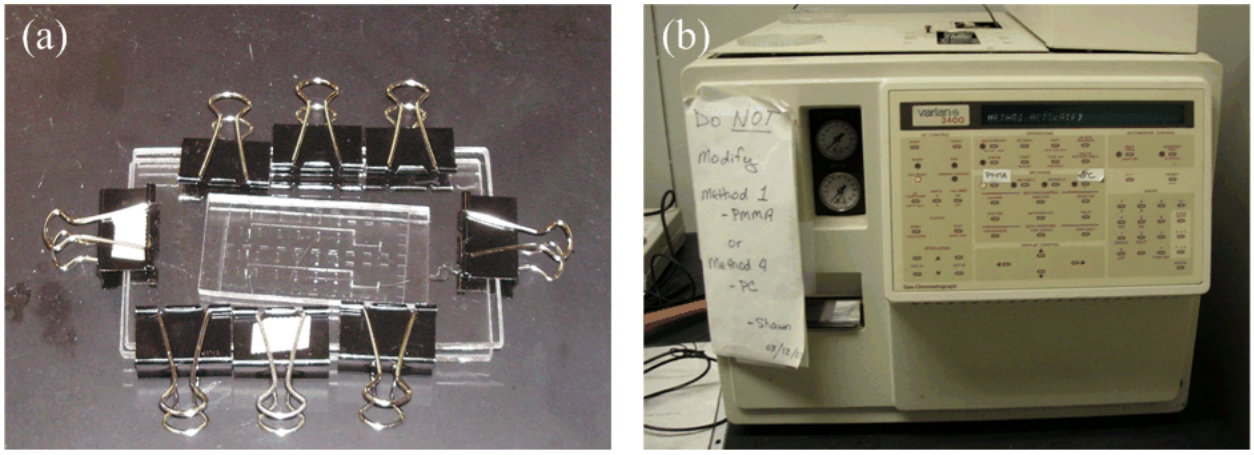


Figure 4-2. (a) The picture of pre-assembly device for thermal bonding. (b) A convection oven.

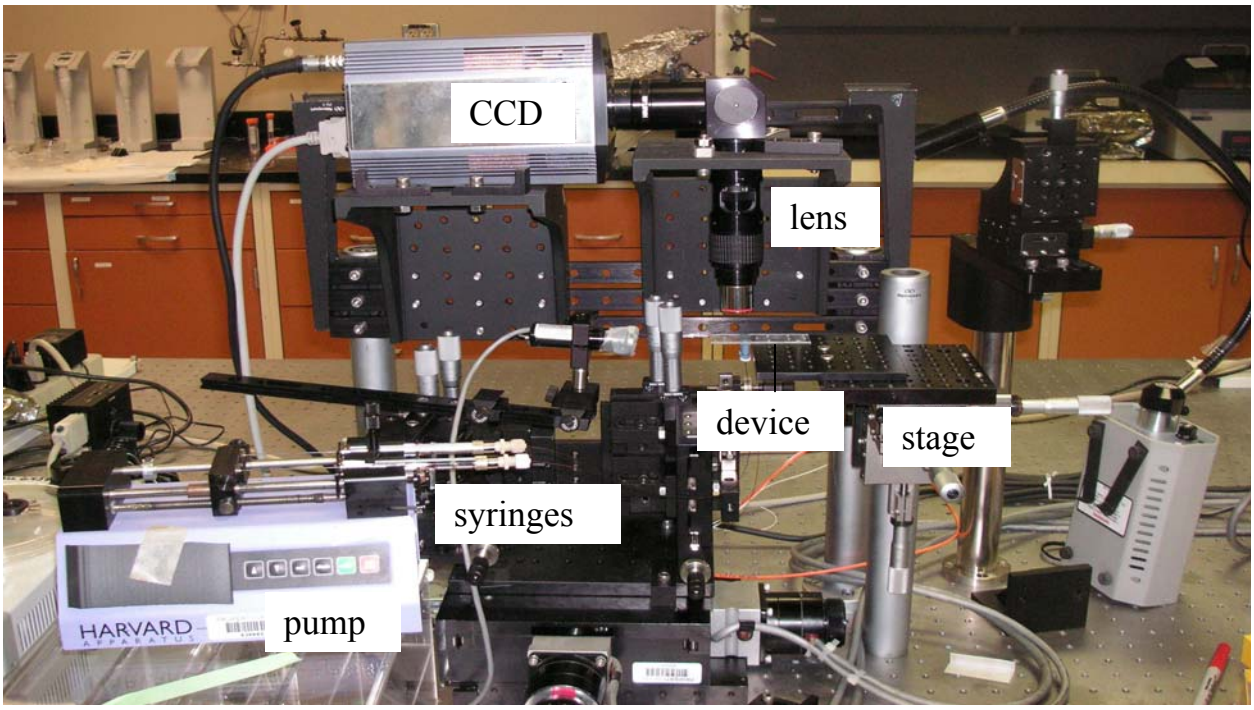


Figure 4-3. Photograph of experimental setup for bioluminescent reaction.

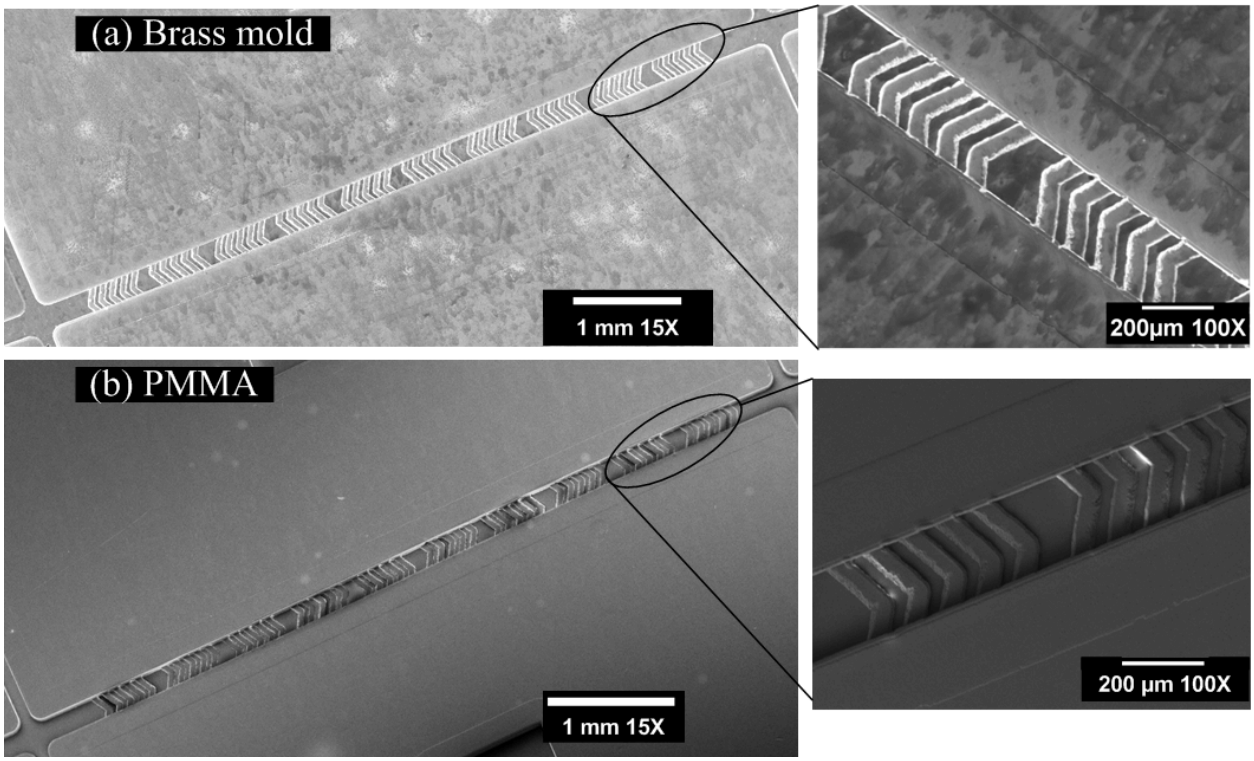


Figure 4-4. SEM pictures of a portion of the channel with the herringbone structure. (a) The brass mold. (b) A representative PMMA substrate. The length of the scaling bars is 1 mm in pictures and 200 μm in the exploded view.

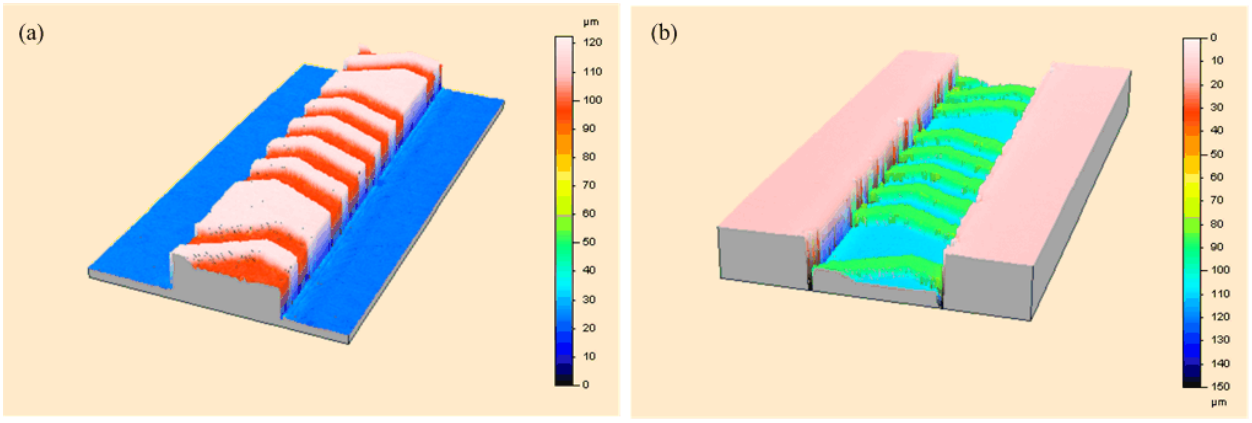


Figure 4-5. Typical 3-D profiler results. (a) The brass mold. (b) A representative PMMA substrate.

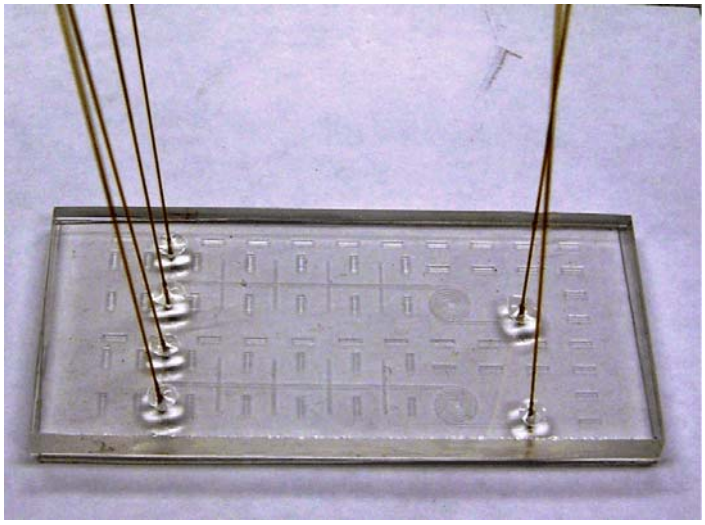

Figure 4-6. The picture of the integrated plastic device.

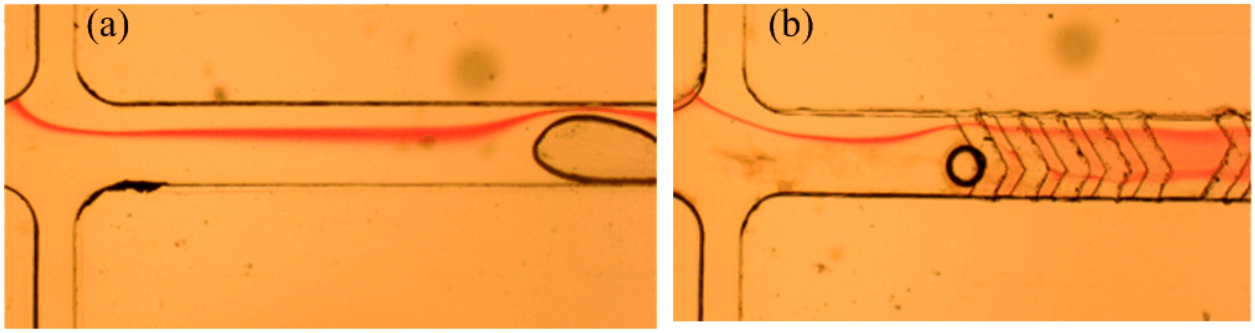


Figure 4-7. The images of air bubbles produced inside the channel. (a) Device I. (b) Device II

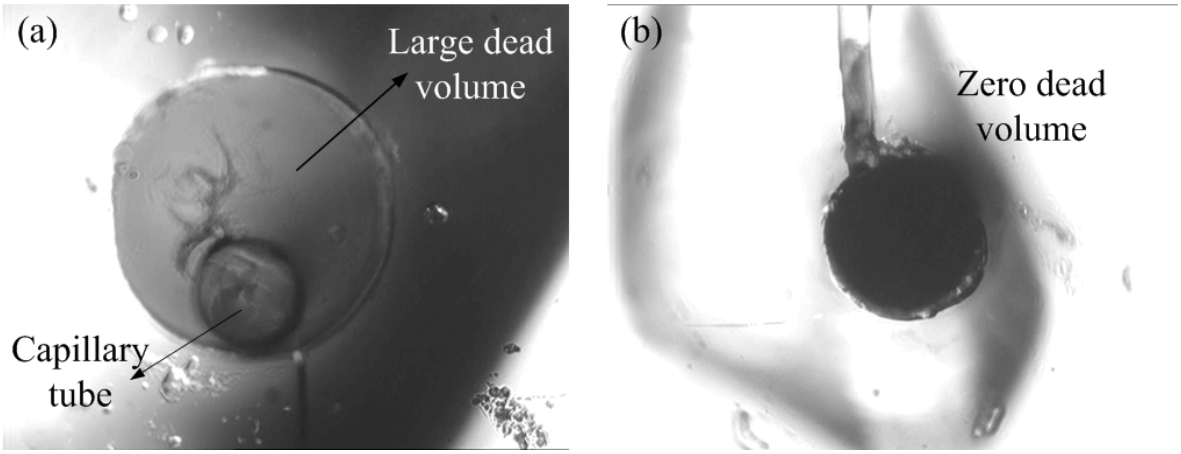


Figure 4-8. The images of a capillary with OD 360 µm inserting into a hole. (a) A mechanically drilled 1 mm-diameter hole. (a) A laser drilled hole of 400 µm.

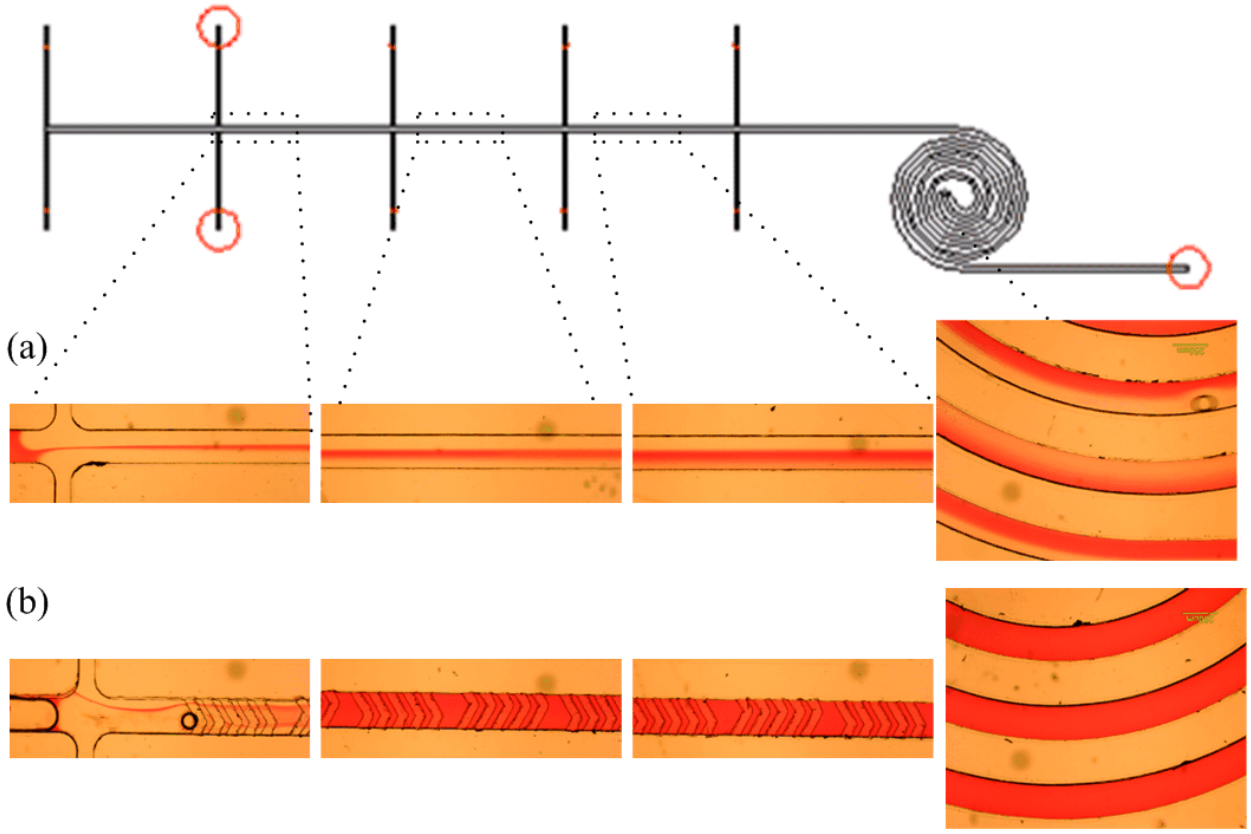


Figure 4-9. Mixing of phenolphthalein and NaOH at the flow rate of 1 μL/min at the indicated locations. (a) Microfluidic device I and (b) Microfluidic device II.

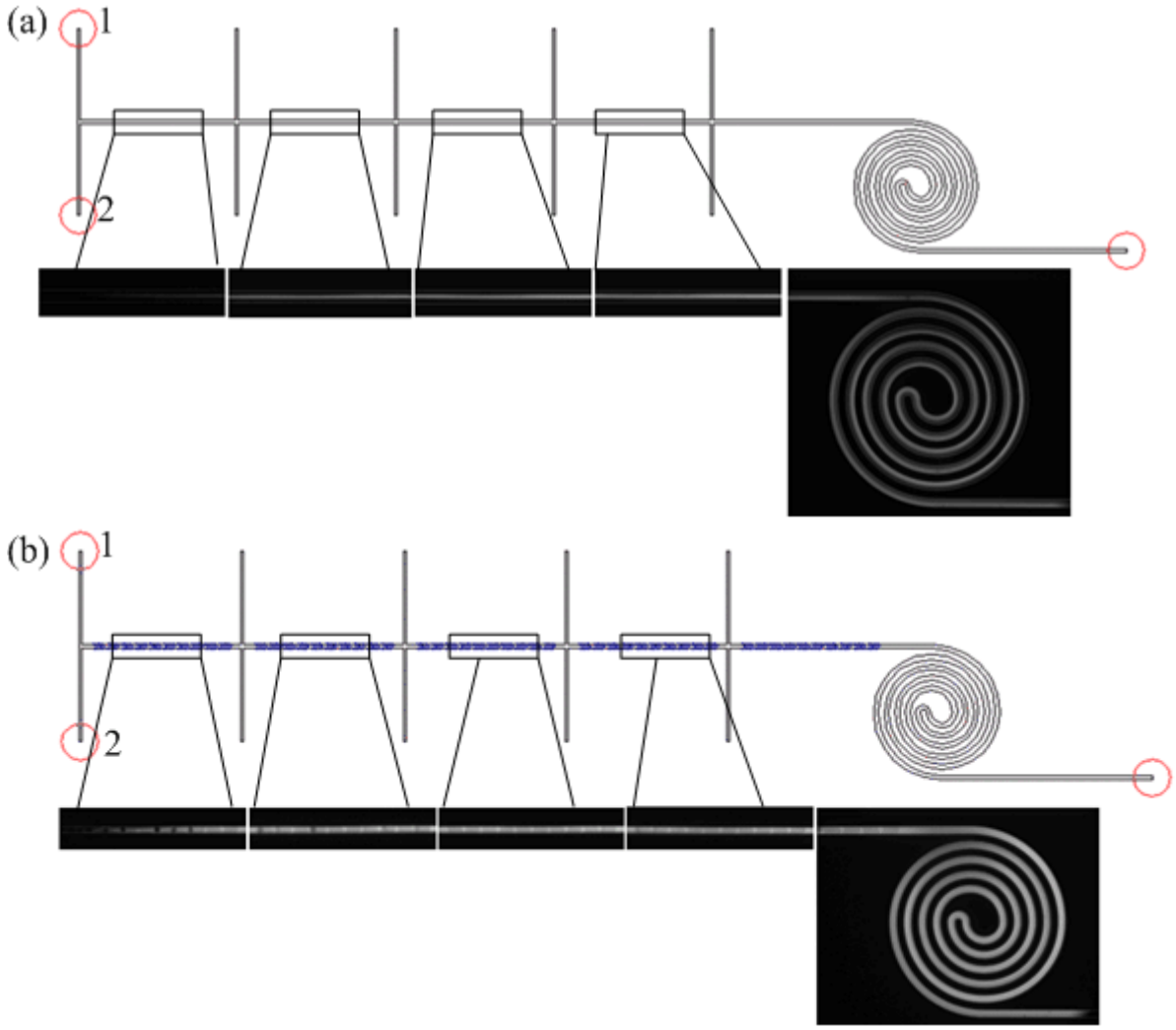


Figure 4-10. CCD camera image of the luminescence at the indicated location in the microfluidic devices. (a) Microfluidic device I; (b) Microfuidic device II.

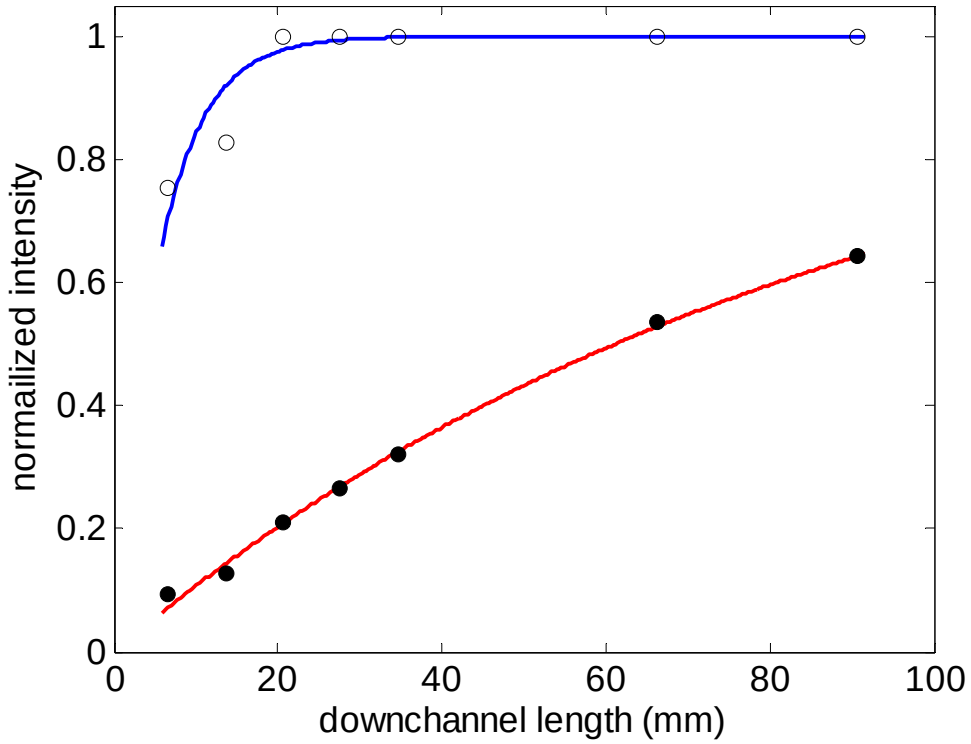


Figure 4-11. Normalized luminescence intensity changes along the channel direction within microfluidic device I (solid circle) and microfluidic device II (open circle) with flow rate of 1 μL/min. Symbols: experimental data, and trend line with $I=1-\exp(-x/\lambda)$.

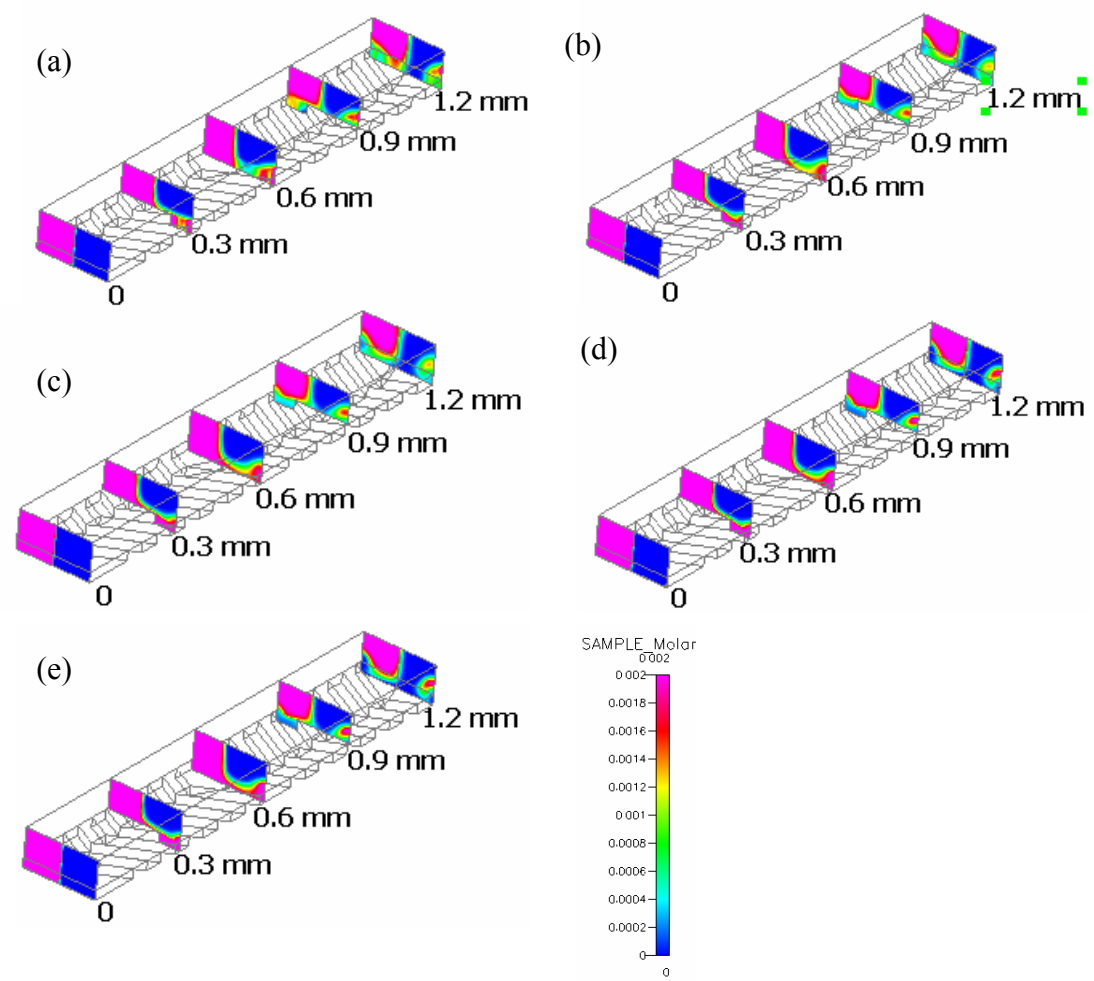


Figure 4-12. CFD results of concentration distributions in the ridge region for different number of the mesh elements: (a) 167910; (b) 180554; (c) 205842; (d) 256418; (e) 344826.


Figure 4-13. The computational residue plot.

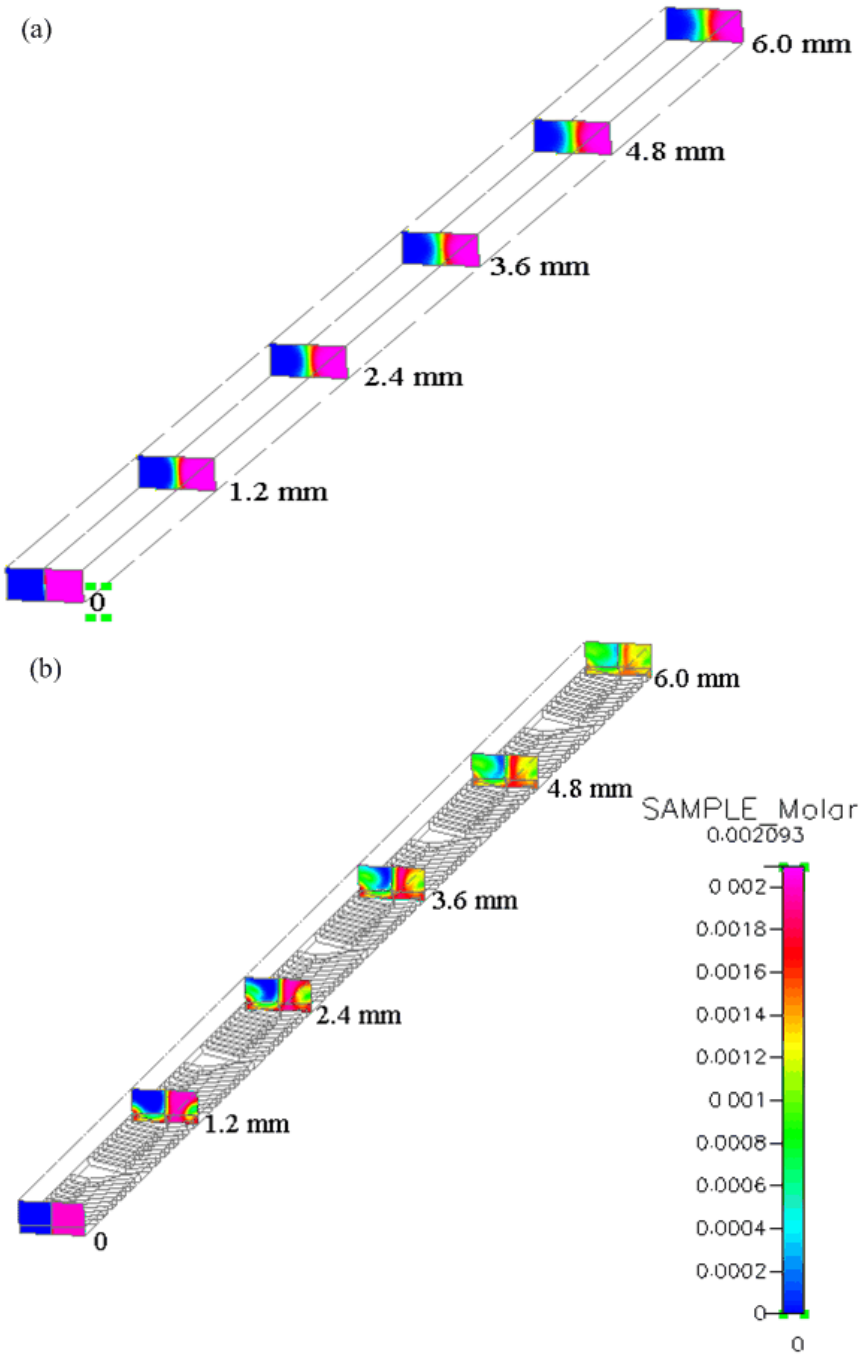


Figure 4-14. CFD results of concentration distributions and the interface between two solutions at the flow rate of 1 μL/min. (a) Microfluidic device I; (b) Microfluidic device.

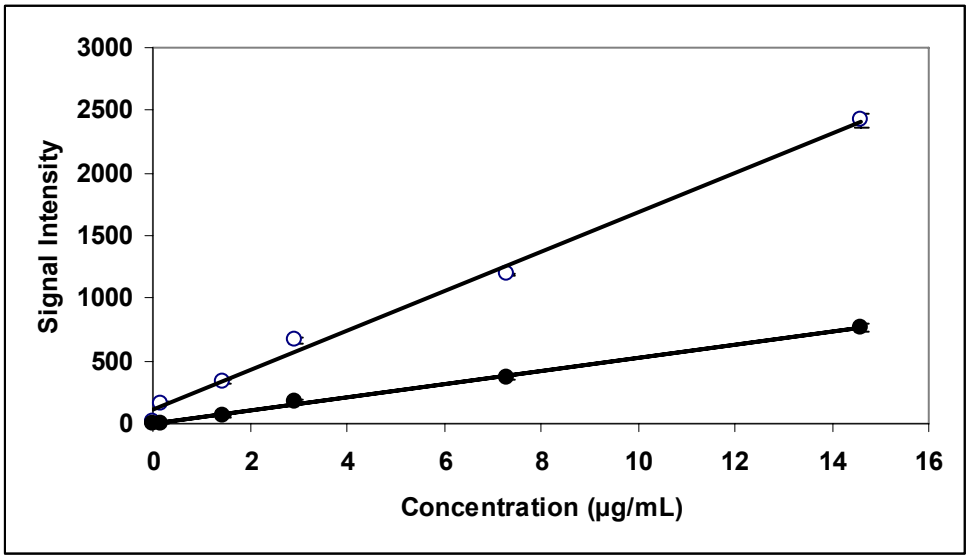


Figure 4-15. Calibration curves for bioluminescent assay using microfluidic device I (solid circles) and microfluidic device II (open circles).

(a)

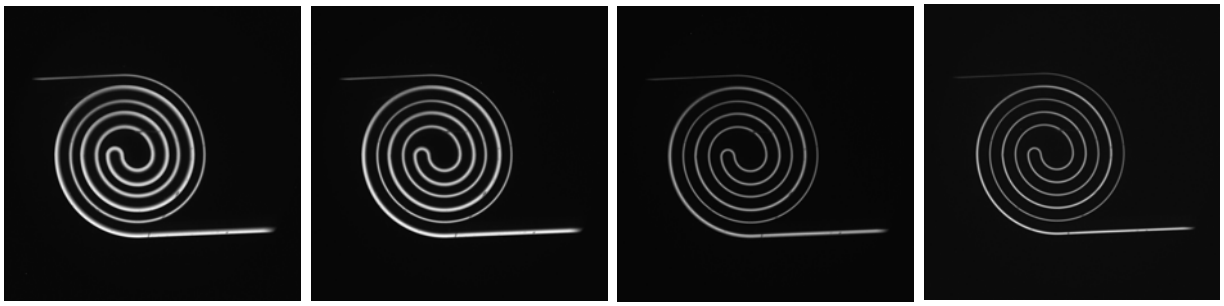

(b)

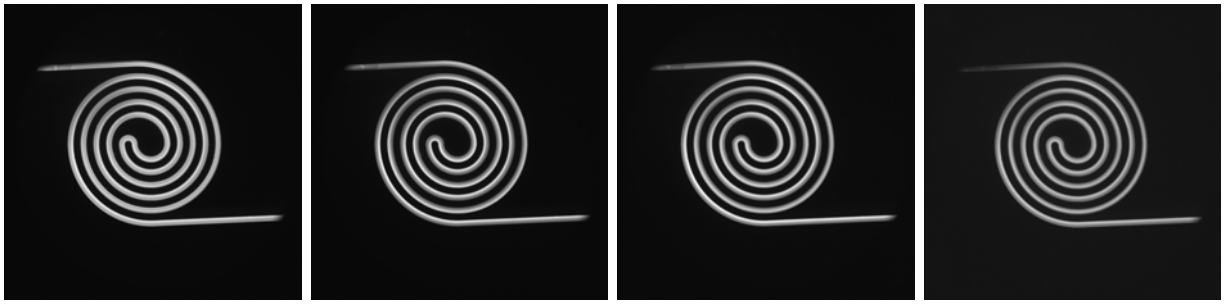

Figure 4-16. CCD image of the luminescence at the spiral channel at the flow rate of 1 µL/min, 2 µL/min, 4 µL/min and 8 µL/min from left to right. (a) Microfluidic device I; (b) Microfuidic device II.

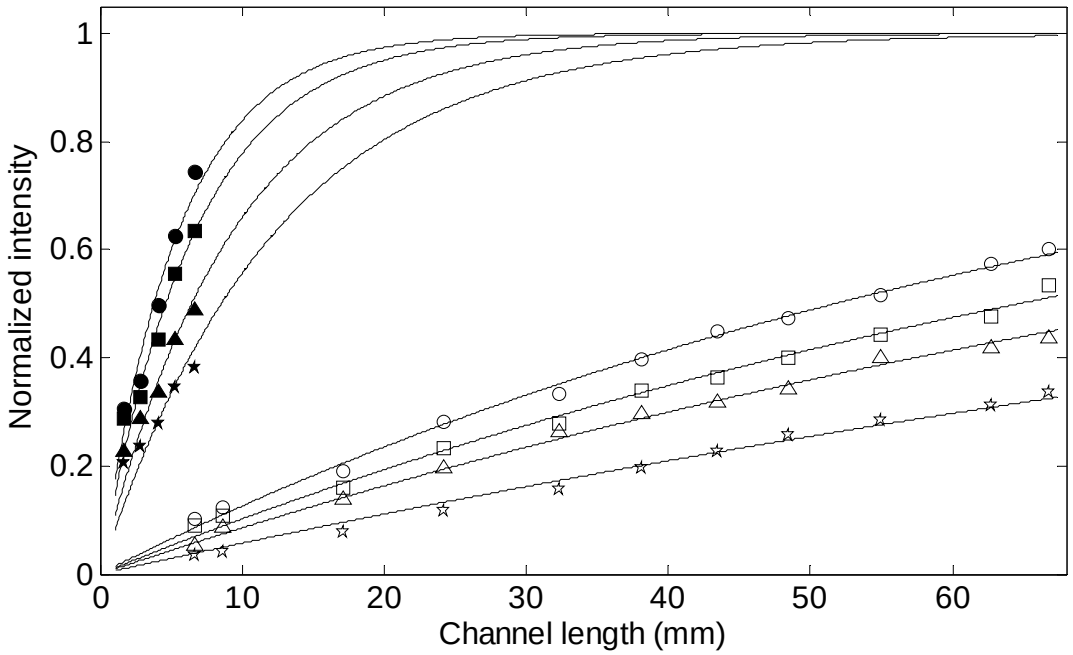


Figure 4-17. Effect of the flow rate on the luminescent intensity along the channel direction in microfluidic device I (open) and microfluidic device II (solid) for flow rate of 1 μL/min (circle), 2 μL/min(rectangle), 4 μL/min (triangle) and 8 μL/min(pentagram).

Figure 4-18. Detection of synthesized luciferase using device II.

# CHAPTER 5
# SUMMARY AND FUTURE DIRECTION

## 5.1 Summary

The objective of this research is to fabricate and develop the miniaturized devices for high yield and high-throughput protein production and its downstream applications. The combination of microfabrication technology and *in vitro* protein synthesis provides a state-of-the-art platform for producing a large number of proteins at low cost. Moreover, such a platform can be used for simple, fast and sensitive toxin detection.

The background information about fabrication and applications of miniaturized devices is first reviewed in Chapter 1. The methods for large scale protein synthesis from *in vivo* to *in vitro* are described. The development and challenges of *in vitro* protein synthesis in microchips are discussed.

Chapter 2 presents a microwell array device made from acrylic by micromilling. The array device has been demonstrated for *in vitro* synthesis of GFP, CAT and luciferase in prokaryotic or eukaryotic expression system. The device is then used to demonstrate the concept of toxin detection based on the mechanism that toxin inhibits biological protein synthesis, while tetracycline (TC) and cycloheximide (CH) are selected as toxin simulants. It is confirmed that TC has an inhibitory effect on the expression of GFP and CAT in the prokaryotic expression system, whereas CH has a negligible effect. In contrast, TC has a negligible effect on the production of luciferase in the eukaryotic expression system, while CH has an inhibitory effect. In addition, the response pattern of TC and CH in a 3 X 4 array microwell device shows the potential of toxin detection based on the mechanisms of toxin actions.

The major shortcoming of the microwell array device is the limited reaction time, thus leading to a low yield of synthesized proteins. For example, expression of CAT and GFP ceased

after 4 h and 1.5 h, respectively. To addresses this challenge, a nested-well device is designed and it incorporates continuous exchange cell free (CECF) technology as discussed in chapter 3. The nested-well device consists of a tray and a well separated by a dialysis membrane. In this device, the reaction byproducts ($P_i$ and NMPs) are removed, and the consumable substrates (amino acids, NTPs, and energy-regenerating compounds) are continuously supplied through the porous membranes. As a result, the nested-well device allows protein expression to continue for up to 20 h with a high protein yield, because the accumulation of inhibitory byproducts and the exhaustion of substrates are avoided. The performances of protein synthesis in a tube and the device are compared. In addition, the use of the device for ricin detection is demonstrated. Compared with traditional labor-intensive and time-consuming ELISA method, this detection method is simpler and faster. The detection limit of 1 pg/μL of ricin is at least comparable to the reported ELISA method and at least one order of magnitude more sensitive than most other reported detection methods.

Chapter 4 focuses on development of the microfluidic devices based on hot embossing technique and its application for enzymatic reactions. The microfludic device is composed of the straight channel with herringbone ridges at the bottom wall and a spiral channel for luminescence detection. The advantages of using herringbone ridge mixer for biological reactions are emphasized. Bioluminescence produced by the enzymatic reaction between luciferase and luciferin is detected by a cooled CCD camera, which allows us to visualize fluid behavior. Diffusion-based mixing and chaotic mixing in the microfluidic device are investigated and compared. In addition, the device is demonstrated to detect luciferase synthesized off chip so that the device may be uesd for online *in vitro* protein synthesis and detection.

## 5.2 Future Work

As summarized in the previous section, miniaturized protein expression systems have been successfully established and their potential applications have also been demonstrated in this dissertation. In this section, the future work is proposed and discussed.

### 5.2.1 Device Design and Fabrication

A two-part, nested-well array is described in the dissertation for protein synthesis. The upper part, or tray, functions as the reaction chamber for protein synthesis; each well has a dialysis membrane on the bottom to hold DNA template, cell extract or lysate, RNA, and synthesized proteins. The lower part, well, contains the feeding solution, including amino acid and energy source. As described in Chapter 3, the lower parts are milled in the lab. Alternatively, a commercially available 96-well plate can be used as a substitute. This will allow the use of commercial well-plate readers to measure the protein expression yield directly. Although the current design is designed in agreement with 96-well plate format, the device with a smaller number of wells is not compatible with commercial plate readers. Well size and alignments corresponding to 384-well plates could also theoretically be developed, though the issues related to injection of tray must be addressed.

The nested-well device consists of two parts, which are separated by a dialysis membrane. Dialysis membrane is glued to tray, which leads to several limitations. First, the glue needs to be carefully chosen and tested for biocompatibility. Second, it is difficult to ensure the uniformity of glue thickness since it depends on the size of a microwell and contact area of the membrane. Third, leakage is always possible. Finally, it is difficult to automate fabrication of device. These limitations may be addressed by laminating a nanoporous membrane with the tray. Moreover, the membranes must meet the following criteria: (1) the pore size is large enough for nutrient supplies and byproduct removal and small enough to keep the synthesized proteins; (2) the

membrane is compatible with lamination process. The pore structures must be maintained during the sealing. Nanoporous PC membranes with the pore size of 10 nm and 15 nm are under testing.

### 5.2.2 Protein Expression System

In this dissertation, we employ *E. coli* extract and wheat germ extract to demonstrate prokaryotic and eukaryotic protein expression system. Theoretically, any organism that makes a large amount of proteins can be used for *in vitro* protein expression, but the discussion on the future work is still focused on commercial systems above.

Many different DNA templates may be designed and tested. Successful *in vitro* protein expression depends on a correct starting DNA template, which consists of a gene encoding a target protein and the necessary regulatory elements including promoter, terminator, ribosome binding site and tags. Although GFP, CAT and luciferase have been expressed from corresponding vectors provided by kit, a variety of different T7 driven plasmids, such as pIVEX, pET, and pEXP for *in vitro* protein expression are available and DNA coding sequence can be inserted into these plasmids by standard cloning procedures.

An alternative method is to use PCR to generate linear DNA template to avoid time-consuming and labor-intensive steps of plasmid preparation. The advantages of this method include: (1) easy deletion and insertion of sequences; (2) easy introduction of point mutations and random mutations; (3) easily and fast fuse of different proteins. The disadvantage of this method is that the yield of protein synthesis is lower than using plasmid. The low yield may be caused either by the fast decay of linear DNA templates by the exonuclease presented in the cell-free extracts or by the limited accessibility of transcription and translation factors due to the secondary structure in DNA or RNA. In chapter 2, we tried to use a PCR amplified template for protein expression, but failed to obtain detectable amount of protein. We suspect that the

sequence of mRNA preceding the translation factor binding site may form the secondary structure and the binding sites are embedded.

### 5.2.3 Protein Detection

In this work, three proteins, CAT, GFP and luciferase, were successfully synthesized in the miniaturized devices. After expression, the synthesized protein was detected and quantified by one or more methods. CAT and GFP were quantified by Western blotting. GFP was also detected by fluorescence whereas luciferase is detected by luminescence. Western blotting is the most commonly-used method for protein detection. However, it takes long time and it is difficult to be integrated with the miniaturized device. Fluorescence detection based on GFP is a good approach, since GFP is a relatively small protein and many proteins have been successfully fused with GFP. Compared with fluorescence, luminescence based on luciferase requires no excitation light source, simplifying the design and fabrication of the microfluidic device. Imaging setup discussed in chapter 5 can be used to detect synthesized luciferase or extended for other targeted proteins, if the protein can be fused with luciferase.

### 5.2.4 Applications

In this dissertation, the feasibility of using *in vitro* protein synthesis system for detecting inhibitory effects of different toxin simulants/drugs has been demonstrated. Other toxin simulants can be tested and the response pattern (or signature) database of the array device can then be constructed. The database may be used as a tool for detection and identification of known and unknown toxins.

Other potential applications of in vitro protein expression array may include (1) high throughput cloning and screening of mutant and engineered proteins; (2) construction of the protein library from cDNA library for functional genomic and proteomic research.

Inspired by Feynman's talk "There is plenty of room at the bottom— an invitation to enter a new field of physics", I have accomplished this research. I would like to end this thesis with an invitation, "there is plenty of chemistry and biology in miniaturized devices". The door is open; scientists and engineers from different disciplinary are welcome to explore such a marvelous small world.

LIST OF REFERENCES


(1) Feynman, R. *Journal of Microelectromechanical systems* **1992**, *1*, 60-66.

(2) Feynman, R. *Journal of Microelectromechanical systems* **1993**, *2*, 4-14.

(3) Dittrich, P. S.; Manz, A. *Nat Rev Drug Discov* **2006**, *5*, 210-218.

(4) Auroux, P. A.; Iossifidis, D.; Reyes, D. R.; Manz, A. *Anal Chem* **2002**, *74*, 2637-2652.

(5) Vilkner, T.; Janasek, D.; Manz, A. *Anal Chem* **2004**, *76*, 3373-3385.

(6) Gad-el-Hak, M. *The MEMS Handbook*, 2nd edition ed.; CRC Press: Boca Raton, 2002.

(7) Hsu, T.-R. *MEMS and Microsystems: Design and Manufacture*; McGraw Hill: Boston, 2002.

(8) Rai-Choudhury, P. *Handbook of Microlithography, Micromachining, and Microfabrication.*, 1st edition ed.; SPIE: Bellingham, 1997.

(9) Terry, S. C.; Jerman, J. H.; Angell, J. B. *IEEE Transactions on Electron Devices* **1979**, *ED-26*, 1880-1886.

(10) Manz, A.; Miyahara, Y.; Miura, J.; Watanabe, Y.; Miyagi, H.; Sato, K. *Sensors and Actuators, B: Chemical* **1990**, *B1*, 249-255.

(11) van Lintel, H. T. G. *Sensors and Actuators* **1988**, *15*, 153-167.

(12) Smits, J. G. *Sensors and Actuators A: Physical* **1990**, *21*, 203-206.

(13) Esashi, M.; Shoji, S.; Nakano, A. *Sensors and Actuators* **1989**, *20*, 163-169.

(14) Shoji, S.; Nakagawa, S.; Esashi, M. *Sensors and Actuators A: Physical* **1990**, *21*, 189-192.

(15) van de Pol, F. C. M.; van Lintel, H. T. G.; Elwenspoek, M.; Fluitman, J. H. J.; van Lintel, H. T. G.; Elwenspoek, M.; Fluitman, J. H. J. *Sensors and Actuators A: Physical* **1990**, *21*, 198-202.

(16) van de Pol, F. C. M.; Wonnink, D. G. J.; Elwenspoek, M.; Fluitman, J. H. J. *Sensors and Actuators* **1990**, *17*, 139-143.

(17) Madou, M. J. *Fundamentals of Microfabrication: The Science of Miniaturization*, 2nd edition ed.; CRC Press: Boca Raton, 2002.

(18) Rai-Choudhury, P. *Handbook of Microlithography, Micromachining, and Microfabrication*, 1st edition ed.; SPIE: Bellingham, 1997.

(19) Sadia National Laboratories. *Microsystems*, http:// www.sadia.gov/mstc/index.html, November 1st, **2007**

(20) NUXUS III Report. Market Analysis for MEMS and Microsystems. http:// www.utc-consult.de/english/r_n3_e.html, April 8th, **2006**

(21) Manz, A.; Graber, N.; Widmer, H. M. *Sensors and Actuators, B: Chemical* **1990**, *B1*, 244-248.

(22) Kovacs, G. T. *Micromachined Transducers Sourcebook*, 1st edition ed.; McGraw-Hill Science: Boston, 1998.

(23) Wise, K. D.; Najafi, K. *Science* **1991**, *254*, 1335-1342.

(24) Kopp, M. U.; Mello, A. J.; Manz, A. *Science* **1998**, *280*, 1046-1048.

(25) Quake, S. R.; Scherer, A. *Science* **2000**, *290*, 1536-1540.

(26) Madou, M.; Florkey, J. *Chem Rev* **2000**, *100*, 2679-2692.

(27) Boone, T. D.; Fan, Z. H.; Hooper, H. H.; Ricco, A. J.; Tan, H.; Williams, S. J. *Anal Chem* **2002**, *74*, 78A-86A.

(28) Soper, S. A.; Ford, S. M.; Qi, S.; McCarley, R. L.; Kelly, K.; Murphy, M. C. *Anal Chem* **2000**, *72*, 642A-651A.

(29) Xia, Y.; Whitesides, G. M. *Annual Review of Materials Science* **1998**, *28*, 153-184.

(30) Whitesides, G. M.; Ostuni, E.; Takayama, S.; Jiang, X.; Ingber, D. E. *Annu Rev Biomed Eng* **2001**, *3*, 335-373.

(31) Peppas, N. A. *Hydrogels in Medicine and Pharmacy*, 1st edition ed.; CRC Press: Boca Raton, 1986.

(32) Beebe, D. J.; Moore, J. S.; Bauer, J. M.; Yu, Q.; Liu, R. H.; Devadoss, C.; Jo, B. H. *Nature* **2000**, *404*, 588-590.

(33) Vogel, S. D., Kathryn K. *Cats' Paws and Catapults: Mechanical Worlds of Nature and People*; W. W. Norton & Company: Norton, 2000.

(34) Fan, Z. H.; Harrison, D. J. *Analytical Chemistry* **1994**, *66*, 177-184.

(35) Sia, S. K.; Whitesides, G. M. *Electrophoresis* **2003**, *24*, 3563-3576.

(36) Stoyanov, A. V.; Das, C.; Fredrickson, C. K.; Fan, Z. H. *Electrophoresis* **2005**, *26*, 473-479.

(37) Vreeland, W. N.; Locascio, L. E. *Anal Chem* **2003**, *75*, 6906-6911.

(38) Lai, S.; Wang, S.; Luo, J.; Lee, L. J.; Yang, S. T.; Madou, M. J. *Anal Chem* **2004**, *76*, 1832-1837.

(39) Tan, W.; Fan, Z. H.; Qiu, C. X.; Ricco, A. J.; Gibbons, I. *Electrophoresis* **2002**, *23*, 3638-3645.

(40) Holden, M. A.; Jung, S. Y.; Cremer, P. S. *Anal Chem* **2004**, *76*, 1838-1843.

(41) Paegel, B. M.; Blazej, R. G.; Mathies, R. A. *Curr Opin Biotechnol* **2003**, *14*, 42-50.

(42) Song, S.; Singh, A. K.; Shepodd, T. J.; Kirby, B. J. *Anal Chem* **2004**, *76*, 2367-2373.

(43) Huber, D. L.; Manginell, R. P.; Samara, M. A.; Kim, B. I.; Bunker, B. C. *Science* **2003**, *301*, 352-354.

(44) Hong, J. W.; Studer, V.; Hang, G.; Anderson, W. F.; Quake, S. R. *Nat Biotechnol* **2004**, *22*, 435-439.

(45) Schmalzing, D.; Belenky, A.; Novotny, M. A.; Koutny, L.; Salas-Solano, O.; El-Difrawy, S.; Adourian, A.; Matsudaira, P.; Ehrlich, D. *Nucleic Acids Res* **2000**, *28*, E43.

(46) Harrison, D. J.; Fluri, K.; Seiler, K.; Fan, Z. H.; Effenhauser, C. S.; Manz, A. *Science* **1993**, *261*, 895-897.

(47) Harrison, D. J.; Manz, A.; Fan, Z. H.; Ludi, H.; Widmer, H. M. *Analytical Chemistry* **1992**, *64*, 1926-1932.

(48) Fan, Z. H.; Mangru, S.; Granzow, R.; Heaney, P.; Ho, W.; Dong, Q.; Kumar, R. *Anal Chem* **1999**, *71*, 4851-4859.

(49) Li, Y.; Buch, J. S.; Rosenberger, F.; DeVoe, D. L.; Lee, C. S. *Anal Chem* **2004**, *76*, 742-748.

(50) Woolley, A. T.; Mathies, R. A. *Proc Natl Acad Sci U S A* **1994**, *91*, 11348-11352.

(51) Burns, M. A.; Mastrangelo, C. H.; Sammarco, T. S.; Man, F. P.; Webster, J. R.; Johnsons, B. N.; Foerster, B.; Jones, D.; Fields, Y.; Kaiser, A. R.; Burke, D. T. *Proc Natl Acad Sci U S A* **1996**, *93*, 5556-5561.

(52) Woolley, A. T.; Hadley, D.; Landre, P.; deMello, A. J.; Mathies, R. A.; Northrup, M. A. *Anal Chem* **1996**, *68*, 4081-4086.

(53) Woolley, A. T.; Mathies, R. A. *Analytical Chemistry* **1995**, *67*, 3676-3670.

(54) Aborn, J. H.; El-Difrawy, S. A.; Novotny, M.; Gismondi, E. A.; Lam, R.; Matsudaira, P.; Mckenna, B. K.; O'Neil, T.; Streechon, P.; Ehrlich, D. J. *Lab on a Chip* **2005**, *5*, 669-674.

(55) Kakuta, M.; Bessoth, F. G.; Manz, A. *The Chemical Record* **2001**, *1*, 395-405.

(56) Janickea, M. T.; Kestenbauma, H.; Hagendorfa, U.; Schutha, F.; Fichtnerb, M.; Schubertb , K. *Journal of Catalysis* **2000**, *191*, 282-293.

(57) Losey, M. W.; Schmidt, M. A.; Jensen, K. F. *Industrial & Engineering Chemistry Research* **2001**, *40*, 2555-2562.

(58) Chambers, R. D.; Spink, R. C. H. *Chemical Communications* **1999**, 883-884.

(59) De Bellefon, C.; Tanchoux, N.; Caravieilhes, S.; Grenoullet, P.; Hessel, V. *Angewandte Chemie, International Edition* **2000**, *39*, 3442-3445.

(60) Hisamoto, H.; Saito, T.; Tokeshi, M.; Hibara, A.; Kitamori, T. *Chemical Communications* **2001**, 2662-2663.

(61) Ismagilov, R. F.; Ng, J. M.; Kenis, P. J.; Whitesides, G. M. *Anal Chem* **2001**, *73*, 5207-5213.

(62) Kikutani, Y.; Horiuchi, T.; Uchiyama, K.; Hisamoto, H.; Tokeshi, M.; Kitamori, T. *Lab Chip* **2002**, *2*, 188-192.

(63) Neils, C.; Tyree, Z.; Finlayson, B.; Folch, A. *Lab Chip* **2004**, *4*, 342-350.

(64) DiTursi, M. K.; Cha, J.; Newman, M. R.; Dordick, J. S. *Biotechnol Prog* **2004**, *20*, 1705-1709.

(65) Dittrich, P. S.; Jahnz, M.; Schwille, P. *Chembiochem* **2005**, *6*, 811-814.

(66) He, M.; Taussig, M. J. *Nucleic Acids Res* **2001**, *29*, E73-73.

(67) Ramachandran, N.; Hainsworth, E.; Bhullar, B.; Eisenstein, S.; Rosen, B.; Lau, A. Y.; Walter, J. C.; LaBaer, J. *Science* **2004**, *305*, 86-90.

(68) Angenendt, P.; Nyarsik, L.; Szaflarski, W.; Glokler, J.; Nierhaus, K. H.; Lehrach, H.; Cahill, D. J.; Lueking, A. *Anal Chem* **2004**, *76*, 1844-1849.

(69) Steffen, J.; von Nickisch-Rosenegk, M.; Bier, F. F. *Lab Chip* **2005**, *5*, 665-668.

(70) de Figueiredo, P.; Roberts, R. L.; Nester, E. W. *Proteomics* **2004**, *4*, 3128-3140.

(71) Zahn, J. D.; Hsieh, Y. C.; Yang, M. *Diabetes Technol Ther* **2005**, *7*, 536-545.

(72) Grayson, A. C. R.; Shawgo, R. S.; Johnson, A. M.; Flynn, N. T.; Li, Y.; Cima, M. J.; Langer, R. *Proceedings of The IEEE* **2004**, *92*, 6-21.

(73) Ziaie, B.; Baldi, A.; Lei, M.; Gu, Y.; Siegel, R. A. *Adv Drug Deliv Rev* **2004**, *56*, 145-172.

(74) Alberts, B.; Johnson, A.; Lewis, J.; Raff, M.; Roberts, K.; Walter, P. *Molecular Biology of the Cell*, 4 Edition ed.; Garland Science: New York, 2002.

(75) Crick, F. *Nature* **1970**, *227*, 561-563.

(76) Temin, H. M.; Baltimore, D. *Adv Virus Res* **1972**, *17*, 129-186.

(77) Mulder, C.; Arrand, J. R.; Delius, H.; Keller, W.; Pettersson, U.; Roberts, R. J.; Sharp, P. A. *Cold Spring Harb Symp Quant Biol* **1975**, *39 Pt 1*, 397-400.

(78) Cech, T. R. *Nature* **1989**, *339*, 507-508.

(79) Cech, T. R. *Biochem Int* **1989**, *18*, 7-14.

(80) Littlefield, J. W.; Keller, E. B.; Gross, J.; Zamecnik, P. C. *J Biol Chem* **1955**, *217*, 111-123.

(81) Lamborg, M. R.; Zamecnik, P. C. *Biochim Biophys Acta* **1960**, *42*, 206-211.

(82) Nirenberg, M. W.; Matthaei, J. H. *Proc Natl Acad Sci U S A* **1961**, *47*, 1588-1602.

(83) Roberts, B. E.; Paterson, B. M. *Proc Natl Acad Sci U S A* **1973**, *70*, 2330-2334.

(84) Pelham, H. R.; Jackson, R. J. *Eur J Biochem* **1976**, *67*, 247-256.

(85) Spirin, A. S.; Baranov, V. I.; Ryabova, L. A.; Ovodov, S. Y.; Alakhov, Y. B. *Science* **1988**, *242*, 1162-1164.

(86) Endo, Y.; Otsuzuki, S.; Ito, K.; Miura, K. *J Biotechnol* **1992**, *25*, 221-230.

(87) Kigawa, T.; Yokoyama, S. *J Biochem (Tokyo)* **1991**, *110*, 166-168.

(88) Kim, D. M.; Choi, C. Y. *Biotechnol Prog* **1996**, *12*, 645-649.

(89) Kim, D. M.; Kigawa, T.; Choi, C. Y.; Yokoyama, S. *Eur J Biochem* **1996**, *239*, 881-886.

(90) Yamane, T.; Kawarasaki, Y.; Nakano, H. *Ann New York Acad Sci* **1995**, *750*, 146-157.

(91) Alakhov, Y. B.; Baranov, V. I.; Ovodov, S. J.; Ryabova, L. A.; Spirin, A. S.; Morozov, I. Y.; United States Patent: USA, 1995.

(92) Baranov, V. I.; Spirin, A. S. *Methods Enzymol* **1993**, *217*, 123-142.

(93) Betton, J. M. *Curr Protein Pept Sci* **2003**, *4*, 73-80.

(94) Hosokawa, K.; Fujii, T.; Nojima, T.; Shoji, S.; Yotsumoto, A.; Endo, I. *Journal of Micromechatronics* **2000**, *1*, 85-98.

(95) Nojima, T.; Fujii, T.; Hosokawa, K.; Yotsumoto, A.; Shoji, S.; Endo, I. *Bioprocess Engineering* **2000**, *22*, 13-17.

(96) Yamamoto, T.; Nojima, T.; Fujii, T. *Lab on a Chip* **2002**, *2*, 197-202.

(97) Tabuchi, M.; Hino, M.; Shinohara, Y.; Baba, Y. *Proteomics* **2002**, *2*, 430-435.

(98) Kinpara, T.; Mizuno, R.; Murakami, Y.; Kobayashi, M.; Yamaura, S.; Hasan, Q.; Morita, Y.; Nakano, H.; Yamane, T.; Tamiya, E. *J Biochem (Tokyo)* **2004**, *136*, 149-154.

(99) Mei, Q.; Fredrickson, C. K.; Jin, S.; Fan, Z. H. *Anal Chem* **2005**, *77*, 5494-5500.

(100) Hahn, G. H.; Asthana, A.; Kim, D. M.; Kim, D. P. *Anal Biochem* **2007**, *365*, 280-282.

(101) Kigawa, T.; Yabuki, T.; Yoshida, Y.; Tsutsui, M.; Ito, Y.; Shibata, T.; Yokoyama, S. *FEBS Lett* **1999**, *442*, 15-19.

(102) Spirin, A. S. *Trends Biotechnol* **2004**, *22*, 538-545.

(103) Gilbert, M.; Albala, J. S. *Current Opinion in Chemical Biology* **2002**, *6*, 102-105.

(104) Jewett, M. C.; Swartz, J. R. *Biotechnol Bioeng* **2004**, *87*, 465-472.

(105) Katzen, F.; Chang, G.; Kudlicki, W. *Trends Biotechnol* **2005**, *23*, 150-156.

(106) Gold, L. M.; Schweiger, M. *Proc Natl Acad Sci U S A* **1969**, *62*, 892-898.

(107) Gold, L. M.; Schweiger, M. *Methods Enzymol* **1971**, *20*, 537-542.

(108) Lederman, M.; Zubay, G. *Biochim Biophys Acta* **1967**, *149*, 253-258.

(109) Schweiger, M.; Gold, L. M. *Proc Natl Acad Sci U S A* **1969**, *63*, 1351-1358.

(110) Zubay, G. *Annu Rev Genet* **1973**, *7*, 267-287.

(111) Zubay, G.; Lederman, M.; DeVries, J. K. *Proc Natl Acad Sci U S A* **1967**, *58*, 1669-1675.

(112) DeVries, J. K.; Zubay, G. *Proc Natl Acad Sci U S A* **1967**, *57*, 1010-1012.

(113) Shimizu, Y.; Inoue, A.; Tomari, Y.; Suzuki, T.; Yokogawa, T.; Nishikawa, K.; Ueda, T. *Nat Biotechnol* **2001**, *19*, 751-755.

(114) Ohashi, H.; Shimizu, Y.; Ying, B. W.; Ueda, T. *Biochem Biophys Res Commun* **2007**, *352*, 270-276.

(115) Oleinikov, A. V.; Gray, M. D.; Zhao, J.; Montgomery, D. D.; Ghindills, A. L.; Dill, K. *Journal of Proteome Research* **2003**, *2*, 313-319.

(116) Elbaz, Y.; Steiner-Mordoch, S.; Danieli, T.; Schuldiner, S. *Proc. Natl. Acad. Sci. USA* **2004**, *101*, 1519-1524.

(117) Tao, S. C.; Zhu, H. *Nat Biotechnol* **2006**, *24*, 1253-1254.

(118) Tian, J.; Gong, H.; Sheng, N.; Zhou, X.; Gulari, E.; Gao, X.; Church, G. *Nature* **2004**, *432*, 1050-1054.

(119) Sawasaki, T.; Hasegawa, Y.; Tsuchimochi, M.; Kamura, N.; Ogasawara, T.; Kuroita, T.; Endo, Y. *FEBS Lett* **2002**, *514*, 102-105.

(120) Jung, G. Y.; Stephanopoulos, G. *Science* **2004**, *304*, 428-431.

(121) Yamamoto, T.; Fujii, T.; Nojima, T. *Lab Chip* **2002**, *2*, 197-202.

(122) Spirin, A. S. In *In cell-free translation systems.*; Spirin, A. S., Ed.; Springer: Berlin, 2002, pp 3-22.

(123) Bujard, H.; Gentz, R.; Lanzer, M.; Stueber, D.; Mueller, M.; Ibrahimi, I.; Haeuptle, M. T.; Dobberstein, B. *Methods Enzymol* **1987**, *155*, 416-433.

(124) Coen, D. M.; Bedbrook, J. R.; Bogorad, L.; Rich, A. *Proc Natl Acad Sci U S A* **1977**, *74*, 5487-5491.

(125) Lewis, J. B.; Anderson, C. W.; Atkins, J. F.; Gesteland, R. F. *Cold Spring Harb Symp Quant Biol* **1975**, *39 Pt 1*, 581-590.

(126) Stueber, D.; Ibrahimi, I.; Cutler, D.; Dobberstein, B.; Bujard, H. *Embo J* **1984**, *3*, 3143-3148.

(127) Spirin, A. S. In *Frontiers in Bioprocessiong II*; Todd, P., K., S. S., Beer, M., Eds.; Washington,DC: ACS, 1991, pp 31-43.

(128) Craig, D.; Howell, M. T.; Gibbs, C. L.; Hunt, T.; Jackson, R. J. *Nucleic Acids Res* **1992**, *20*, 4987-4995.

(129) Jermutus, L.; Ryabova, L. A.; Pluckthun, A. *Curr Opin Biotechnol* **1998**, *9*, 534-548.

(130) Endo, Y.; Sawasaki, T. *J Struct Funct Genomics* **2004**, *5*, 45-57.

(131) Jackson, A. M.; Boutell, J.; Cooley, N.; He, M. *Brief Funct Genomic Proteomic* **2004**, *2*, 308-319.

(132) ImageJ. http://rsb.info.nih.gov/ij, July 18$^{th}$, **2007**

(133) Tsien, R. Y. *Annu Rev Biochem* **1998**, *67*, 509-544.

(134) Prendergast, F. G. In *Green fluorescent proteins*; Sullivan, K. F., Kay, S. A., Eds.; Academic press: San Diego, 1999, pp 1-18.

(135) Bucdavari, S. *The Merck Index*; Merck &Co.: Whitehouse Station,NJ, 1996.

(136) Watson, J. D.; Baker, T. A.; Bell, S. P.; Gann, A.; Kevine, M.; Losich, R. *Molecular biology of the gene*, 12th edition ed.; CSHL press: Cold Spring Harbor,NJ, 2004.

(137) Salyers, A. A.; Whitt, D. D. *Bacterial pathogenesis: a molecular approach*, 2nd edition ed.; ASM press: Washington, DC, 2002.

(138) Terpe, K. *Appl Microbiol Biotechnol* **2003**, *60*, 523-533.

(139) Buchel, C.; Morris, E.; Orlova, E.; Barber, J. *J Mol Biol* **2001**, *312*, 371-379.

(140) Mei, Q.; Fredrickson, C. K.; Lian, W.; Jin, S.; Fan, Z. H. *Anal Chem* **2006**, *78*, 7659-7664.

(141) Mei, Q.; Fredrickson, C. K.; Simon, A.; Knouf, R.; Fan, Z. H. *Biotechnology Progress* **2007**, *23*.

(142) Moreno-Bondi, M. C.; Alarie, J. P.; Vo-Dinh, T. *Anal Bioanal Chem* **2003**, *375*, 120-124.

(143) Phillips, K. S.; Cheng, Q. *Anal Chem* **2005**, *77*, 327-334.

(144) Liu, W.; Montana, V.; Chapman, E. R.; Mohideen, U.; Parpura, V. *Proc Natl Acad Sci U S A* **2003**, *100*, 13621-13625.

(145) Taitt, C. R.; Anderson, G. P.; Lingerfelt, B. M.; Feldstein, M. J.; Ligler, F. S. *Anal Chem* **2002**, *74*, 6114-6120.

(146) Tao, L.; Yu, X.; Snyder, A. P.; Li, L. *Anal Chem* **2004**, *76*, 6609-6617.

(147) Mothershed, E. A.; Cassiday, P. K.; Pierson, K.; Mayer, L. W.; Popovic, T. *J Clin Microbiol* **2002**, *40*, 4713-4719.

(148) Lagally, E. T.; Emrich, C. A.; Mathies, R. A. *Lab Chip* **2001**, *1*, 102-107.

(149) Koh, C. G.; Tan, W.; Zhao, M. Q.; Ricco, A. J.; Fan, Z. H. *Anal Chem* **2003**, *75*, 4591-4598.

(150) Belgrader, P.; Young, S.; Yuan, B.; Primeau, M.; Christel, L. A.; Pourahmadi, F.; Northrup, M. A. *Anal Chem* **2001**, *73*, 286-289.

(151) CDC, http://www.bt.cdc.gov/agent/agentlist-category.asp, March 16th, **2005**.

(152) Teter, K.; Holmes, R. K. *Infect Immun* **2002**, *70*, 6172-6179.

(153) Crowther, J. R. *ELISA : theory and practice*; Humana Press: Totowa, N.J., 1995.

(154) Olsnes, S.; Refsnes, K.; Pihl, A. *Nature* **1974**, *249*, 627-631.

(155) Lord, J. M.; Roberts, L. M.; Robertus, J. D. *Faseb J* **1994**, *8*, 201-208.

(156) Lord, M. J.; Jolliffe, N. A.; Marsden, C. J.; Pateman, C. S.; Smith, D. C.; Spooner, R. A.; Watson, P. D.; Roberts, L. M. *Toxicol Rev* **2003**, *22*, 53-64.

(157) Vitetta, E. S.; Thorpe, P. E.; Uhr, J. W. *Trends in Pharmacological Sciences* **1993**, *14*, 148-154.

(158) Uckun, F. M.; Frankel, A. *Leukemia* **1993**, *7*, 341-348.

(159) Franz, D. R.; Jaax, N. K. In *Medical Aspects of Chemical and Biological Warfare*; Sidell, F. R., Takafuji, E. T., Franz, D. R., Eds.; Borden Institute, Walter Reed Army Medical Center: Washington, D.C., 1997, pp 632.

(160) Bigalke, H.; Rummel, A. *Toxicology* **2005**, *214*, 210-220.

(161) Poli, M. A.; Rivera, V. R.; Hewetson, J. F.; Merrill, G. A. *Toxicon* **1994**, *32*, 1371-1377.

(162) Godal, A.; Olsnes, S.; Pihl, A. *Journal of Toxicology and Environmental Health* **1981**, *8*, 409-417.

(163) Wadkins, R. M.; Golden, J. P.; Pritsiolas, L. M.; Ligler, F. S. *Biosensors & Bioelectronics* **1998**, *13*, 407-415.

(164) Stine, R.; Pishko, M. V. *Analytical Chemistry* **2005**, *77*, 2882-2888.

(165) Shankar, K.; Zeng, K.; Ruan, C.; Grimes, C. A. *Sensors and Actuators B* **2005**, *107*, 640-648.

(166) Alakhov, Y. B. B., V. I.; Ovodov, S. J.; Ryabova, L. A.; Spirin, A.S.; Morozov,I. Y.; United States Patent: USA, 1995.

(167) Madin, K.; Sawasaki, T.; Ogasawara, T.; Endo, Y. *Proc Natl Acad Sci U S A* **2000**, *97*, 559-564.

(168) Yamamoto, Y.; Sugimoto, S.; Shen, X. C.; Nagamune, T.; Yao, S. L.; Suzuki, E. *Biochemical Engineering Journal* **1999**, *3*, 151-155.

(169) Martin, G. A.; Kawaguchi, R.; Lam, Y.; DeGiovanni, A.; Fukushima, M.; Mutter, W. *Biotechniques* **2001**, *31*, 948-950, 952-943.

(170) Angenendt, P.; Nyarsik, L.; Szaflarski, W.; Glokler, J.; Nierhaus, K. H.; Lehrach, H.; Cahill, D. J.; Lueking, A. *Anal. Chem.* **2004**, *76*, 1844-1849.

(171) Kolb, V. A.; Makeyev, E. V.; Spirin, A. S. *Embo J* **1994**, *13*, 3631-3637.

(172) Salyers, A. A.; Whitt, D. D. *Bacterial pathogenesis: a molecular approach*, 2nd ed.; ASM Press: Washington, D.C., 2002.

(173) Endo, Y.; Mitsui, K.; Motizuki, M.; Tsurugi, K. *J Biol Chem* **1987**, *262*, 5908-5912.

(174) Endo, Y.; Tsurugi, K. *J Biol Chem* **1987**, *262*, 8128-8130.

(175) Harley, S. M.; Beevers, H. *Proceedings of the National Academy of Sciences of the United States of America-Biological Sciences* **1982**, *79*, 5935-5938.

(176) Harley, S. M.; Beevers, H. *Plant Science Letters* **1984**, *36*, 1-5.

(177) Cawley, D. B.; Hedblom, M. L.; Houston, L. L. *Arch Biochem Biophys* **1978**, *190*, 744-755.

(178) Ramakrishnan, S.; Eagle, M. R.; Houston, L. L. *Biochimica Et Biophysica Acta* **1982**, *719*, 341-348.

(179) Leith, A. G.; Griffiths, G. D.; Green, M. A. *Journal of the Forensic Science Society* **1988**, *28*, 227-236.

(180) Narang, U.; Anderson, G. P.; Ligler, F. S.; Burans, J. *Biosensors and Bioelectronics* **1997**, *12*, 937-945.

(181) Dill, K.; Montgomery, D. D.; Ghindilis, A. L.; Schwarzkopf, K. R.; Ragsdale, S. R.; Oleinikov, A. V. *Biosensors and bioelctronics* **2004**, *20*, 736-742.

(182) Rubina, A. Y.; Dyukova, V. I.; Dementieva, E. I.; Stomakhin, A. A.; Nesmeyanov, V. A.; Grishin, E. V.; Zasedatelev, A. S. *Anal Biochem* **2005**, *340*, 317-329.

(183) Yu, X.; Zhao, L.; Jiang, H.; Wang, H.; Yin, C.; Zhu, S. *Sensors and Actuators B* **2001**, *76*, 199-202.

(184) Shyu, R. H.; Shyu, H. F.; Liu, H. W.; Tang, S. S. *Toxicon* **2002**, *40*, 255-258.

(185) Kudlicki, W.; Kramer, G.; Hardesty, B. *Anal Biochem* **1992**, *206*, 389-393.

(186) Kigawa, T.; Yabuki, T.; Yokoyama, S. *Tanpakushitsu Kakusan Koso* **1999**, *44*, 598-605.

(187) Klammt, C.; Lohr, F.; Schafer, B.; Haase, W.; Dotsch, V.; Ruterjans, H.; Glaubitz, C.; Bernhard, F. *Eur J Biochem* **2004**, *271*, 568-580.

(188) Shirokov, V. A. S., P. N.; Biryukov, S. V.; Spirin, A. S. In *In cell-free translation*; Spirin, A. S., Ed.; Spiringer: Berlin, 2002, pp 91-107.

(189) Budisa, N. In *In cell-free protei expression*; Swartz, J. R., Ed.; Springer: Berlin, 2003, pp 89-98.

(190) Nemetz, C. W., S.; Krupka, S.; Watzele, M; Mutter, W. In *In cell-free translation systems*; Spirin, A. S., Ed.; Springer: Berlin, 2000, pp 157-163.

(191) Madin, K. W., Manfred; Hoffmann, Michael; Metzler, Thomas; Rode, Hans-Jürgen; Schmid, Markus; Mayr, Dora; Nikolaus, Thomas; Schlossman, Thilo; Obermeier, Wolfgang; Reichhuber, Rolf ; Buchberger, Bernd *Biochemica* **2005**, 33-36.

(192) HosoKawa, K.; Fujii, T.; Nojima, T.; Shoji, S.; Yotsumoto, A.; Endo, I. *Journal of Micromechatronics* **2000**, *1*, 85-98.

(193) Service, R. F. *Science* **1998**, *282*, 400-400.

(194) Schwesinger, N.; Frank, T.; Wurmus, H. *Journal of Micromechanics and Microengineering* **1996**, *6*, 99-102.

(195) Liu, R. H.; Lenigk, R.; Grodzinski, P. *Journal of Microlithography Microfabrication and Microsystems* **2003**, *2*, 178-184.

(196) Burns, M. A.; Johnson, B. N.; Brahmasandra, S. N.; Handique, K.; Webster, J. R.; Krishnan, M.; Sammarco, T. S.; Man, P. M.; Jones, D.; Heldsinger, D.; Mastrangelo, C. H.; Burke, D. T. *Science* **1998**, *282*, 484-487.

(197) Kricka, L. J.; Wilding, P. *Anal Bioanal Chem* **2003**, *377*, 820-825.

(198) Bilitewski, U.; Genrich, M.; Kadow, S.; Mersal, G. *Anal Bioanal Chem* **2003**, *377*, 556-569.

(199) Golbig, K.; Kursawe, A.; Hohmann, M.; Taghavi-Moghadam, S.; Schwalbe, T. *Chemical Engineering Communications* **2005**, *192*, 620-629.

(200) Liu, R. H.; Lenigk, R.; Druyor-Sanchez, R. L.; Yang, J. N.; Grodzinski, P. *Analytical Chemistry* **2003**, *75*, 1911-1917.

(201) Schwalbe, T.; Autze, V.; Wille, G. *Chimia* **2002**, *56*, 636-646.

(202) Ehrfeld, W.; Golbig, K.; Hessel, V.; Lowe, H.; Richter, T. *Industrial & Engineering Chemistry Research* **1999**, *38*, 1075-1082.

(203) Benz, K.; Jackel, K. P.; Regenauer, K. J.; Schiewe, J.; Drese, K.; Ehrfeld, W.; Hessel, V.; Lowe, H. *Chemical Engineering & Technology* **2001**, *24*, 11-17.

(204) Yang, Z.; Goto, H.; Matsumoto, M.; Maeda, R. *Electrophoresis* **2000**, *21*, 116-119.

(205) Yang, Z.; Matsumoto, S.; Goto, H.; Matsumoto, M.; Maeda, R. *Sensors and Actuators a-Physical* **2001**, *93*, 266-272.

(206) Zhu, X.; Kim, E. S. *Sensors and Actuators a-Physical* **1998**, *66*, 355-360.

(207) Wu, H. Y.; Liu, C. H. *Sensors and Actuators a-Physical* **2005**, *118*, 107-115.

(208) Lu, L. H.; Ryu, K. S.; Liu, C. *Journal of Microelectromechanical Systems* **2002**, *11*, 462-469.

(209) Oddy, M. H.; Santiago, J. G.; Mikkelsen, J. C. *Anal Chem* **2001**, *73*, 5822-5832.

(210) Lemoff, A. V.; Lee, A. P. *Sensors and Actuators B-Chemical* **2000**, *63*, 178-185.

(211) Liu, R. H.; Stremler, M. A.; Sharp, K. V.; Olsen, M. G.; Santiago, J. G.; Adrian, R. J.; Aref, H.; Beebe, D. J. *Journal of Microelectromechanical Systems* **2000**, *9*, 190-197.

(212) Stroock, A. D.; Dertinger, S. K. W.; Ajdari, A.; Mezic, I.; Stone, H. A.; Whitesides, G. M. *Science* **2002**, *295*, 647-651.

(213) Stroock, A. D.; Dertinger, S. K.; Whitesides, G. M.; Ajdari, A. *Analytical Chemistry* **2002**, *74*, 5306-5312.

(214) Park, S. J.; Kim, J. K.; Park, J.; Chung, S.; Chung, C.; Chang, J. K. *Journal of Micromechanics and Microengineering* **2004**, *14*, 6-14.

(215) Bessoth, F. G.; deMello, A. J.; Manz, A. *Analytical Communications* **1999**, *36*, 213-215.

(216) Jen, C. P.; Wu, C. Y.; Lin, Y. C.; Wu, C. Y. *Lab on a Chip* **2003**, *3*, 77-81.

(217) Jeon, M. K.; Kim, J. H.; Noh, J.; Kim, S. H.; Park, H. G.; Woo, S. I. *Journal of Micromechanics and Microengineering* **2005**, *15*, 346-350.

(218) Kim, D. S.; Lee, I. H.; Kwon, T. H.; Cho, D. W. *Journal of Micromechanics and Microengineering* **2004**, *14*, 1294-1301.

(219) Kim, D. S.; Lee, S. W.; Kwon, T. H.; Lee, S. S. *Journal of Micromechanics and Microengineering* **2004**, *14*, 798-805.

(220) Kim, D. S.; Lee, S. H.; Kwon, T. H.; Ahn, C. H. *Lab on a Chip* **2005**, *5*, 739-747.

(221) Kim, D. J.; Oh, H. J.; Park, T. H.; Choo, J. B.; Lee, S. H. *Analyst* **2005**, *130*, 293-298.

(222) Kirner, T.; Albert, J.; Gunther, M.; Mayer, G.; Reinhackel, K.; Kohler, J. M. *Chemical Engineering Journal* **2004**, *101*, 65-74.

(223) Lee, N. Y.; Yamada, M.; Seki, M. *Analytical and Bioanalytical Chemistry* **2005**, *383*, 776-782.

(224) Lee, Y. K.; Shih, C.; Tabeling, P.; Ho, C. M. *Journal of Fluid Mechanics* **2007**, *575*, 425-448.

(225) Mae, K.; Maki, T.; Hasegawa, I.; Eto, U.; Mizutani, Y.; Honda, N. *Chemical Engineering Journal* **2004**, *101*, 31-38.

(226) Melin, J.; Gimenez, G.; Roxhed, N.; van der Wijngaart, W.; Stemme, G. *Lab on a Chip* **2004**, *4*, 214-219.

(227) Chung, Y. C.; Hsu, Y. L.; Jen, C. P.; Lu, M. C.; Lin, Y. C. *Lab on a Chip* **2004**, *4*, 70-77.

(228) Hassell, D. G.; Zimmerman, W. B. *Chemical Engineering Science* **2006**, *61*, 2977-2985.

(229) Howell, P. B.; Mott, D. R.; Fertig, S.; Kaplan, C. R.; Golden, J. P.; Oran, E. S.; Ligler, F. S. *Lab on a Chip* **2005**, *5*, 524-530.

(230) Hong, C. C.; Choi, J. W.; Ahn, C. H. *Lab on a Chip* **2004**, *4*, 109-113.

(231) Johnson, T. J.; Ross, D.; Locascio, L. E. *Anal Chem* **2002**, *74*, 45-51.

(232) Chew, Y. T.; Xia, H. M.; Shu, C.; Wan, S. Y. M. *Modern Physics Letters B* **2005**, *19*, 1567-1570.

(233) Xia, H. M.; Wan, S. Y. M.; Shu, C.; Chew, Y. T. *Lab on a Chip* **2005**, *5*, 748-755.

(234) Xia, H. M.; Shu, C.; Wan, S. Y. M.; Chew, Y. T. *Journal of Micromechanics and Microengineering* **2006**, *16*, 53-61.

(235) Vijayendran, R. A.; Kathleen, M. M.; Beebe, D. J.; Leckband, D. E. *Langmuir* **2003**, *19*, 1824-1828.

(236) Yang, J. T.; Huang, K. J.; Lin, Y. C. *Lab on a Chip* **2005**, *5*, 1140-1147.

(237) Fu, X.; Liu, S. F.; Ruan, X. D.; Yang, H. Y. *Sensors and Actuators B-Chemical* **2006**, *114*, 618-624.

(238) Aubin, J.; Fletcher, D. F.; Bertrand, J.; Xuereb, C. *Chemical Engineering & Technology* **2003**, *26*, 1262-1270.

(239) Wang, H. Z.; Iovenitti, P.; Harvey, E.; Masood, S. *Journal of Micromechanics and Microengineering* **2003**, *13*, 801-808.

(240) Lynn, N. S.; Dandy, D. S. *Lab on a Chip* **2007**, *7*, 580-587.

(241) Hupert, M. L.; Guy, W. J.; Llopis, S. D.; Shadpour, H.; Rani, S.; Nikitopoulos, D. E.; Soper, S. A. *Microfluidics and Nanofluidics* **2007**, *3*, 1-11.

(242) DeLuca, M.; McElroy, W. D. *Biochemistry* **1974**, *13*, 921-925.

(243) David, R.; Lintz, H. G. *Chemie Ingenieur Technik* **1984**, *56*, 104-110.

# BIOGRAPHICAL SKETCH

Qian Mei was born in 1977 in China. She was raised in Luoyang, a beautiful city in central China, known as the "city of peonies." She entered Southeast University in Nanjing, China, in 1996, and earned her Bachelor of Science in biomedical engineering four years later. She then proceeded to her graduate studies in the same university and she received a Master of Science in biomedical engineering in 2003. In the same year, she enrolled in biomedical engineering at the Health Science Center of theUniversity of Tennessee at Memphis. In the spring of 2004, she relocated to Florida and started to pursue her Ph.D. in mechanical engineering in University of Florida.